Biogeosystem Technique

Issued since 2014.

E-ISSN 2413-7316
2025. 12(1). Issued 2 times a year

Journal is indexed by: **Cross Ref (USA), Electronic scientific library (Russia), MIAR (Spain), Open Academic Journals Index (USA), CiteFactor – Directory of International Reseach Journals (Canada).**

All manuscripts are peer reviewed by experts in the respective field. Authors of the manuscripts bear responsibility for their content, credibility and reliability.

Editorial board doesn't expect the manuscripts' authors to always agree with its opinion.

Postal Address: 13906, Polarstone Ct., Houston, TX, 77044 USA

Website: https://bgt.cherkasgu.press
E-mail: kalinitch@mail.ru

Founder and Editor: Cherkas Global University

Release date 25.06.25
Format 21 × 29,7/4.

Headset Georgia.

Order B-27.

Biogeosystem Technique

2025

Is. 1

C O N T E N T S

Articles

Published in the USA
Biogeosystem Technique
Issued since 2014.
E-ISSN: 2413-7316
2025. 12(1): 3-14

DOI: 10.13187/bgt.2025.1.3
https://bgt.cherkasgu.press

Articles

Monitoring the Condition of Hydraulic Structures during the Inter-Flood Period

Rafek R. Abdullin [a], Maxim V. Dyuldin [b], Denis A. Egorov [a], Natalia V. Krupenina [a], Evgeniy O. Olkhovik [a], Yuriy K. Smirnov [a], Alexey V. Cheremisin [b], Igor A. Chernov [a], Dilan Kouam [c], Chenxi Guo [d], Vasliy Y. Rud [a, e, *]

[a] Admiral Makarov State University of Maritime and Inland Shipping, Saint-Petersburg, Russian Federation
[b] Peter the Great St. Petersburg Polytechnic University, Saint-Petersburg, Russian Federation
[c] Université de Yaoundé, Yaoundé, Cameroon
[d] Lanzhou Shi, Gansu University, China
[e] Ioffe Institute, St.-Petersburg, Russian Federation

Paper Review Summary:
Received: 2025, May 21
Received in revised form: 2025, June 25
Acceptance: 2025, June 25

Abstract

The article is devoted to the issues of operational monitoring of the state of the infrastructure of hydraulic structures in the inter-flood period after the active impact of a powerful water flow during an ice break. For the design of repair and restoration works, a thorough examination of the condition of the riverbed and walls of hydraulic structures is necessary, on the basis of which a visual three-dimensional model is built. For visual observation, it is proposed to use a water drone equipped with pressure and temperature sensors, as well as a gyroscope-accelerometer and a magnetic compass. The main objective of the study is to plan the trajectory of a water drone in the reservoir area in order to build the most adequate model of its depths, the condition of the mooring walls and coastal slopes, with the recording of sensor readings in a database and operational visualization of the data obtained. To examine the condition of the walls of hydraulic structures, both visual and instrumental built-in monitoring tools are used to track the values of the main indicators of the condition of reinforced concrete structures. Monitoring of the groundwater level is a prerequisite for the adequate functioning of hydraulic structures. This is necessary for modeling the hydrological balance, which allows making informed decisions on water resources management and preventing negative consequences for the environment. It is also very important to monitor the depths of the fairway and the condition of the coastal slopes.

Keywords: riverbed fairway, hydraulic structures, condition monitoring, measurement filtering, measurement sensors, autonomous drones.

[*] Corresponding author
E-mail addresses: ecobaltica@gmail.com (V.Y. Rud)

1. Introduction

River valleys and floodplains are naturally designed to handle so-called "large water" flow. However, humans have always settled near riverbanks because rivers served as means of communication, water supply, energy, irrigation, and recreation. Many floodplains and low-lying areas are built up with houses and outbuildings despite the risk of flooding. One major downside of living near water is the potential for flooding during high water periods, especially in spring or during prolonged rains (Budin, 2008). Free river flow is regulated by hydraulic structures, and riverbeds are obstructed by dams and locks (Figure 1), which increases pollutant runoff due to higher flow velocity, reduced sedimentation, and natural floodplain purification. This also increases the risks of flooding, waterlogging, and inundation.

Fig. 1. Dam of a hydraulic structure

2. Objective of the Study

The main objective of the study is to develop a methodology for rapid automated monitoring of the condition of hydraulic structures and riverbeds after a flood to construct a visual 3D model for restoration work planning.

3. Discussion

Problem Statement

The primary task of the research is to build a model of the river fairway and hydraulic structure walls to create the most accurate representation of their condition, along with the state of quay walls and coastal slopes, recording sensor readings in a database and providing real-time visualization of the obtained data for planning repair and restoration work.

Solution Methods

The main research device proposed is the underwater drone "Oceanica Bathyscaphe" and a set of sensors embedded in hydraulic structures. The "Oceanica Bathyscaphe" is a smart robot capable of operating in both seawater and freshwater. The drone is fully controlled via a remote control unit included in the package. The operator can control the underwater movement speed of the robot, which supports three different speed modes. The drone's configuration includes an external navigation module equipped with sensors: a six-axis gyroscope-accelerometer, a three-axis magnetic compass, a pressure sensor, and a temperature sensor. The core of the Oceanica Bathyscaphe is the Raspberry Pi3 microcomputer (Figure 2; Jiang, 2025).

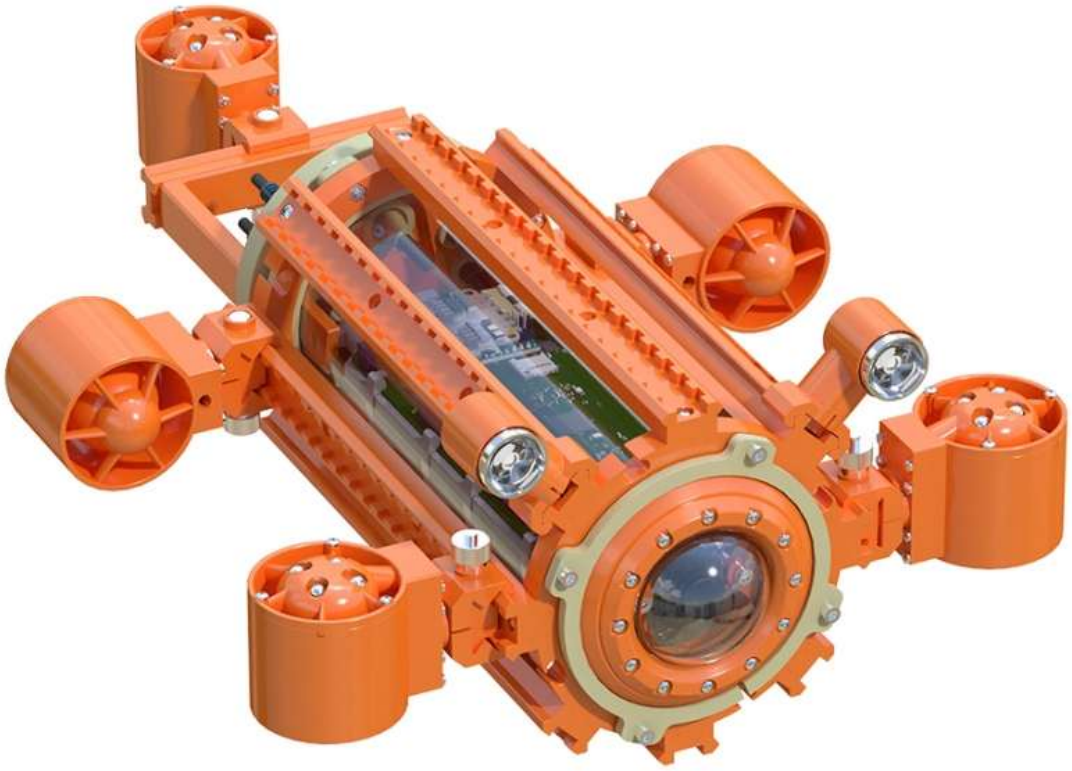

Fig. 2. Oceanica Bathyscaphe Robot

This robot is capable of:

– Diving to depths of up to 50 meters in both freshwater and saltwater;

– Recording video and taking photos underwater on a mobile device and saving them in memory;

– Capturing images with 8-megapixel resolution and recording Full HD video;

– Turning powerful lights on/off with adjustable brightness;

– Moving in six directions: up, down, forward, backward, right, and left;

– Transmitting system status data to a mobile device display;

– Collecting objects, lifting metal items, and monitoring water conditions;

– Moving underwater at three different speeds;

– Capturing photos and videos underwater while simultaneously viewing the captured images;

– Maintaining a connection with a mobile device at distances up to 30 meters.

Monitoring the Condition of Quay Walls

During the operation of quay structures, mechanical damage, metal corrosion, and concrete erosion are commonly encountered. The destruction of a pier begins from the moment the structure is commissioned. The slow degradation of construction materials occurs under the influence of the environment (Figure 3). Unlike mechanical damage, corrosion and erosion involve the dispersion and oxidation of the affected metal, often resulting in irreversible loss. Any construction material can be subject to corrosive or erosive damage.

In addition to these types of material degradation, others may also occur. For organic materials (wood), biological degradation caused by bacteria, fungi, or insects is often the main issue. For materials such as plastics, paints, and rubber, aging processes – gradual irreversible changes in internal structure and properties – are hazardous, often occurring in undesirable directions.

Fig. 3. Destruction of quay structures

All issues related to the operation of hydraulic structures, quay structures, and dams inevitably encounter the problem of ice impact.

The following types of ice impact on hydraulic structures (HST) are distinguished (Budin, 2008; Peschansky, 1967; Fomicheva, Kofeeva, 2022):

– Static pressure of a continuous ice cover during thermal expansion caused by air temperature changes;

– Impact of ice adhering to the structure during water level fluctuations;

– Static pressure of freely floating ice fields when pushed against the structure by wind and current;

– Dynamic pressure of freely floating ice fields and ice floes caused by ice drift, current, or wind;

– Dynamic impact of ice jams or blockages;

– Abrasive impact of ice floes on the structure surface during their movement influenced by wind, current, and water level fluctuations.

Additionally, for detecting metal corrosion and concrete erosion, visual inspection of quay walls using aerial and underwater drones is necessary.

Monitoring the Condition of Lock Walls.

The main feature of hydraulic structures (HST) is the need for continuous observation of their condition to prevent or timely address emergencies due to the influence of technogenic and natural hazards.

Safety monitoring of hydraulic structures is essential since these types of facilities are potentially dangerous, and any accident can result in catastrophic consequences. Therefore, implementing modern methodologies and equipment for control today is a necessity. Two types of HST condition observation are distinguished (Bolgov et al., 2013; Fomicheva, 2019; Panfilov, 1965; Korzhavin, 1973; Tsilikin, 1972):

– **Visual**: Involves visual inspection and the use of simple measuring instruments. These allow identifying defects, such as cracks that appear after natural disasters.

– **Instrumental**: Includes the use of control and measurement equipment, enabling continuous or short-interval monitoring**.**

Modern safety monitoring of HST primarily relies on automatic systems incorporating a complex of sensors, software, and equipment necessary for decoding signals from sensors and displaying them on the dispatcher's monitor. Such equipment allows continuous tracking of the technical condition of HST and automatically alerts the dispatcher and personnel of any malfunctions, enabling timely repairs or evacuation. As we can see, automatic HST monitoring ensures the safety of both the facility and the working personnel.

An automated monitoring system should track:

– Stress-strain state (SSS) of concrete structures;

– Piezometric head and filtration flow rate;

– Horizontal plane displacement of the structure or its elements;

– Structural settlement;

– Deviations from the normal angle.

For continuous monitoring of the technical condition of HST, a wide range of various sensors is employed. Most accurately, information is displayed from sensors installed in hydraulic structures during the construction stage. Among such equipment, the following can be highlighted:

– Piezometers on hydraulic structures ensure control of filtration head.

– Inclinometers measure the degree of horizontal soil deformation and structural settlement.

– Crackmeters determine the displacement of parts of the structure relative to each other.

– Strain gauges monitor the SSS of concrete structural elements.

Complex hydraulic structures (HST), such as hydroelectric power plants, dams, embankments, and marine port infrastructure objects (docks, locks, piers, etc.), are among the most dangerous objects in terms of potential accident consequences. To predict, prevent accidents timely, and assess HST safety, continuous monitoring of the technical condition of these hydraulic structures is required. Piezometry is widely used in automated industrial safety control systems for HST as a basic methodology for production measurement of hydrostatic or hydrodynamic pressure of liquids and solid deformations. Using various types of piezometers within the structure of automated geotechnical monitoring systems for HST, the following critical control tasks are addressed:

– Filtration pressure on the foundations of concrete hydraulic structures (dams, embankments), filtration deformations of the structure and foundations;

– Piezometric heads and hydraulic regime of HST, their foundations, and shore joints;

– Stresses in construction materials, at monitoring points in various zones inside the structures (including pore pressure);

– Level and temperature parameters of groundwater, allowing assessment of changes in the density and permeability of HST soils during long-term operation and the impact of these processes on the reliability of their foundations;

– Vertical and horizontal displacements of HST, settlements, mutual displacements of their elements and foundations;

– Zones, magnitudes, and sizes of structure deformations, length, and crack opening.

Classification, Device, and Principles of Piezometer Installation.

1) By installation method:

– Embedded – installed during the construction of the hydraulic structure;

– Drop-in – used in constructing and constructed HST.

2) By location of the measuring instrument's water intake:

– Surface;

– Deep;

– Point;

3) By location of the sensor mouth:

– Non-pressure;

– Pressure.

Principle of Operation of a String Piezometer.

The principle of operation depends on the frequency of string oscillations according to their tension degree. When water pressure changes in the structure where the sensor is installed, the tension of the string, which is the measuring element, changes. The oscillation frequency of the sensor string is proportional to the water pressure in the structure. One end of the string is fixed inside the sensor body, and the other is on a sensitive diaphragm. Piezometer data is transmitted to a reading device through a signal cable attached to the sensor.

Control of Filtration Heads.

Non-pressure piezometers, consisting of a pipe up to 35-40 m long, a filter located at the lower end of the pipe, and a head, control filtration heads. Piezometers are installed in pre-drilled piezometric wells in the structure. During piezometer installation in the piezometric well, a watertight "plug" is created above it (and if necessary, below it). The filter communicates with the surface through two hollow tubes where measurements are taken.

Water level (mm) in non-pressure piezometers is measured using a tape measure with a bell or whistle lowered into the well on a marked rope. The accuracy of the device is 1 cm at well depths up to 10 m and 2-3 cm at depths over 25 m.

The number and location of piezometers are determined in each specific project based on control tasks, design scheme, structure of the hydraulic structure, geological and hydrological features of the object, and other conditions.

For various designs of earthen dams, embankments, and typical engineering-geological foundation conditions, principal schemes of piezometric (observation) cross-section equipment are developed. On dams or embankments, piezometric cross-sections are located 100-150 m apart in the riverbed part and 150-250 m apart in the floodplain. At least three cross-sections are placed in the body of the HST and in the shore joints. Each cross-section must have at least three piezometers and a minimum of one in the downstream area of the hydraulic structures.

Application of Piezometers for Measuring Pore Pressure in Soil Mass.

Automatic piezometers with sensors of various types (electrical or vibrating string piezometer) are often used in geotechnical monitoring projects of HST. Sensors are installed in dispersive soils for automatic monitoring of pore pressure changes in hydraulic structures and groundwater levels (GWL) in the soil mass foundation of HST. Such devices can be equipped with filters of various pore diameters for solving complex measurement tasks. Automatic piezometers allow:

– Monitoring changes in hydrostatic pressure and gradient during HST operation;

– Evaluating the effectiveness of anti-filtration measures;

– Creating hydrogeodynamic models.

Piezometers can be used to observe changes in hydrogeological parameters (groundwater dynamics) in isolated aquifers.

Groundwater level is a key indicator of the state of underground water resources.

Monitoring Groundwater Levels

Monitoring groundwater levels is crucial for various sectors, including agriculture, construction, and ecology. High groundwater levels can lead to flooding and damage agricultural lands, as well as structures and building foundations. Conversely, low groundwater levels can cause drought and reduce the availability of drinking water.

Changes in groundwater levels can have serious environmental consequences. Rising groundwater levels can alter landscapes, reduce soil quality, and degrade ecosystems. On the other hand, declining groundwater levels can dry up rivers and lakes, negatively affecting animals and vegetation.

Various methods are used to monitor groundwater levels, including well monitoring, measuring underground water levels, and modeling the hydrological balance. This data helps make informed decisions about water resource management and preventing negative environmental impacts.

Well monitoring can utilize the Solinst Levelogger recorder and telemetry LevelSender 9500.

The Solinst Levelogger is a compact recorder that measures water level and temperature in a well. It is equipped with high-accuracy sensors and can record data to its internal memory.

The LevelSender 9500 is a telemetry system that transmits data from the Solinst Levelogger via email. Thus, obtaining monitoring data without physical presence at the well becomes possible (Figure 4).

Fig. 4. Solinst Levelogger Recorder

Monitoring groundwater levels is an integral part of managing underground water resources. Understanding the importance of this indicator and its consequences helps ensure sustainable use of underground water and environmental protection.

This sensor conveniently measures water levels at any time, as the device is lowered into a specially installed piezometric tube with a mounted submersible pump, rather than directly on its own cable into the water intake well. Piezometric measurements can be conducted manually or automatically.

The implementation of an automated monitoring system provides real-time comprehensive and reliable information about the state of the hydraulic object, thus minimizing the risks of accidents, emergencies, and eliminating material and human losses.

Monitoring the Condition of Coastal Slopes

The process of bank collapse is most pronounced in newly created reservoirs. The initial shape of the coastal zone often no longer corresponds to the project after exposure to water masses, primarily waves and currents. These discrepancies lead to intense deformations in the coastal zone and the creation of new bank forms, particularly the formation of a coastal shallows, altering both the above-water and underwater parts of the slopes.

Longshore currents, especially destructive during floods, play a significant role in bank formation. With good transport capacity due to high velocities and turbulence, currents move erosion products from erosion zones (headlands) to accumulation zones (bays and coves), where bars and spits form, narrowing the fairway and complicating ship approaches to piers.

Bank destruction by ice is due to its significant force both during ice movements and during the ice drift period. Ice floes and lateral ice jams annually destroy river banks. As a result of ice jams, river slopes are undercut, then they weather and erode, gradually widening river channels and shallowing the fairway *(*Volosukhin, Bandurin, 2017).

Ice jams also play a significant role in channel reformation. If a jam forms in the main channel, the ice flow bypasses it, eroding side channels.

Considering all these factors, periodic monitoring of the condition of navigable riverbank slopes and guaranteed fairway depths becomes relevant.

Monitoring the Condition of the Fairway

Each river has a source — an origin, which can be a lake, swamp, glacier, spring, etc., and a mouth — the place where the river ends and flows into the sea, lake, or another river (Volosukhin, Bandurin, 2017).

The water horizon, or river water level, fluctuates from maximum during high water periods, when part of the valley – the floodplain – is flooded, to minimum during low water periods — a low-water state of the river. Maximum and minimum horizons in the river almost annually change depending on the river's feeding. Rivers have more water in snowy and rainy years and less in low-snow and dry years.

River water levels depend on the presence of hydraulic structures, wind-induced surge phenomena, and tides and ebbs at river mouths.

The longitudinal profile of the riverbed has a jagged shape, constantly changing and descending in steps from the source to the mouth. Deep-water sections – pools – are located between sandy shallow sections – shoals. Each river has its longitudinal profile and slope, so the water level varies along different sections of the river. Typically, the upper part – the upper pool – has a steeper slope, the stream cuts through the rock, the flow velocity is high, and the depth is relatively shallow. Navigation on such a river is difficult. For example, the Volga in the upper pool. In the lower pool of the river, the slope is usually minimal, the flow velocity sharply decreases, contributing to sediment deposition in the channel.

The moving river stream continuously finds its way and primarily erodes places where the soil is weak, depositing sediments elsewhere in the form of mid-channel bars, islands, and most often spits. Thus, river bends form, and their erosion intensifies with increased flow around curves. Bank erosion and sediment deposition are especially intense during ice drift.

River bends vary in length and shape (Figure 5). Long bends of the low-water channel together with the valley are called meanders. A very long river bend, where the distance between the start and end is significantly less than the bend's length, is called a loop. A long bend inside the valley is called a meander, and a steep short meander is called a knee. As the river erosion increases, the start and end of the meander may connect during high water periods. This natural straightening of the river is called a chute, and navigation may occur through it during high water and then during low water periods. Over time, the chute becomes deeper and wider and may turn into the main channel. Meanwhile, the meander itself fills with sediments, gradually becoming

shallow, turning into an old channel – an oxbow lake or abandoned riverbed.

Considering all the above, continuous monitoring of the fairway condition in the pre-navigation period becomes relevant to ensure shipping channel depth during the navigation period.

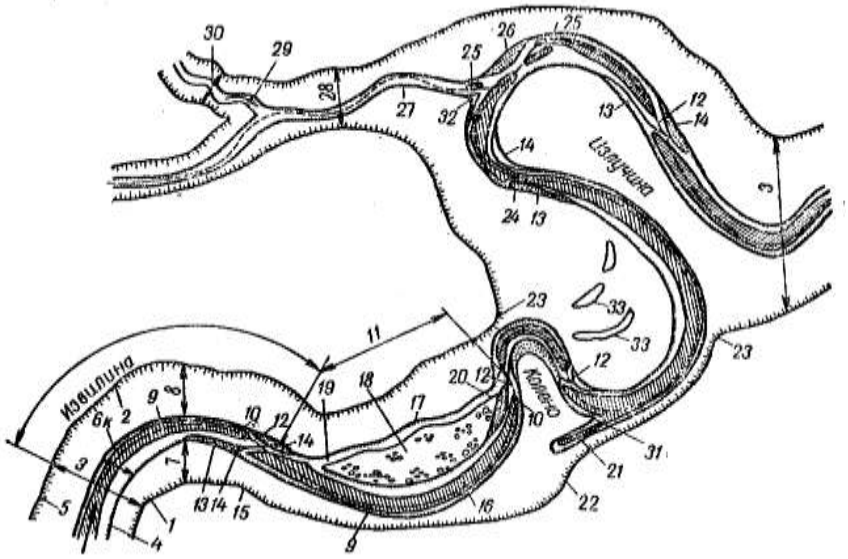

Fig. 5. River bends

Methods of Processing Data Obtained from Sensors

Preparatory filtering algorithm

Data read from sensors undergo primary processing by an Arduino processor to prevent highly noisy data from entering the operational database. Then, in real-time, data is collected and accumulated in the Blender 3D package database to create a three-dimensional computer graphic model (Ponomarenko, Karavaev, 2014; Ametov et al., 2016).

Quality noise filtering can reduce measurement errors and improve sensor measurement accuracy. It is necessary to combat two types of noise: constant noise (additive white Gaussian noise) with relatively stable amplitude and random impulses caused by external factors.

The arithmetic mean method effectively combats random noise, storing several previous measurement values in a buffer. When a new value is added to the buffer at the end of the sequence, the "window" of viewed values moves along it. A drawback of this method is some slowdown in data processing due to the need for floating-point calculations, but these are still faster than data exchange operations, thus negligibly affecting sensor reading speed (Ponomarenko, Karavaev, 2014).

The median filter method is convenient for combating random impulses within a single measurement. Combined with the arithmetic mean method, it yields acceptable results on experimental data.

After preliminary filtering, processed data is transmitted via WiFi to a control computer, where it undergoes more thorough processing.

Primary data processing includes:

– Median filter for combating random impulses.
– Arithmetic mean method.
– Preliminary filtering on-board the drone.
– Optimal filter setup parameters:
– Median filter window size: 5-7 measurements.
– Averaging period: 3-5 seconds.
– Threshold deviation value: 3σ.

Model refinement algorithm

The drone's algorithm for navigating within a water body to refine depths is based on a uniform grid. In areas with significant depth differences, the distances between successive drone trajectories on the water surface are reduced, and intermediate point data is collected. For depth refinement, the drone can be manually directed to any accessible point in the water body. The model constructs the water bed surface using linear interpolation, but before sending the sensor-obtained data to the database for model construction, these data are filtered using the

"Caterpillar" method (SSA) implemented in GNU Octave software (Alekseev, Chesnokova, 2012).

Data transmitted over communication channels are subject to "jitter" — undesirable disruption of signal temporal periodicity. In communication channels, jitter represents oscillation of the information signal's temporal position relative to its nominal value. Jitter in data transmission channels is caused by synchronization instability and path fluctuations. Jitter typically has two components: purely random and quasi-deterministic, usually low-frequency, referred to as "wander" in digital systems (Baklanov, 1998).

Particular interest lies in filtering the quasi-deterministic component, whose presence is mainly determined by the characteristics of the used equipment. To extract this component, the "Caterpillar" time series analysis method is proposed, whose main advantage is the lack of need for an a priori jitter model. "Caterpillar" or Singular Spectrum Analysis (SSA) allows for higher-quality analysis of various time series compared to common traditional methods.

The main goal of SSA is to decompose a series into interpretable components such as trend, periodic components, and noise. The essence of the method is transforming a one-dimensional series into multidimensional using a one-parameter shift procedure (hence the name "Caterpillar"), examining the resulting multidimensional trajectory using Principal Component Analysis (singular decomposition), and reconstructing (approximating) the series from selected principal components. The result of applying the method is the decomposition of the time series into simple components – slow trends and other periodic or oscillatory components, as well as noise components.

After undergoing such a filtering process, data cleaned from noise effects – slow trends – are used to build a 3D model of the water body.

Main stages of implementing the "Caterpillar" (SSA) method consist of four stages:

Stage 1. Embedding Transformation

Embedding is the process of converting certain data into numbers, vectors, which machines can not only store but also manipulate.

The original time series x(t) is transformed into a multidimensional series by creating a trajectory matrix. For this, a decomposition window L (100-200 points) is chosen, and each sequence of L points forms a row vector of matrix X.

Stage 2. Singular Value Decomposition

The resulting matrix X undergoes singular value decomposition: $X = U \Sigma V$,

where U and V are orthogonal matrices, and Σ is a diagonal matrix of singular values. Singular value decomposition can be reformulated geometrically as follows: a linear operator mapping elements of space R^n into itself can be represented as sequentially performed linear operators of rotation and stretching. Therefore, the components of singular value decomposition vividly show the geometric changes when a linear operator A maps a set of vectors from vector space into itself or into a vector space of another dimension.

Stage 3. Component Grouping and Principal Component Analysis

Principal components are identified based on the analysis of singular values. Usually, 3-5 components exceeding the noise threshold of 0.05 are used.

Stage 4. Reconstruction of the Filtered Signal

The filtered signal is reconstructed by inverse transformation of the selected components:

$X^* = \sum_{i=1}^{k} \sigma_i u_i v_i^*$,

where k is the number of selected components.

SSA Method Parameters for Implementation in GNU Octave Package:

– Decomposition window length: 100-200 points.
– Number of components for reconstruction: 3-5.
– Noise cutoff threshold: 0.05.

Algorithm Characteristics:

– Adaptability to changes in data.
– No need for preliminary settings for different types of signals.
– High processing speed due to matrix operations.
– Robustness to outliers and anomalies in data.

Quality of filtering is evaluated by the following metrics:

– Noise suppression coefficient.
– Correlation with the original signal.
– Root mean square error of reconstruction.
– Temporal stability of results.

This algorithm ensures an optimal balance between preserving useful information and removing noise components, which is critically important for measurement accuracy during dredging operations.

Modern analogues

Algorithmic compensation of measurement errors is the main method for improving the accuracy of modern monitoring systems. Its implementation requires the synthesis of estimation algorithms, which includes forming a model of the estimated state vector of a dynamic system. The type and order of the model affect the accuracy and quality of the obtained filtered estimates. Various information processing methods are applied to solve the problem of algorithmic error compensation, often using the Kalman filter – an algorithm that estimates the state vector of a dynamic system based on current measurements.

Determining coordinates and corresponding depths with the highest possible accuracy from a sequence of measurements generated by radar or optoelectronic systems is the central task of any monitoring system. A significant number of algorithms have been developed to solve this problem, mainly based on the well-known recursive Kalman filter algorithm, efficiently implemented on digital computers.

However, the problem cannot yet be considered definitively solved. This is due to many factors, and one of the most significant is the nonlinear nature of motion and measurement models in many practical problems. Nonlinearity arises for many reasons — due to nonlinear relationships between coordinate systems used in observation object and measurement equations, or due to the inherently nonlinear nature of the equations themselves.

Ignoring nonlinearities and overly simplifying the situation can significantly reduce the effectiveness of coordinate and velocity estimation algorithms in real target tracking systems. In practice, nonlinear estimation algorithms are used, but mainly limited to simpler variants such as the extended Kalman filter. More powerful algorithms exist but are rarely used because they require significant computational costs. However, the rapid growth of computing capabilities over many recent years quite allows using many of these algorithms in practice.

Comparison with Existing Methods

– **Kalman Filter** – An efficient recursive filter estimating the state vector of a dynamic system using a series of incomplete and noisy measurements. The Kalman filter is designed for recursive estimation of the state vector of an a priori known dynamic system, meaning calculating the current state requires knowing the current measurement and the previous state of the filter itself. Thus, like other recursive filters, the Kalman filter is implemented in the time domain rather than the frequency domain, but unlike other similar filters, it operates not only with state estimates but also with uncertainty estimates (probability density) of the state vector, based on Bayes' conditional probability formula.

The algorithm works in two stages. In the first stage – prediction stage – the Kalman filter extrapolates the state variable values and their uncertainties. In the second stage, based on the measurement data (obtained with some error), the extrapolation result is refined. Due to its step-by-step nature, the algorithm can track the object's state in real-time (without looking ahead, using only current measurements and information about the previous state and its uncertainty) (Shakhtarin, 2008a, 2008b; Egorushkin, Salychev, 2018).

– **Fourier Analysis** – A direction in analysis studying how general mathematical functions can be represented or approximated as a sum of simpler trigonometric functions. Fourier analysis arose from studying the properties of Fourier series and is named after Joseph Fourier, who showed that representing a function as a sum of trigonometric functions greatly simplifies the study of heat transfer. Fourier analysis finds application in solving a wide range of mathematical problems. In science and engineering, decomposing a function into oscillatory components is called Fourier analysis, and operating and reconstructing functions from those parts is called Fourier synthesis. For example, determining which frequency components are present in a musical note involves applying Fourier analysis to the selected musical note. Afterward, the same sound can be synthesized using the frequency components detected during the analysis.

– **Wavelet Transform** – A method that decomposes a signal into a linear combination of shifted and scaled versions of a mother wavelet. Since this is a multi-resolution approach, it provides excellent time and frequency localization of the signal representation. This integral transform represents the convolution of the wavelet function with the signal. Wavelet transform

translates the signal from the time domain into the frequency-time domain.

A method of transforming a function (or signal) into a form that either makes some quantities of the original signal more amenable to study or allows compressing the original dataset. Wavelet signal transformation is a generalization of spectral analysis. The term (wavelet) in English translation means "small wave." Wavelets are the general name for mathematical functions of a certain shape that are localized in time and frequency, and all functions are derived from one base function by modifying it (shifting, stretching). Wavelet transform of a function is an improved version of the Fourier transform. Fourier transform is a powerful tool for analyzing components of stationary signals, but it is not suitable for analyzing non-stationary signals, whereas wavelet transform allows analyzing components of non-stationary signals.

Advantages of the proposed SSA approach lie in the fact that the caterpillar method can extract polynomial and exponential trends. Moreover, unlike regression, SSA does not require pre-specification of a parametric model, which can provide a significant advantage when conducting exploratory analysis of a series and there is no obvious model, as happens in monitoring systems. Algorithms based on the caterpillar method possess:

– High data processing speed;
– Adaptability to changing conditions;
– Ease of implementation.

Results of data filtering

The result of the conducted research is the development of a method for performing rapid filtering of field research data on depths and bottom relief of newly formed reservoirs in the drying sea or river basin.

Quantitative indicators:

– Noise reduction: 40-50 %;
– Measurement accuracy improvement: 25-30 %;
– Data processing time: 0.2-0.3 seconds.

Comparison with traditional methods:

– Accuracy is 15-20 % higher compared to simple averaging;
– Processing speed is 2-3 times faster than Kalman filtering;
– Stability of results under various conditions.

Quality of filtering is evaluated by the following metrics:

– Noise suppression coefficient;
– Correlation with the original signal;
– Root mean square error of reconstruction;
– Temporal stability of results.

This algorithm ensures an optimal balance between preserving useful information and removing noise components, which is critically important for measurement accuracy during dredging operations.

4. Results

The developed method of rapid data filtering improves the efficiency of fairway parameter measurements and thereby increases the accuracy of dredging work planning by 15-20 %. Implementation of the proposed methodology provides:

– Increased accuracy of bottom relief measurements;
– Reduced influence of external interference;
– Accelerated data processing;
– Improved quality of created 3D models of reservoirs.

The proposed approach can be successfully applied in real conditions to optimize the process of water area monitoring and dredging work planning.

5. Conclusion

The result of the conducted research is the development of a method for monitoring and rapidly visualizing field research on depths and bottom relief of the fairway, as well as the state of coastal slopes of the shipping channel and quay walls.

The presented method of rapid monitoring with simultaneous visualization of field measurements, cleaned from noise, data on depth and bottom relief and coastal slopes of the shipping channel, as well as the state of piers and walls of hydraulic structures in the post-flood

period of the river, can be used for designing restoration and dredging works and can increase their efficiency by 15-20 %.

References

Alekseev, Chesnokova, 2012 – *Alekseev, E.R., Chesnokova, O.V.* (2012). Introduction to Octave for Mathematicians and Engineers. Moscow: ALT Linux. 368 p.

Ametov et al., 2016 – *Ametov, F.R., Mevlut, I.Sh., Adilshaeva, E.I.* (2016). Blender Program as the Main 3D Modeling Environment for Game Development in UNITY. *Tavricheskiy Scientific Reviewer*. 6(11): 190-192.

Baklanov, 1998 – *Baklanov, I.G.* (1998) Measurement Technologies in Modern Telecommunications Moscow: ECO-TRENDS, 1998. 140 p.

Bolgov et al., 2013 – *Bolgov, M.V., Borsch, S.V., Khaziakhmetov, R.M.* (2013). Dangerous Hydrological Phenomena: Methods of Analysis, Calculation, and Prediction, Mitigation of Negative Consequences. Abstracts of Reports. VII All-Russian Hydrological Congress. Saint-Petersburg. Pp. 6-12.

Budin, 2008 – *Budin, V.A.* (2008). Dangerous Hydrological Phenomena. SPb, RGGMU Publishing, , 228 p.

Egorushkin, Salychev, 2018 – *Egorushkin, A.Yu., Salychev, O.S.* (2018). Peculiarities of using the Kalman filter for algorithmic compensation of inertial navigation system errors. *Engineering journal: Science and Innovation*. 12. DOI: 10.18698/2308-6033-6033-2018-12-1834

Fomicheva, 2019 – *Fomicheva, N.N.* (2019). Hydraulic Modeling in Studying Ice Passage Through Hydraulic Structures. *Innovations and Investments*. 11: 298-300.

Fomicheva, Kofeeva, 2022 – *Fomicheva, N.N., Kofeeva, V.N.* (2022). Ice-Free Passage Through Hydrounits During Operation. In: Scientific Problems of Water Transport. *Russian Journal of Water Transport*. 72(3): 231-238.

Jiang, 2018 – *Jiang, Y.* (2018). Computational Fluid Dynamics Study of Hydrodynamic and Motion Stability of an Autonomous Underwater Helicopter. Master Thesis, Zhejiang University, Zhoushan, Zhejiang, China.

Korzhavin, 1973 – *Korzhavin, K.N.* (1973). Ice Passage During Construction and Operation of Hydrounits. Moscow: Energiya, 1973. 160 p.

Panfilov,1965 – *Panfilov D.F.* (1965). Destruction of Ice Fields Under Local Water Level Changes. Hydraulic Engineering. 1965. 12: 21-25.

Peschansky, 1967 – *Peschansky, I.S.* (1967). Ice Science and Ice Technology. Leningrad, Hydrometeorological Publishing. 462 p.

Ponomarenko, Karavaev, 2014 – *Ponomarenko, V.I., Karavaev, A.S.* (2014). Use of the ARDUINO Platform in Measurements and Physical Experiments. *Proceedings of Universities "PND"*. 22(4): 77-89.

Shakhtarin, 2008a – *Shakhtarin, B.I.* (2008). Wiener and Kalman filters. Moscow: Helios ARV. 408 p.

Shakhtarin, 2008b – *Shakhtarin B.I.* (2008) Nonlinear optimal filtering in examples and problems. Moscow: Helios ARV. 344 p.

Tsilikin, 1972 – *Tsilikin, V.F.* (1972). Modeling Ice Passage During Laboratory Hydraulic Research. Research and Calculations of Ice Jams. Issues of Ice Thermics and Hydrodynamics. Leningrad: Hydrometeoizdat. 192: 30-36.

Volosukhin, Bandurin, 2017 – *Volosukhin, V.A., Bandurin, M.A.* (2017). Multifactor survey monitoring realization in the conditions of the hydraulic structures safety deficit growth. *Izvestiya Vuzov. North-Caucasian region. Technical sciences*. 1: 76-78.

Published in the USA
Biogeosystem Technique
Issued since 2014.
E-ISSN: 2413-7316
2025. 12(1): 15-24

DOI: 10.13187/bgt.2025.1.15
https://bgt.cherkasgu.press

The Problem of Data Compromise in the Era of Quantum Computing

Rafek R. Abdullin [a], Maxim V. Dyuldin [b], Denis A. Egorov [a], Natalia V. Krupenina [a], Eugeny O. Olkhovik [a], Vladimir V. Karetnikov [a], Yuri K. Smirnov [a], Vasily Y. Rud [a, c, *], Daria A. Valiullina [d], Zhenyue Yuan [e], Van Yuikun [f], Alexey V. Cheremisin [b], Igor A. Chernov [a]

[a] Admiral Makarov State University of Maritime and Inland Shipping, Saint-Petersburg, Russian Federation
[b] Peter the Great St. Petersburg Polytechnic University, Saint-Petersburg, Russian Federation
[c] Ioffe Physico-Technical Institute, Saint-Petersburg, Russian Federation
[d] Kazan State Academy of Veterinary Medicine named after N.E. Bauman, Kazan, Russian Federation
[e] Shenyang Institute of Technology, Fushun, China
[f] Wenzhou University, Wenzhou, China

Paper Review Summary:
Received: 2025, June 18
Received in revised form: 2025, June 25
Acceptance: 2025, June 25

Abstract

Solving modern problems of ecology and the environment requires the use of large amounts of data and, accordingly, the use of quantum computers and artificial intelligence. This article examines the challenges associated with ensuring secure information exchange in the context of integrating quantum computers into communication networks. These quantum computers possess significantly higher processing speeds compared to standard von Neumann architecture computers. Considering that symmetric and asymmetric encryption algorithms rely on the assumption that breaking the used ciphers within a reasonable timeframe is practically impossible, the advent of quantum computers with their immense computational power calls into question the long-term stability of these ciphers. The primary threat posed by quantum computers is data compromise, which involves intercepting and accumulating encrypted data for future decryption attempts. To mitigate this threat, it is proposed to use a neural network to classify suspicious logs recorded by the operating system's security subsystem.

Keywords: quantum computing, post-quantum cryptography, cybersecurity, encryption algorithms, data compromise.

1. Introduction

Currently, there is rapid development in quantum technologies (Dushkin, 2018). With this progress comes the need to rethink existing approaches to data security. Classical encryption algorithms, both symmetric (e.g., AES) and asymmetric (e.g., RSA), have long served as the foundation for information protection. However, the emergence of quantum computers, capable of

* Corresponding author
E-mail addresses: ecobaltica@gmail.com (V.Y. Rud)

solving problems underlying these algorithms exponentially faster than classical computers, raises questions about their viability and resilience to new threats.

The main threats to standard encryption algorithms arising from quantum computers include attacks using Shor's algorithm, Grover's algorithm, and the compromise of long-term data (INFARS, 2025).

Symmetric encryption algorithms, such as DES and AES, use the same key for both encryption and decryption. While they are efficient and fast, their main drawback lies in the necessity of securely transmitting the shared key between sender and receiver. If the key is intercepted by an attacker, the entire security system becomes vulnerable.

An attack using Grover's algorithm, executed by a quantum computer, reduces the time required to brute-force keys by half, thereby weakening symmetric ciphers like AES. Although increasing key length can partially mitigate this vulnerability, it is insufficient in the long term (Burlakovs et al., 2020).

Most modern information systems utilize the asymmetric RSA encryption algorithm, which operates based on public-key cryptography. Its cryptographic strength relies on the difficulty of factoring large numbers, enabling a system where the public key is used for encryption and the private key for decryption. This innovation circumvented the problem of securely transmitting secret keys and revolutionized digital security.

The most cryptographically robust systems currently employ 1024-bit or larger numbers. However, increasing key size cannot be indefinite, as it prolongs encryption times and slows down data transmission.

Shor's algorithm is a quantum algorithm that performs factorization of large numbers in polynomial time, unlike classical methods, which require exponential time (Shor, 1997). This algorithm acts as a "cryptographic breaker." RSA relies on the complexity of this task for its security; thus, if quantum computers achieve sufficient power, they could easily derive private keys from public ones, rendering RSA entirely vulnerable.

The compromise of long-term data involves copying and storing intercepted data, even if quantum computers have not yet broken cryptographic algorithms. Attackers may already be collecting encrypted data today to decrypt it in the future when quantum technologies become widely accessible.

Considering all of the above, the most pressing issue in protecting information from quantum computer attacks is the problem of data compromise.

2. Objective of the Study

The primary problem under consideration is data compromise, i.e., situations where confidential information becomes publicly accessible due to leakage, interception, or unauthorized access. In the modern digital world, this can involve personal data (e.g., credit card passwords or passport details) as well as corporate, banking, or governmental information.

Compromise is particularly dangerous when it concerns long-term data. This means that even if data is encrypted using current algorithms at the time of transmission, its interception and subsequent storage by attackers could lead to potential exposure in the future, when numerous quantum computers surpassing classical von Neumann architecture machines in speed will operate globally. Encrypted records of bank transactions, medical records, or personal information protected today by RSA-2048 could become vulnerable in a few years due to advancements in quantum computing or improved cryptanalysis methods. Thus, while data may currently be protected, its long-term storage without regular updates to security mechanisms could result in serious issues.

3. Problem Statement

The most common and difficult-to-control factor is human error. Even the most complex and well-designed security systems are not immune to vulnerabilities like a password sticker attached to a monitor. Errors can also occur during implementation, as algorithms may be compromised due to implementation flaws or incorrect use of cryptographic libraries. This includes:

– Poor quality random number generation for key creation.
– Improper storage or transmission of cryptographic keys.
– Use of default security parameters that are easily predictable for attackers.

If credentials, passwords, and encryption keys are compromised, attackers gain immediate access

to previously encrypted information. The history of information security is replete with examples of master key breaches leading to extensive security violations. A notable example is the 2011 breach of DigiNotar, a Dutch certification authority, where hackers generated approximately 500 fake SSL certificates. This led to severe consequences, including a major man-in-the-middle attack on Gmail services, loss of DigiNotar's reputation, and eventual bankruptcy. Following this incident, Public Key Infrastructure (PKI) was reevaluated, and new protection mechanisms were implemented.

With the advent of new technologies like artificial intelligence (AI) and machine learning, the process of analyzing and extracting information has become significantly easier. Modern AI technologies enable faster and more accurate analysis of encrypted data, identifying patterns or minor deviations that can be exploited to attack cryptographic algorithms. Such systems can detect weaknesses in algorithm design, significantly increasing the risk of compromise. Additionally, many solutions rely on publicly available and widely used libraries, which can pose risks partly due to human factors. If a vulnerability is discovered in a popular cryptography library, it could jeopardize vast amounts of data protected by its tools.

3.1. Compromise identifiers (SIEM)

In MaxPatrol SIEM, there is functionality to check previously obtained events for the presence of indicators of compromise based on tabular lists. An indicator of compromise is a sign of suspicious activity or a malicious object within an organization's IT infrastructure; such signs may indicate an ongoing attack by adversaries. Indicators of compromise can include, for example, an IP address or domain name of a node where suspicious activity has been registered, or the hash value of a malicious file.

– To search for indicators of compromise in events, a task must be created to check events using one of the profiles of the "batcheventsearch" module. Standard profiles have been created for checking events based on data from reputational tabular lists:

– IOC search for IP addresses – for checking against IP addresses from the "repListIP" tabular list.

– IOC search for URLs – for checking against addresses or domain names from the "repListMasks" tabular list.

– IOC search for domain names – for checking against domain names from the "repListDomains" tabular list.

– IOC search for hash values – for checking against file checksum values from the "repListHashes" tabular list.

Based on these standard profiles, custom profiles can be created. Typically, a SIEM system is deployed over the protected information system and has an architecture of "data sources" → "data storage" "application server" (Figure 1).

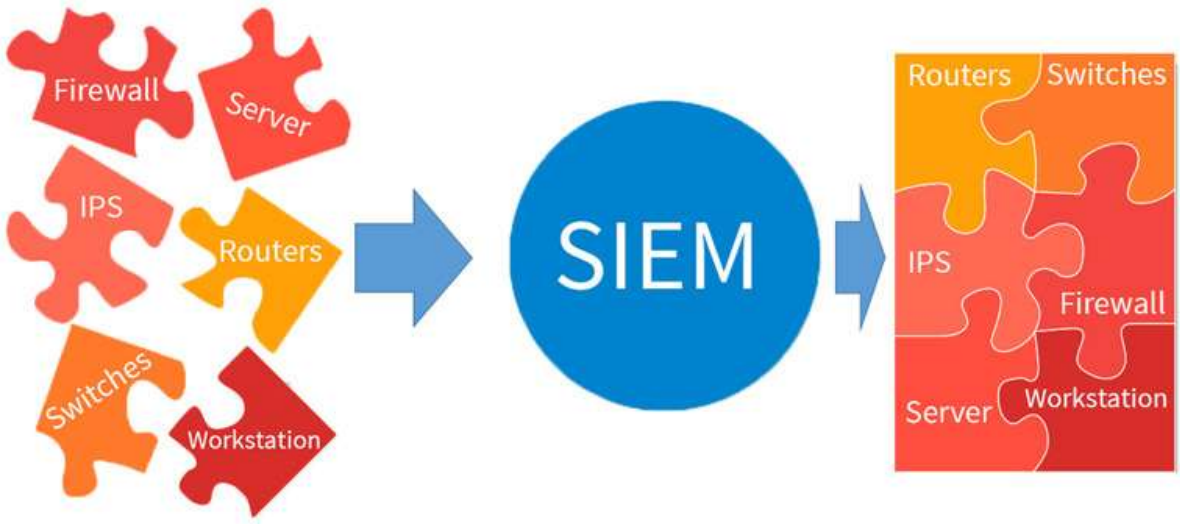

Fig. 1. SIEM-system

3.2. Indicators of Compromise (XDR)

Extended Detection and Response (XDR) is a multi-layered security technology that protects

IT infrastructure. This is achieved by collecting and correlating data from multiple security layers, including endpoints, applications, email, cloud environments, and networks, providing greater transparency into the organization's technological environment. This allows security teams to quickly and effectively detect, investigate, and respond to cyber threats.

XDR is considered a more advanced version of Endpoint Detection and Response (EDR). While EDR focuses on endpoints, XDR takes a broader approach, focusing on multiple security control points to detect threats faster through deep analytics and automation (Figure 2).

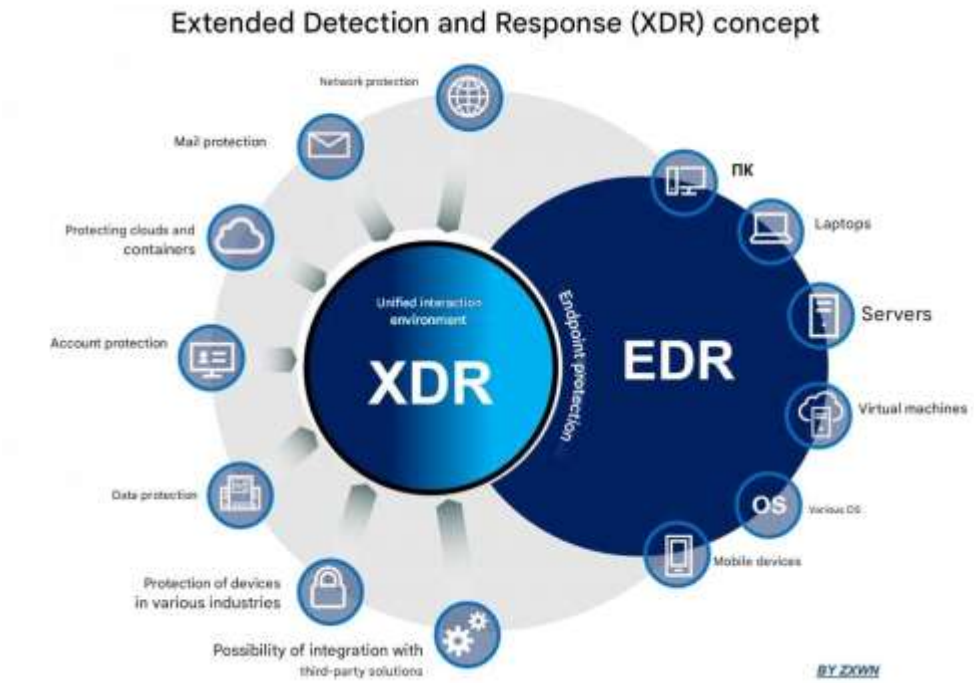

Fig. 2. XDR Conception

3.3. Key Indicators of Compromise

Key indicators of compromise serve as warning signs that an attack has been attempted, is ongoing, or has already occurred. Below are some of the main indicators:

3.1. Traffic Anomalies

Most organizations have a certain "profile" of normal network traffic. This profile reflects the expected behavior of users, applications, and services. For example, employees might typically transfer a specific amount of data during working hours. An indicator of compromise could be a sudden increase in outgoing traffic at night or connections to external IP addresses outside the trusted group. Such events may indicate data leakage or the presence of malware transmitting information to a control server.

3.2. Unusual Login Attempts

User work habits are generally predictable. They log in from specific geographic locations, during certain hours, and from the same devices. However, suspicious actions include:

– Attempting to log in at night if the user usually works during the day.

– Logging in from an IP address belonging to another country.

– Multiple failed login attempts for a single account, indicating a possible brute-force password attack.

3.3. Privileged Account Anomalies

Accounts with elevated privileges (e.g., administrator accounts) are prime targets for attackers because they provide access to sensitive data and critical systems. Signs that administrator rights are compromised include:

– Attempts to change access levels.

– Logins by administrators from unusual devices.

– Actions inconsistent with the user's usual responsibilities, such as mass deletion of data.

To protect privileged accounts, organizations implement Privileged Access Management (PAM) systems, multi-factor authentication, and action monitoring logs.

3.4. System Configuration Changes

Changes in system configurations may indicate the presence of malicious code, especially if:
– Security services or antivirus software have been disabled.
– Remote access has been enabled.
– Firewall settings have been altered.

Such actions are often performed during the early stages of an attack to prepare the infrastructure for exploitation.

3.5. Unexpected Software Installation or Updates

The sudden appearance of new software without IT approval may indicate an attempt at compromise. This type of software can appear due to employee negligence or phishing attacks. Examples of malicious software activity include
– The appearance of new executable files.
– Changes in startup processes.
– Installed services mimicking system services.

3.6. Multiple Requests for a Single File

If numerous accesses to the same file occur within a short time frame, this may indicate an attempt to bypass access restrictions or preparation for data theft.

To detect indicators of compromise, signs of digital attacks are recorded in log files. In cybersecurity practices utilizing IoCs, teams regularly monitor digital systems for suspicious activity. Modern SIEM and XDR solutions simplify this process using AI and machine learning algorithms, which establish baseline metrics for normal operations within an organization and then alert the team to anomalies. Additionally, it is important to educate employees who are not part of the security team, as they may receive suspicious emails or accidentally download infected files. Effective security training programs help employees better identify compromised emails and provide them with ways to report anomalies (Schöffel, 2021).

3.7. Solution Methods

Indicators of compromise (IoC) based on artificial intelligence (AI) allow for the detection of cyberattacks at early stages by analyzing not only static data but also behavioral patterns. Therefore, the problem of constructing a neural network for classifying threats based on Windows Security logs is highly relevant.

The illustration below demonstrates how the neural network will be trained based on data obtained from Windows Security logs, where the neural network learns from a CSV file derived from a security report.

The initial data for the program to classify threat logs is a CSV table containing the following fields (Figure 3. Part of the logs):
– Keywords,
– Date and time,
– Source,
– Event ID,
– Task category,
– Description/additional information.

Fig. 3. Part of the logs

Next, the data must be transformed for loading into the neural network:
– Removing rows with missing values,
– Processing CSV/text: accounting for comma-separated errors, merging columns,
– Encoding "EventID" values into classes 1, 2, and 3 based on severity.
Part of the code for label encoding and searching is shown in (Figure 4. Part of the code for labels).

```
# ============================
# 3. Assigning threat labels based on EventID
# ============================

# Example of mapping. Change it if necessary according to your requirements.
# Here:
# - 0: very dangerous
# - 1: you need to pay attention
# - 2: normal
mapping = {
    4624:2, # normal event
    4625: 0, # unsuccessful entry attempt is high-risk
    4648:1, # an attempt to log in with explicit authentication requires attention
    4672: 0, # privileged entry is very dangerous
    4720: 1, # account creation - requires attention
    4724:1, # password reset - requires attention
    4732: 1, # adding to a group requires attention
    4735:1, # group policy change - requires attention
    4738: 1 # Account change - requires attention
}

# Creating a new column with the threat label
df['ThreatLevel'] = df['Event_code'].map(mapping)
print("Example of threat labels:")
df[['Event_code', 'ThreatLevel']].shape
```

Fig. 4. Part of the code for labels

A neural network needs to be built for analysis and prediction based on network or personal computer logs to anticipate and predict attacks on devices or networks.
As the development environment, JupyterLab – an open-source integrated development environment – was chosen. The programming language and libraries used include:
– Python – a versatile programming language well-suited for big data analysis,
– Pandas – an analytical tool for big data analysis,
– Keras – a high-level library for building and training neural networks.
The choice of tool for the neural network was made based on an analysis of existing solutions for building neural networks (Table 1).

Table 1. Comparison of Libraries for Neural Networks

Name	Features	Language
TensorFlow	From Google, low-level, powerful, flexible. Used as a backend for Keras.	Python, C++
PyTorch	From Facebook, popular in academia, dynamic computation graph, flexible.	Python
Scikit-learn	Not for neural networks, but offers many ML models for classical tasks.	Python
MXNet	Supported by Amazon, cross-platform, scalable.	Python, R, Scala
JAX	From Google, optimized for acceleration and autodifferentiation.	Python

The Keras library was chosen due to its advantages, including:

– **Simplicity and ease of use**: Keras provides an intuitive API for rapid prototyping of neural networks, allowing developers and researchers to experiment with different model architectures easily.

– **Modularity**: Keras is organized into separate modules (layers, activation functions, loss functions, optimizers, etc.) that can be combined to create complex models, making the code more organized and maintainable.

– **Support for multiple backends**: Initially, Keras could operate on several computational engines (TensorFlow, Theano, CNTK). Currently, TensorFlow is the primary backend, ensuring broad support and integration with other tools in the TensorFlow ecosystem.

– **Large community and documentation**: Thanks to its extensive developer community and high-quality documentation, Keras has become a popular tool in both academic and industrial settings, facilitating the search for examples, templates, and support during model development.

– **Versatility**: With Keras, both simple models and complex deep learning architectures can be built for tasks such as classification, regression, image processing, text analysis, and more.

For building the neural network, the data is split into 80 % for training and 20 % for testing. The layers are then created as follows:

– **First Layer**: A fully connected (Dense) layer with 64 neurons and ReLU activation. The “input_dim” parameter specifies the number of features in the input vector. A Dropout layer with a probability of 0.3 randomly deactivates some neurons during training to prevent overfitting.

– **Second Layer**: A fully connected layer with 32 neurons and ReLU activation. Dropout is applied again.

– **Third Layer**: An additional layer with 16 neurons if a deeper network is required.

– **Output Layer**: Contains 3 neurons (corresponding to three threat classes). The softmax activation function converts output values into probabilities for each class.

The model is compiled with the Adam optimizer and the “sparse_categorical_crossentropy” loss function, suitable for multiclass classification tasks with integer labels.

Thus, a neural network has been constructed for training on prepared data to classify events by threat levels.

After all transformations, network training, and data classification, the built system distributes and outputs the results for convenient analysis by specialists. The program saves the obtained data in separate files, including:

– Training model graphs,

– Accuracy levels for each class,

– Overall model accuracy,

– Confusion matrix,

– Comparison with previous training iterations, showing how the neural network improved or changed.

On the graph below, we observe successful predictions by the neural network (Figure 5. Training Graph).

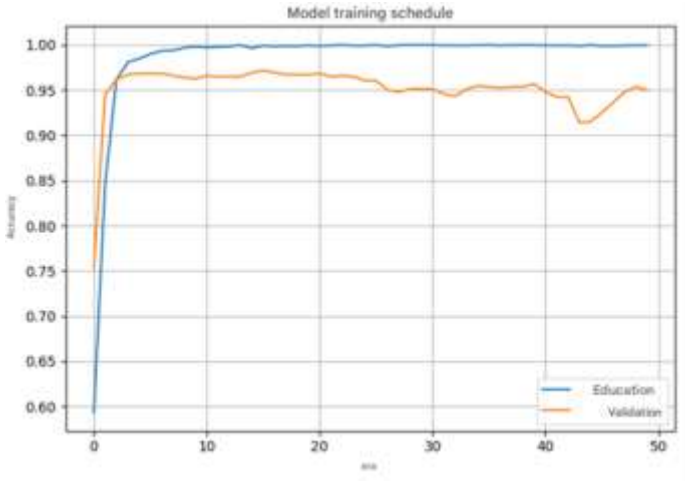

Fig. 5. Training Model Graph

In the screenshot below, we see accuracy on the test set, followed by precision, recall, F1-score, and the number of objects per class (Figure 6. Accuracy Table).

Точность на тестовой выборке: 0.9466

	precision	recall	f1-score	support
0	1.00	0.95	0.98	532
1	0.16	0.85	0.27	13
2	1.00	0.94	0.97	559
accuracy			0.95	1104
macro avg	0.72	0.91	0.74	1104
weighted avg	0.99	0.95	0.96	1104

Fig. 6. Accuracy Table

In Figure 7, the confusion matrix by classes is presented. For example, for class 0, 507 were correctly predicted, 25 were confused with class 1, and 0 were confused with class 2.

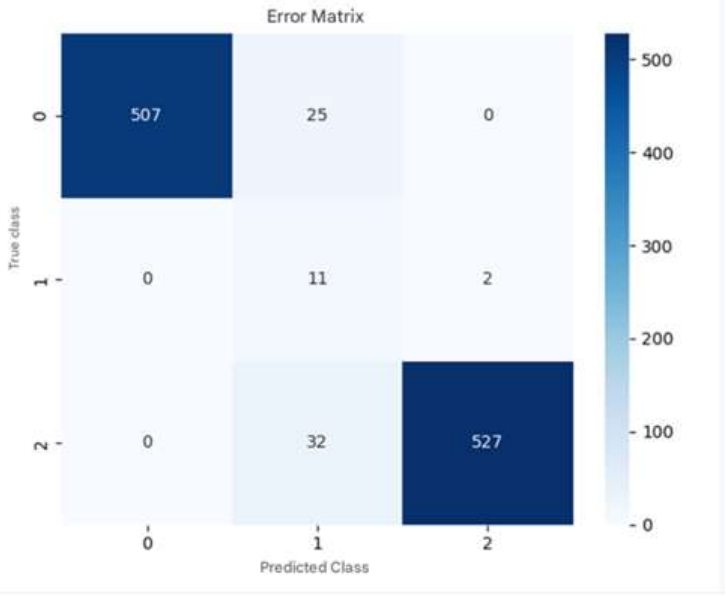

Fig. 7. Confusion Matrix

In Figure 8, a comparison with the previous model is shown. As seen, the new iteration did not improve compared to the previous model.

📊 Comparison with the previous model:
test accuracy: 0.4819 ↓ (-0.4647)
Test loss: 1.1260 ↓ (0.4641)
Accuracy: 0.5317 ↓ (-0.4565)
Completeness: 0.4819 ↓ (-0.4647)
f1 dimension: 0.4669 ↓ (-0.4971)

Fig. 8. Comparison with the Previous Model

4. Results

Thus, a neural network-based system for assessing and classifying security incidents based on Windows logs has been implemented programmatically. The system evaluates the potential

danger of each event and qualifies it into one of three classes with a probability of over 90 %. The remaining percentage represents potentially unclassified errors and threats, ensuring automation of analysis and threat detection. This system is a step toward building an automated protection system for computer networks and/or personal computers against attacks (Davydov et al., 2020; Li, 2017; Markley, 2014).

Through the creation of this program, the convenience of analyzing and predicting potential attacks on a network/computer has also been demonstrated.

To ensure security in the era of quantum computing (Hidary, 2019), quantum-resistant algorithms such as lattice-based algorithms (e.g., NTRU), Goppa codes, and isogeny-based elliptic curve systems must be used. These algorithms are considered sufficiently robust even against quantum computers (Hao, 2018). Additionally, further directions for implementing quantum-resistant algorithms are being developed, including:

– **Lattice-based cryptography**: Utilizes the complexity of finding the shortest vector in a lattice. Examples include NTRUEncrypt and Kyber.

– **Code-based cryptography**: Based on the difficulty of decoding random linear codes. A notable example is the McEliece algorithm.

– **Multivariate polynomial cryptography**: Relies on solving systems of nonlinear polynomials, such as Rainbow and GeMSS.

– **Quantum-secure cryptographic hash functions and protocols**, such as ring and supercode cryptography, offering new approaches to data protection.

These algorithms are in the process of standardization, and their implementation will help secure data in the post-quantum era.

5. Conclusion

Although quantum computers threaten many existing cryptographic systems, algorithms resistant to quantum attacks are continually being refined. These algorithms are being developed within the framework of post-quantum cryptography and are based on mathematical problems that cannot be efficiently solved even by quantum computers.

The analysis shows that while classical algorithms continue to provide the necessary level of security under von Neumann architecture, they face long-term threats from quantum attacks. This is particularly relevant for "harvest now, decrypt later" scenarios, where attackers copy encrypted information with the intention of decrypting it in the future. In this context, protecting long-term data becomes critically important.

The practical outcome of this work is the creation of a prototype system for intelligent analysis of Windows security logs using a neural network for threat classification. This demonstrates the potential of integrating machine learning methods into modern information security and data compromise monitoring systems.

Finalizing, the development of quantum technologies necessitates a reevaluation of existing approaches to information protection. The future of cryptography lies in the development of post-quantum algorithms, the implementation of hybrid cryptosystems, and the use of quantum cryptography. However, measures must already be taken today to protect long-term data by strengthening the implementation of cryptographic protocols, increasing key lengths, and introducing predictive threat analysis mechanisms.

References

Burlakovs et al., 2020 – *Burlakovs, J. Hogland, W., Vincevica-Gaile, Z., Kriipsalu, M.,Klavins, M., Jani, Y., Hendroko Setyobudi R., Bikse, J., Rud, V., Tamm, T.* (2020). Environmental Quality of Groundwater in Contaminated Areas—Challenges in Eastern Baltic Region. Water Resources Quality and Management in Baltic Sea Countries. Negm, A., Zelenakova, M., Kubiak-Wójcicka, K. (eds). Springer Water. Springer, Cham. DOI: https://doi.org/10.1007/978-3-030-39701-2_4

Davydov et al., 2020 – *Davydov, R.V., Rud, V.Yu. and Yushkova, V.V.* (2020). On the possibility of analysis using the wavelet transform of the pulse waveform from the bloodstream. *J. Phys.: Conf. Ser.* 1695 012064 DOI: 10.1088/1742-6596/1695/1/012064

Dushkin, 2018 – *Dushkin, R.V.* (2018). Overview of the Current State of Quantum Technologies. *Computer Research and Modeling*. 10(2): 165-179. DOI: 10.20537/2076-7633-2018-10-2-165-179

Hao, 2018 – *Hao, Y., Xu, A.A.* (2018). Modified Extended Kalman Filter for a Two-Antenna GPS/INS Vehicular Navigation System. *Sensors*. 8: 3809.

Hidary, 2019 – *Hidary, J.D.* (2019). Quantum Computing: An Applied Approach. Springer International Publishing. Pp. 104-107.

INFARS, 2025 – INFARS. Post-Quantum Cryptography. 2025. [Electronic resource]. URL: https://infars.ru/blog/post-quantum-cryptography-kak-kvantovye-kompyutery-ugrozhayut-bezopasnosti-dannykh// (date of access: 03.05.2025).

Li, 2017 – *Li, T., Su, J., Liu, W., Corchado, J.M.* (2017). Approximate Gaussian conjugacy: Parametric recursive filtering under nonlinearity, multimodality, uncertainty, and constraint, and beyond. *Front. Inf. Technol. Electron. Eng*. 18: 1913-1939.

Markley, 2014 – *Markley, F.L., Crassidis, J.L.* (2014). Fundamentals of Spacecraft Attitude Determination and Control. Springer: New York, NY, USA.

Schöffel, 2021 – *Schöffel, M., Lauer, F., Rheinländer, C.C., Wehn, N.* (2021). On the Energy Costs of Post-Quantum KEMs in TLS-based Low-Power Secure IoT. Proceedings of the International Conference on Internet-of-Things Design and Implementation. Charlottesvle. VA, USA, 18–21 May. Pp. 158-168.

Shor, 1997 – *Shor, P.W.* (1997). Polynomial-Time Algorithms for Prime Factorization and Discrete Logarithms on a Quantum Computer. *SIAM J. Comput*. 26(5): 1484-1509.

Published in the USA
Biogeosystem Technique
Issued since 2014.
E-ISSN: 2413-7316
2025. 12(1): 25-35

DOI: 10.13187/bgt.2025.1.25
https://bgt.cherkasgu.press

Medico-Ecological Approaches to Plant Research

Artyom Kirakosyan [a], Astghik Sukiasyan [b, *], Alla Okolelova [c], Silva Gevorgyan [d], Tatiana Stratulat [e], Anahit Atoyants [f]

[a] Yerevan State Base Medical College, Yerevan, Armenia
[b] Institute of General and Inorganic Chemistry, National Academy of Sciences of the Republic of Armenia, Yerevan, Armenia
[c] Volgograd State Technical University, Volgograd, Russian Federation
[d] B-On Biotechnology Laboratory of the Foundation for Armenian Science and Technology of the Armenian National Agrarian University, Yerevan, Armenia
[e] National Institute of Applied Research in Agriculture and Veterinary Medicine, Chisinau, Republic of Moldova
[f] Research Institute of Biology at Yerevan State University, Yerevan, Armenia

Paper Review Summary:
Received: 2025, March 28
Received in revised form: 2025, April 18
Acceptance: 2025, April 26

Abstract

The primary task of environmental protection is to ensure the safety of territories and promote their sustainable development. At the same time, analysing the current ecological situation in a specific area, including identifying spatio-temporal changes within its boundaries, is a complex undertaking that requires an integrated approach. This article proposes methods that use annual and perennial plants as natural targets for analysing the accumulation and migration of potentially toxic elements in the soil. In this sense, studying plant ecotypes already adapted to specific growing conditions is of significant practical importance. To gain a complete understanding of current circumstances, the study compared the indicators of geoecological indices related to the accumulation and migration of potentially toxic elements in the soil with the antioxidant potential of plants and their bioaccumulate capacity is important to emphasise, as the accumulation of potentially toxic elements in plants is most influenced by their genotype. Primary and secondary metabolic processes also play a role in the process of peroxidation in lipid-containing structures that are sensitive to pH, temperature, and other physicochemical parameters. Therefore, the acquisition of quantitative and qualitative data on the movement of potentially toxic elements in the soil-plant system is essential for a reliable assessment of the degree of environmental pollution.

Keywords: plants, potentially toxic elements, environmental pollution, geo-ecological index.

* Corresponding author
E-mail addresses: sukiasyan.astghik@gmail.com (A. Sukiasyan)

1. Introduction

Conservation and rational use of biological and landscape diversity have become global priorities. However, scientific and technological progress and climate change have had an irreversible impact on ecosystems due to anthropogenic factors. In this context, significant changes have occurred in plant cover, primarily altering the endemic diversity of the region (Terschanski et al., 2024). The substantial descriptive material accumulated for most plants continues to serve as a valuable source for obtaining and using natural compounds that are of significant interest in medicine, veterinary medicine, biochemistry, and culinary studies, among others (Torosyan, 1983). In certain cases, this knowledge has been meticulously documented in historical scientific and applied works, which have served as a foundation for contemporary biological and clinical research (Khamkar et al., 2015).

Many nationalities have a unique collection of traditional plants that are endemic to their specific geographical locations. It is equally important to recognise that the use of such plants has consistently produced favourable results, thus validating their efficacy (Ekor, 2013). Here the tradition of the name of drug plants (DPs) has its origin. Numerous investigations on DPs, many of which were founded on subjective assessments of the plants' taste, smell and appearance, as well as on the spices, infusions, tinctures and other preparations derived from them. In some cases, this knowledge has been meticulously documented in historical scientific and applied works, which have served as a foundation for contemporary biological and clinical research (Petrovska, 2012). Integration of geo-ecological and biochemical studies is driven by the necessity to evaluate and predict the anthropogenic impact on the environment, to address one of the most significant fundamental ethno-geological challenges, namely the analysis of biologically active compounds found in plants. Armenia's landscape is notable for its pronounced relief features and vertical zonation, which can be defined by ten distinct climate and landscape regions. Consequently, this results in the formation of rich and unique plant diversity. The considerable biodiversity of the Armenian flora is attributable to a confluence of geographical, geological and topographical factors (Hayrapetyan, 2016).

Consequently, the study of plant ecotypes adapted to specific growth conditions is a pertinent research area. The aim of the presented work is to compare the antioxidant potential of plants with their bioaccumulation potential.

2. Materials and methods

The geographic coordinates for each sampling site are presented in Table 2. Soil sampling was conducted in accordance with the specified criteria, employing the envelope method as outlined by (43). All the elemental analysis of soil samples was conducted using a Termo Scientific™ Niton™ portable XRF analyzer and the geoaccumulation index and biomobility index were calculated using (Muller, 1981; Sukiasyan, 2018).

The concentrations of primary (diene conjugates) and secondary (malonic dialdehyde) oxidation products of lipid-containing structures of DPs extracts of diene conjugates and malonic dialdehyde were determined by the method of (Stalnaya, Garishvili, 1977). The antioxidant potential of corn (malonic dialdehyde, FRAP, polyphenol, flavonoids) was determined according to the protocol described in (Sukiasyan, 2016; Sukiasyan, 2019). The value of the redox potential was determined in DPs extracts by the potentiometric method using a potentiometer, measuring the electromotive force of the chain according to (Sumarukov, 1970).

Bioassay for determining the extent of clastogenicity in the contaminated soil is included in the International Programme for Monitoring and Testing of Environmental Contaminants (Mišík et al., 2019).

All experiments had up to 5 technical replicates. The data were statistically processed. The Student's t-criterion was used to process the results. The observed differences are statistically significant. The calculated values of the criterion were greater than the critical value at a significance level of $p < 0.05$.

3. Results and discussion

Nowadays, the forecasts are not encouraging and entail the destruction and transformation of many species of plants. In the context of anticipated changes in temperature and precipitation, a scenario of progressive upward displacement of landscape zones can be postulated (Figure 1).

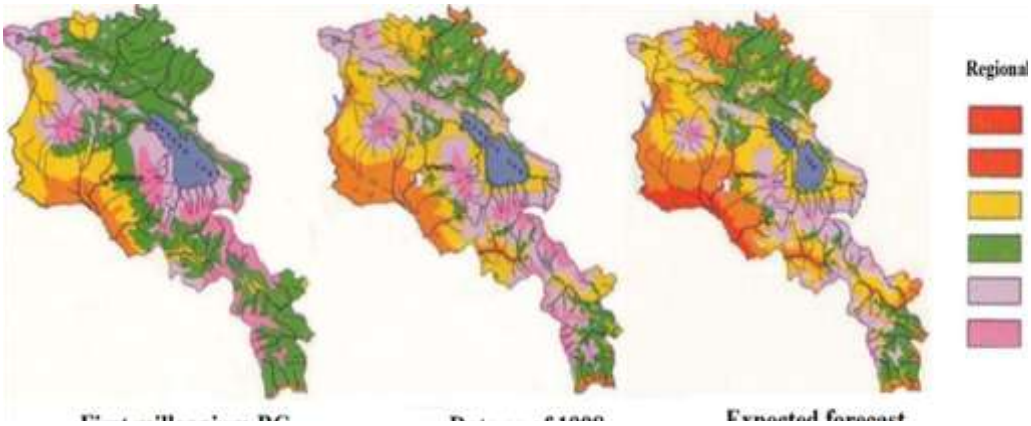

Fig. 1. Prognosis of dynamics of the spatial distribution of flora zones in Armenia
Source: Hayrapetyan, 2016

Recent years have seen rapid advancements in the field of biogeochemistry, with the development of novel methodologies including the use of plants for the monitoring of changes in the concentration of potentially toxic elements (PTEs) in soil. In this context, biochemical analysis of plant organism metabolism, particularly changes in antioxidant status, has been instrumental (Thalassinos et al., 2023; Sukiasyan et al., 2024).

Nevertheless, the response of secondary metabolite formation in plants to metal stress remains to be fully elucidated. It is imperative to acknowledge that a certain concentration pool of PTEs with variable valence is necessary also for plants as an example of a living organism (Figure 2). It is well established that such elements are actively involved in many metabolic processes that are integral to the growth and development of plants (Reshi et al., 2023).

Fig. 2. The borders of the concentration pool of potentially toxic elements with variable valency necessary for a living organism

Uncontrolled concentration changes of PTEs are one of the resulting factors responsible for biodiversity decline. However, to comprehensively comprehend the concentration fluctuations of PTEs within the environment, it is imperative to consider geochemical alterations to identify areas of potential risk and to differentiate between abiotic and anthropogenic contamination.

The external anthropogenic threat of environmental pollution is a significant concern for endemic plants, which are not evolutionarily equipped to cope with it. The concentration changes of PTEs in the trophic chain have become a critical issue, as these contaminants can accumulate and migrate in ecosystems via contaminated water, soil, and air (Vodyanitskii, 2008). Consequently, the study of PTEs in the environment, their levels in water, their accumulation in

soil, and their subsequent bioaccumulation in plants is a vital aspect of environmental risk assessment (Sukiasyan, Kirakosyan, 2024; Shtangeeva, 2022; Kaur et al., 2023).

Plants as a natural source of antioxidants. A significant proportion of DPs have been recognized as valuable sources of natural antioxidants for quite some time. The bioactive compounds present in these matrices have been shown to play a pivotal role in regulating speed of oxidative stress. Primary metabolism includes proteins, carbohydrates, fats, vitamins, organic acids, and enzymes, while secondary metabolism consists of alkaloids, phenolic compounds, terpenes, and terpenoids. For example, phenolic compounds, which include tannins, flavonoids and phenolic acids, are a constant source of antioxidant potential in these plants, scavenging free radicals and thereby inhibiting lipid peroxidation (LPO) (Halliwell, Gutteridge, 2015). In addition, tannins have been shown to be superior to phenolic acids in tests of LPO activity (Dorman, Deans, 2000). Conversely, the antioxidant activity (AOA) of plant flavonoids depends on their concentration and type (Manach et al., 2004). The synergistic effect of carnosic acid and other diterpenes has been shown to enhance AOA in lipid-containing structures (Wang et al., 2023). The synergistic effect of mixtures of many plants has been shown to enhance antioxidant efficacy, providing insight into their therapeutic potential (Bahadori et al., 2015; Krzyżek et al., 2023). A distinction is made between primary and secondary metabolism, which are sensitive to pH value, temperature, and other physical and chemical parameters (Table 1).

Table 1. Antioxidant potential of plant extracts depending on their thermal treatment

Plant species	Malondialdehyde. nmol		Diene conjugates. µmol		Eh		rH	
	A	B	A	B	A	B	A	B
Quercus robur L.	4.1±0.5	8.3±0.7	1.52±0.02	1.19±0.03	+347±17	+354±19	20.41	19.34
Urtica dioica L.	8.3±0.8	9.3±0.7	1.78±0.04	1.55±0.03	+70±13	+93±11	17.43	17.76
Salvia officinalis L.	9.9±0.4	12.4±1.0	1.91±0.03	1.90±0.03	+115±14	+183±22	15.33	16.46
Hypericum perforatum L.	11.1±0.5	18.8±0.8	2.53±0.02	2.27±0.03	+264±16	+237±19	18.37	18.04
Chelidonium majus L.	13.1±0.9	13.69±0.9	2.86±0.03	2.27±0.03	+217±20	+200±21	18.37	17.61
Artemisia absinthium L.	21.1±0.9	15.9±1.04	2.86±0.03	2.15±0.02	+233+28	+213±14	18.23	17.36

Notes: A – fresh plant extract. B – hot treatment plant extract

The results of the redox potential (Eh) determination in fresh DPs extracts were positive for all samples (Table 1). The heat treatment of DPs extracts generally did not result in alterations to the Eh levels within the comparison series. The value of the redox potential is contingent on the acid-base environment, and the value of rH was calculated based on this premise, thus allowing for the elimination of the effect of pH. The values of rH for all DPs extracts fall within the range corresponding to the reduction potential of hydrogen (from 0 to 41). This finding is indicative of their antioxidant nature, given that hydrogen ions are the principal reducing agents in free radical oxidation processes.

Plants as bioindicators of contaminated soil. The degree of ecological safety of the environment is typically evaluated by comparing the existing changes with the level of permissible content of pollutants (Sukiasyan, 2018). The impact of PTEs as pollutants is twofold: firstly, they directly affect biodiversity, and secondly, they reduce the tolerance limits of plants, reducing resistance to natural factors (Milyutina et al., 2019; Ali et al., 2013; Bielen et al., 2013; Wuana, Okieimen, 2011). It has been established that an increase in abiotically derived background levels of PTEs is to be expected in response to intensified human activities, which will be compounded by alterations in the water balance of the environment (Bray et al., 2000). In case the river water quality remains tense, but the effect is weakening, since the coastal soil itself acts as a "natural filter" for plants growing in these areas (Sukiasyan, Pirumyan, 2018).

Genotoxic potential of plant use. The accumulation of PTEs in plants is also largely determined by their genotype, but they an excess affects the absorption of water from the soil, reducing the water content in the root system. The initiation of plant response mechanisms in response to the intake of PTEs occurs at the level of the root system (Rucinska-Sobkowiak, 2016; Pirumyan et al., 2011).

The sampling of endemic Artemisia plants was arranged according to the following defined criteria: slightly disturbed natural flora, with fairly uniform saturation, known geochemical and geological study of the region, a certain distance from large industrial centers. The following locations were sampled: Sevan town (site1); Fantan village near Hrazdan town (site 2); Yerevan botanical garden (site 3) and, as a control, soil from the greenhouse of Yerevan State University (site 4).

Thereafter, the concentration values for each of the elements in the plant samples and the corresponding growing soil were determined. Using the values obtained, the biological mobility index coefficient was calculated as follows. The results obtained are summarized in Table 2, which indicates that an index value of less than 1 suggests an increased content of PTE in the soil sample, and vice versa. In practical situations, the assessment of contamination is often difficult to carry out, which hinders the assessment of the toxicity and mutagenicity of potential environmental hazards. In this context, transgenic organisms have emerged as a particularly promising avenue of research (Atoyants et al., 2009). To determine the extent of clastogenicity in the contaminated soil samples in the soil-plant system, Tradescantia (clone 02) was studied as a model plant (Figure 3).

Fig. 3. General view of flowers of the model plant *Tradescantia (clone 02)*

The results of this study showed a significant increase in the frequency of pink cells (PC) in the soil samples compared to the control (Table 2). The elevated incidence of PC frequency observed in the soil samples from points 2 and 4 can be attributed to the elevated concentrations of certain PTEs (Cu, Zn, Pb) in it. It has been demonstrated that under the influence of solutions of Pb^{2+} and Zn^{2+} salts, along with an increase in PC, the frequency of colorless cells (CC) increases linearly.

Furthermore, it was established that ions of the same metals with different valences exhibit a pronounced divergence in mutation activity. Specifically, Cr^{6+} was found to enhance the frequency of recessive mutations by a factor of 1.5 in comparison with the trivalent chromium ion (Table 2).

For certain PTEs ions (Cr^{6+}, Ni^{2+}, As^{3+} and Cd^{3+}), patterns analogous to those previously identified in our research were observed (Huang et al., 2012; Kumar et al., 2015). In addition to the mutational disorders previously described, the treated Tradescantia clone 02 plants exhibited various types of morphological change. Of these, the most prevalent were dwarf and branched hairs (Sukiasyan et al., 2009).

Geo-ecological aspects of plant use. PTEs migration in the soil-plant system also depends on the vegetative cycle of plant growth and development. In soil, PTEs are initially adsorbed by fast reactions (lasting minutes to hours), followed by slow adsorption reactions (lasting days to months). Thereafter, they are redistributed into different chemical forms,

exhibiting excellent biodistribution, mobility, and toxicity. A comparative analysis revealed that annual plants accumulate Cu, Zn and Mo much more intensively than perennial plants. Conversely, a contrasting trend was observed for Pb, with perennial plants exhibiting a fivefold accumulation in comparison to annual plants.

This phenomenon can be attributed to the notion of an "ecological memory" in perennial plants, which refers to the capacity to accumulate pollutants in the growing area. In contrast to annual plants, the accumulation of PTEs in perennial plants is accompanied by their active participation in metabolic processes associated with growth and development throughout the entire growing period (Juc et al., 2006).

Table 2. Induction of clastogenic effects in sporogenic cells of *Tradescantia (clone 02)* in soil samples according to bioassay tests

Soil sampling		Biological mobility index				Genotoxicity analysis			
Site	Coordinates	Cu	Zn	Pb	Cr	Total quantity	Pink cells in stamen hairs (1000±m)	Colorless cells in stamen hairs (1000±m)	Stunted hairs (1000±m)
1	40°37'20.8" N, 44°57'33.5" E	1.26±0.03	0.14±0.01	2.50±0.13	1.97±0.08	15804	0.76±0.22*	2.53±0.4	2.66±0.41
2	40°24'02.9" N. 44°41'34.4" E	0.43±0.02	0.14±0.01	5.71±0.23	1.19±0.05	17204	1.51±0.3***	4.82±0.53	3.78±0.47
3	40°12'41.9" N. 44°33'31.6" E	0.73±0.03	0.12±0.01	0.04±0.002	0.09±0.002	14526	0.96±0.26**	5.44±0.61**	1.86±0.36
4	40°18'29.04" N, 44°52'65.07" E	Concentration of potential toxic elements in soil sample				15322	0.2±0.11	3.59±0.48	1,44±0,31
		2.9	65.2	0.2	4.2				

Notes: biological mobility index is the ratio of an element's concentration in a plant to its content in the soil; statistically significant difference compared to the control is indicated at * – p <0.05, ** – p <0.01, *** – p <0.001.

Conversely, annual plants can serve as bioindicators of soil pollution only within a specific growing season (Figure 4). The reaction of the plant itself to changes in the concentration of PTEs in the environment includes complex signal transduction, according to which PTEs bind to receptors of the plant plasma membrane, generating a stress signal (Yang et al., 2021). As is evidenced by research findings, there is a direct relationship between the study of endemic plants and the ecological condition of their growing region (Sukiasyan et al., 2024; Sukiasyan, 2019).

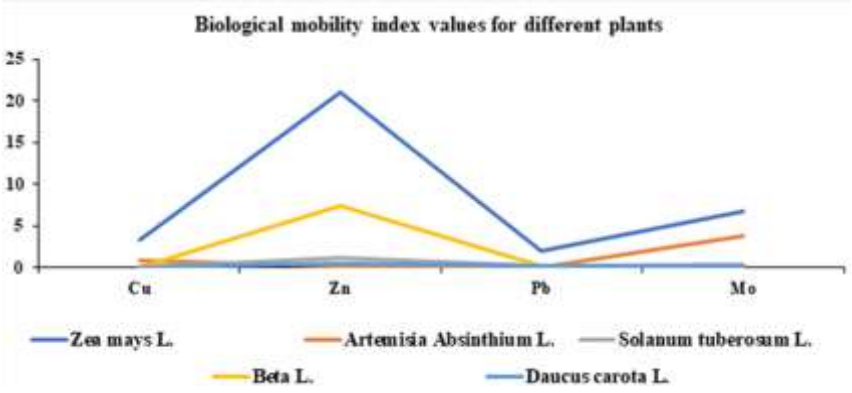

Fig. 4. Biological mobility index for annual and perennial different plant species

The following analysis, the changes in the concentration of TBA-active oxidation products in maize, was grown in the Tekhut and Shnogh regions. The results demonstrate that the plant samples harvested from Tekhut exhibited a 50 % increase in the parameter values compared to the control sample (Figure 5). When studying the samples from the Shnogh settlement, the changes in the malondialdehyde (MDA) value remained within the mean square. Samples of sweet maize from the Armenian population showed variation based on the area of growth, including the

concentration of iron in the soil cover (Sukiasyan, 2016). In addition, concentration changes in the reducted of low-molecular iron by antioxidants (ferric reducing/antioxidant power, FRAP (Benzie, Strain, 1996)) revealed that the level in the maize sample harvested from Tekhut was 2.4 times higher than in others. Polyphenols have been shown to possess strong antioxidant properties, which contribute to the regulation of free radicals within biological systems. Concurrently, flavonoids meticulously regulate the development of individual organs and the entire plant (Brunetti et al., 2023). As was also the case in previous cases, in this instance too, the concentration changes of polyphenols and flavonoids were the most significant in the comparison series (Figure 5) in the samples.

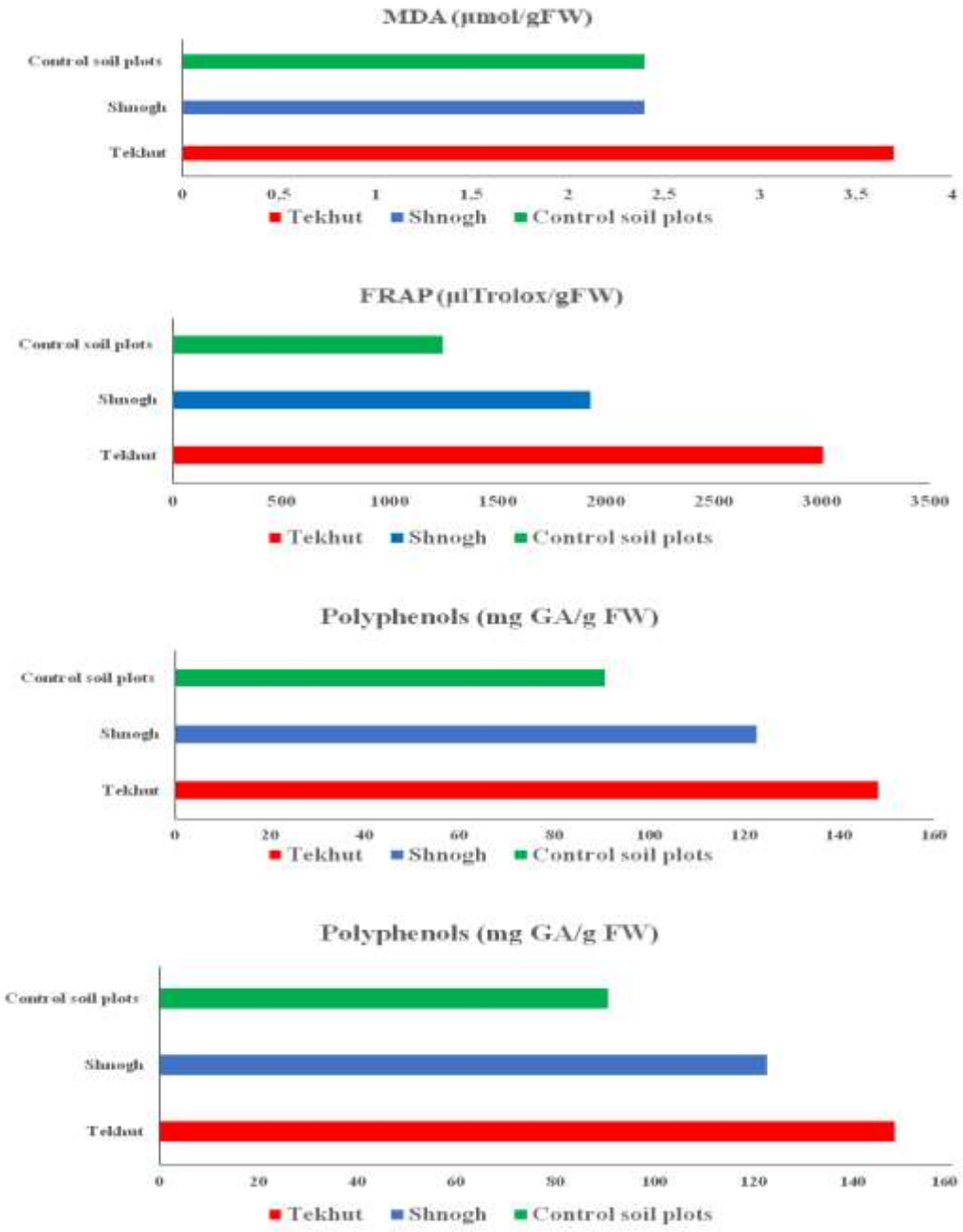

Fig. 5. Comparative analysis antioxidant indicators of samples of *Zea mays L.* plants from different soil-climatic regions of Armenia

The soil has a selective capacity to accumulate certain chemical elements, thereby inducing a change in their accumulation rate in the vegetation growing on it (Brunetti et al., 2023; Tangahu et al., 2011). The capacity of a plant to manifest bioindicative behavior, predicated on the content of PTE in the soil, will be predominantly contingent on the condition of the underlying soil itself (Palansooriya et al., 2000). Information about quantitative alterations in some PTEs within the

soil-plant system is imperative for identifying the level of environmental pollution. Numerical values of several PTEs were determined in soil samples and maize grains (Figure 6). Subsequently, the soils in which the plant is cultivated were classified by the geoaccumulation coefficient (I_{geo}).

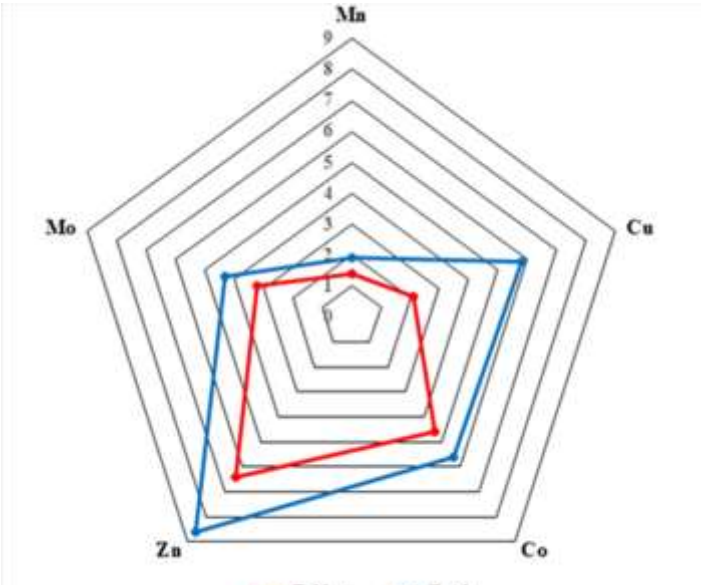

Fig. 6. The value of the geoaccumulation coefficient of some potential toxic elements

The analysis of soil samples from the Tekhut settlement revealed that they were slightly polluted with the concentration of Mo, Mn and Cu, but heavily polluted with Co and Zn. Furthermore, analysis of soil samples from Shnogh indicated their light pollution with manganese, and they were heavily polluted with molybdenum. Concurrently, these soil samples exhibited pronounced levels of copper, cobalt and zinc contamination.

4. Conclusion

The integration of endemic flora as a target indicator of environmental quality has the potential to facilitate the emergence of new types of ecological indicators. This interdisciplinary approach enabled the identification of correlations with respect to the cumulative activity of PTE based on the value of the geoaccumulation index and certain biochemical parameters of antioxidant potential. These parameters primarily depended on soil-climatic conditions and the degree of soil contamination on which the plants grew.

References

Ali et al., 2013 – *Ali, H., Khan, E., Sajad, M.A.* (2013). Phytoremediation of heavy metals-concepts and applications. *Chemosphere*. 91(7): 869-887.

Atoyants et al., 2009 – *Atoyants, A.L., Sukiasyan, A.R., Aghajanyan, E.A., Varzhapetyan, A.S., Avalyan, R.E., Harutyunyan, R.M.* (2009). Application of plant test objects: *Tradescantia* (Clone 02) and *Artemisia absinthium*, for assessment of soil genotoxicity and their pollution with heavy metals. *Biological Journal of Armenia*. 61(4): 51-56.

Bahadori et al., 2015 – *Bahadori, M. B., Valizadeh, H., Asghari, B., Dinparast, L., Farimani, M.M., Bahadori, Sh.* (2015). Chemical composition and antimicrobial, cytotoxicity, antioxidant and enzyme inhibitory activities of *Salvia spinosa* L. *Journal of Functional Foods*. 18(A): 727-736. DOI: https://doi.org/10.1016/j.jff.2015.09.011

Benzie, Strain, 1996 – *Benzie, I.F., Strain, J.J.* (1996). The ferric reducing ability of plasma (FRAP) as a measure of «antioxidant power»: the FRAP assay. *Analytical Biochemistry*. 239: 70-76.

Bielen et al., 2013 – *Bielen, A., Remans, T., Vangronsveld, J., Cuypers, A.* (2013). The influence of metal stress on the availability and redox state of ascorbate, and possible interference with its cellular functions. *International Journal of Molecular Sciences*. 14 (3): 6382-6413.

Bray et al., 2000 – *Bray, E.A., Bailey-Serres, J., Weretilnyk, E.* (2000). Responses to abiotic stress. Biochemistry & molecular biology of plants. In: *Gruissem, W. and Jones, R., Eds., American Society of Plant Physiologists*. Rockville. Pp. 1158-1203.

Brunetti et al., 2013 – *Brunetti, C., Di Ferdinando, M., Fini, A., Pollastri, S., Tattini, M.* (2013). Flavonoids as antioxidants in plants under abiotic stresses. *International Journal of Molecular Sciences*. 14(2): 3540-3555.

Dorman, Deans, 2000 – *Dorman, H.J., Deans, S.G.* (2000). Antimicrobial agents from plants: antibacterial activity of volatile oils. *Journal of Applied Microbiology*. 88(2): 308-316.

Ekor, 2013 – *Ekor, M.* (2013). The growing use of herbal medicines: issues relating to adverse reactions and challenges in monitoring safety. *Front pharmacol.* 4: 177. DOI: 10.3389/fphar.2013.00177

Fayvush, 2007 – *Fayvush, G.M.* (2007). Endemic plants of the flora of Armenia. *Collection of scientific papers. Flora, vegetation and plant resources. Takhtajaniya*. 16: 62-68.

Halliwell & Gutteridge, 2015 – *Halliwell, B., Gutteridge, J.M.C.* (2015). Free radicals in biology and medicine. Oxford University Press.

Hayrapetyan, 2016 – *Hayrapetyan, N.* (2016). The issue of preservation of plants on the verge of extinction in the territory of the RA. *Collection of scientific articles of YSU SSS Proceedings of the Annual Scientific Session of 2015*. Pp. 88-91.

Huang et al., 2012 – *Huang, T.L., Nguyen, Q.T.T., Fu, S.F., Lin, C.Y., Chen, Y.C., Huang, H.J.* (2012). Transcriptomic changes and signalling pathway induced by arsenic stress in rice roots. *Plant Mol. Biol.* 80: 587-608.

Juc et al., 2006 – *Juc, L., Bouvet, Y., Stratulat, T.* (2006). Pollution des sols moldaves par des pesticides organochlorés. *Environnement, Ingénierie & Développement*. 44: 1-4. DOI: https://doi.org/10.4267/dechets-sciences-techniques.2183

Kabata-Pendias, Pendias, 2001 – *Kabata-Pendias, A., Pendias, H.* (2001). Trace Metals in Soils and Plants, CRC Press, Boca Raton, Fla, USA, 2nd edition, 331 p.

Kaur et al., 2023 – *Kaur, H., Kaur, H., Kaur, H., Srivastava, S.* (2023). The beneficial roles of trace and ultra trace elements in plants. *Plant Growth Regulation*. 100: 219-236. DOI: https://doi.org/10.1007/s10725-022-00837-6.

Khamkar et al., 2015 – *Khamkar, A.D., Motghare, V.M., Deshpande, R.* (2015). Ethnopharmacology – A Novel Approach for Drug Discovery. *Indian J Pharm Pharmacol.* 2(4): 222-225.

Krzyżek et al., 2021 – *Krzyżek, P., Junka, A., Słupski, W., Dołowacka-Jóźwiak, A., Płachno, B Krzyżek, J., Sobiecka, A., Matkowski, A., Chodaczek, G., Płusa, T., Gościniak, G., Zielińska, S.* (2021). Antibiofilm and antimicrobial-enhancing activity of *Chelidonium majus* and *Corydalis cheilanthifolia* extracts against multidrug-resistant *Helicobacter pylori*. *Pathogens*. 10: 1033. DOI: https://doi.org/10.3390/pathogens10081033.

Kumar et al., 2015 – *Kumar, V., Singh, A., Mithra, S.V., Krishnamurthy, S.L., Parida, S.K., Jain, S., Tiwari, K.K., Kumar, P., Rao, A.R., Sharma, S.K., Khurana, J.P., Singh, N.K., Mohapatra, T.* (2015). Genome-wide association mapping of salinity tolerance in rice (Oryza sativa). *DNA research: an international journal for rapid publication of reports on genes and genomes*. 22(2):133-145. DOI: https://doi.org/10.1093/dnares/dsu046.

Manach et al., 2004 – *Manach, C., Scalbert, A., Morand, C., Rémésy, C., Jiménez, L.* (2004). Polyphenols: food sources and bioavailability. *The American journal of clinical nutrition*. 79(5): 727-747. DOI: https://doi.org/10.1093/ajcn/79.5.727

Milyutina et al., 2019 – *Milyutina, N., Osmolovskaya, N., Politaeva, N.* (2019). Migration of heavy metal in the soil-plant system in the territory adjacent to the MSW landfill. *2019 IOP Conf. Ser.: Earth Environ. Sci.* 403: 012166. DOI: 10.1088/1755-1315/403/1/012166

Mišík et al., 2019 – *Mišík, M., Pichler, C., Rainer, B., Nersesyan, A., Mišíková, K., Knasmueller, S.* (2019). Micronucleus assay with tetrad cells of Tradescantia. *In: Genotoxicity Assessment. Methods in Mol Biol.* (Eds A. Dhawan, M. Bajpayee), Humana Nev York. DOI: 10.1007/978-1-4939-9646-9_18; 9.

Muller, 1981 – *Muller, G.* (1981). Die Schwermetallbelstung der Sedimente des Neckars und seiner Nebenfl usse: eine estandsaufnahme. *Chemical Zeitung*. 105: 157-164.

Palansooriya et al., 2000 – *Palansooriya, K. N., Shaheen S.M., Chen, S.S., Tsang, D.C.W., Hashimoto, Y., Hou, D., Bolan, N. S., Rinklebe, J., Ok, Y.S.* (2000). Soil amendments for immobilization of potentially toxic elements in contaminated soils: A critical review. *Environment International*. 134: 105046. DOI: https://doi.org/10.1016/j.envint.2019.105046

Petrovska, 2012 – *Petrovska, B.B.* (2012). Historical review of medicinal plants' usage. *Pharmacognosy Rev*. 6(11):1-5. DOI: 10.4103/0973-7847.95849.

Pirumyan et al., 2011 – *Pirumyan, G.P., Vardumyan, L.E., Minasyan, S.G., Vardumyan, E.E.* (2011). Assessment of river water quality using the principal component analysis method. *Water: Chemistry and Ecology*. 11: 22-27. [Electronic resource]. URL: http://watchemec.ru/article/24228

Reshi et al., 2023 – *Reshi, Z.A., Ahmad, W., Lukatkin, A.S., Javed, S.B.* (2023). From Nature to Lab: A review of secondary metabolite biosynthetic pathways, environmental influences, and in vitro approaches. *Metabolites*. 13(8): 895. DOI: 10.3390/metabo13080895

Rucinska-Sobkowiak, 2016 – *Rucinska-Sobkowiak, R.* (2016). Water relations in plants subjected to heavy metal stresses. *Acta Physiol Plant*. 38: 257-269.

Shtangeeva, 2022 – *Shtangeeva, I.* (2022). Accumulation of scandium, cerium, europium, hafnium, and tantalum in oats and barley grown in soils that differ in their characteristics and level of contamination. *Environmental Science and Pollution Research*. 29(27): 40839-40853. DOI: https://doi.org/10.1007/s11356-021-18247-y.

Stalnaya, Garishvili, 1977 – *Stalnaya, I.D., Garishvili, T.G.* (1977). Modern methods in biochemistry. Moscow: Medicine: 66-68.

Sukiasyan, Kirakosyan, 2024 – *Sukiasyan, A.R., Kirakosyan, A.A.* (2024). Seasonal aspects of macro, trace, and ultra trace element changes in soils with different anthropogenic loads. *Sustainable Development of Mountain Territories*. 16(2): 789-802. DOI: https://doi.org/10.21177/1998-4502-2024-16-2-789-802

Sukiasyan, Pirumyan, 2018 – *Sukiasyan, A.R., Pirumyan, G.P.* (2018). Impact of heavy metals content in water and soil on the ecological stress of plants in different climatic zones of the Republic of Armenia. *Water and Ecology: Problems and Solutions*. 2(74): 87-94.

Sukiasyan et al., 2009 – *Sukiasyan, A.R., Atoyants, A.L., Tadevosyan, A.V., Shamiyan, A.G., Kirakosyan, A.A., Ambartsumyan, A.F., Aghajanyan, E.A.* (2009). Determination of the degree of soil pollution with heavy metals using a plant test object. *Bulletin of the Engineering Academy of Armenia*. 3(3): 457-460.

Sukiasyan et al., 2024 – *Sukiasyan, A.R., Kroyan, S.Z., Tovmaysan, S.V., Margaryan, A.A., Kirakosyan, A.* (2024). Comparative analysis of soil pollution in influence zone of cement plants. *MIAB. Mining Inf. Anal. Bull.* (12): 78-91. DOI: 10.25018/0236_1493_2024_12_0_78

Sukiasyan et al., 2024 – *Sukiasyan, A.R., Simonyan, G.S., Atoyants, A.L., Avalyan, R.E., Aghajanyan, E.A., Jhangiryan, T.A., Hunanyan, S.A., Kirakosyan, A.A.* (2024). Assessment of geochemical properties and genotoxicity of soils by macro-and trace elements contained in them. *Journal of Environmental Protection and Ecology*. 25(3): 785-800. [Electronic resource]. URL: https://scibulcom.net/en/article/DxaVqwfOJn6LupBveZxK

Sukiasyan, 2016 – *Sukiasyan, A.R.* (2016). Antioxidant capacity of maize corn under drought stress from the different zones of growing. *International Journal of Biological, Biomolecular, Agricultural, Food and Biotechnological Engineering*. 10(8): 413-416. DOI: 10.1999/1307-6892/10005083

Sukiasyan, 2018 – *Sukiasyan, A.R.* (2018). New approach to determining the environmental risk factor by the biogeochemical coefficients of heavy metals. *South of Russia: ecology, development*. 13(4): 108-118. DOI: 10.18470/1992-1098-2018-4-108-118

Sukiasyan, 2019 – *Sukiasyan, A.R.* (2019). Differential antioxidant response on drought by zones of the growth of maize leaves. *Chemistry of plant raw material*. 2: 169-177. DOI: 10.14258/jcprm.2019024458

Sumarukov, 1970 – *Sumarukov. G.V.* (1970). Oxidative equilibrium and radiosensitivity of organisms. *Atomizdat. Moscow*. P. 10.

Tangahu et al., 2011 – *Tangahu, B. V, Abdullah, S. R. S., Basri, H., Idris, M., Anuar, N., Mukhlisin, M.* (2011). A review on heavy metals (As, Pb, and Hg) uptake by plants through phytoremediation. *International Journal of Chemical Engineering*. 1-32: 939161

Terschanski et al., 2024 – *Terschanski, J., Nunes, M.H., Aalto, I., Pellikka, P., Wekesa, Ch., Maeda, E.E.* (2024). The role of vegetation structural diversity in regulating the microclimate of human-modified tropical ecosystems. *Journal of Environmental Management*. 360: 121128. DOI: https://doi.org/10.1016/j.jenvman.2024.121128

Thalassinos et al., 2023 – *Thalassinos, G., Petropoulos, S.A., Grammenou, A., Antoniadis, V.* (2023). Potentially toxic elements: A review on their soil behavior and plant attenuation mechanisms against their toxicity. *Agriculture*. 13(9): 1684. DOI: https://doi.org/10.3390/agriculture13091684

Torosyan, 1983 – *Torosyan A.A.* (1983). Drug plant of Armenia. Hayastan, Yerevan.

Vodyanitskii, 2008 – *Vodyanitskii, Y.N.* (2008). Heavy metals and metalloids in soils. GNU Soil Institute. V.V. Dokuchaev Russian Academy of Agricultural Sciences. M.

Wang et al., 2023 – *Wang, Y., Xie, X., Ran, X., Chou, S., Jiao, X., Li, E., Zhang, Q., Meng, X., Li, B.* (2018). Comparative analysis of the polyphenols profiles and the antioxidant and cytotoxicity properties of various blue honeysuckle varieties. *Open Chemistry*. 16(1): 637-646. DOI: https://doi.org/10.1515/chem-2018-0072

Wuana, Okieimen, 2011 – *Wuana, R.A., Okieimen, F.E.* (2011). Heavy metals in contaminated soils: a review of sources, chemistry, risks and best available strategies for remediation. *ISRN Ecology*. 2011: 1-21. DOI: 10.5402/2011/402647

Yang et al., 2021 – *Yang, X., Lu, M., Wang, Y., Wang, Y., Liu, Z., Chen, S.* (2021). Response mechanism of plants to drought stress. *Horticulturae*. 7: 50. DOI: https://doi.org/10.3390/horticulturae7030050

Published in the USA
Biogeosystem Technique
Issued since 2014.
E-ISSN: 2413-7316
2025. 12(1): 36-47

DOI: 10.13187/bgt.2025.1.36
https://bgt.cherkasgu.press

Sustainable Management of Saline Soils: Insights into Organic Amendments for Enhancing Soil Health and Crop Resilience

Abhishek Singh [a, *], Armine Chakhmakhchyan [a], Nare Darbinyan [a], Sakshi Singh [a], Ani Hayrapetyan [a], Rupesh Kumar Singh [b], João Ricardo Sousa [b], Derdzyan Tatevik [a], Hrant Khachatryan [a], Karen Ghazaryan [a]

[a] Faculty of Biology, Yerevan State University, Armenia
[b] Centro de Investigação E Tecnologias Agroambientais E Biológicas (CITAB), Universidade de Trás-Os-Montes E Alto Douro, Vila Real, Portugal

Paper Review Summary:
Received: 2024, November 8
Received in revised form: 2025, April 16
Acceptance: 2025, April 18

Abstract

Soil salinization, whether induced by nature or by humans, is an increasingly pressing global issue. This problem threatens agro-ecosystems since salt stress affects most farmed plants, reducing both the quality and amount of food produced. There have been a lot of new strategies and techniques developed in the last several years to help plants deal with salt stress and lessen its effects on crops. Unfortunately, not all of them are eco-friendly. That is why it is so important to find sustainable ways to improve soil production in salty environments without harming them in the long run. A lot more people are starting to pay attention to organic amendments like *vermi-compost (VC), vermi-wash (VW), biochar (BC), and bio-fertilizers (BF)*. The organic supplement lessens the effects of salt stress and boosts the development, growth, and harvest of crops. According various previous research on organic amendments after application of these organic products it enhances plant growth and yield, boost salt tolerance, and modify ionic balance, photosynthetic processes, antioxidant systems, and oxidative stress reduction. This review discusses recent studies on organic amendments in salt-stressed plants and their role in stress alleviation. The current assessment explores both existing and potential future applications of organic amendments.

Keywords: Soil salinization, organic amendments, biochar, vermicompost, vermiwash, bio-fertilizers.

1. Introduction

Worldwide agricultural soil salinity is a major abiotic factor which reducing crop growth, yield, and cultivatable land sustainability. Soil properties and feature is very important for crop cultivation and sustainable development of agriculture and soil health (Figure 1). Salt-damaged soils constitute more than three-quarters of the Earth land surface, affecting 424 million hectares of topsoil and 833 million hectares of subsoil (Mahajan, Tuteja, 2005). Salinity is a problem on a

* Corresponding author
E-mail addresses: sinxabishik@ysu.am (A. Singh), kghazaryan@ysu.am (K. Ghazaryan)

global scale, reducing crop yields (Celleri et al., 2022; Shahid et al., 2018). The situation is deteriorating annually, with 1.2 billion hectares of land already experiencing salinity-related issues. Moreover, the area of agricultural land affected by salinity is expanding by 10 million hectares each year. Salinity impacts plants by causing oxidative stress, osmotic stress, and ion toxicity and all these stresses created hinder in seedling growth and emergence (Balasubramaniam et al., 2023; Nikolić et al., 2023). The crops which grown in saline soil facing the problems related to photosynthetic system and inhibition of chlorophyll (chl) biosynthesis resulting in limitation or fully inhibition is show in photosynthesis process (Grattan, Grieve, 1998; Qin et al., 2010; Rahman et al., 2015; Yamane et al., 2012). High soils salinity also affected the plants nutrients absorption including nitrogen (N), phosphorus (P), potassium (K), and zinc (Zn). Because roots are essential for taking nutrients in, establishing a firm foundation, and sustaining symbiotic connections with rhizosphere microbes (Grattan, Grieve, 1998; Niste et al., 2014; Qin et al., 2010). Lowered metabolic processes, stunted plant development, and lowered agricultural yields were all results of nutrient deficiencies caused by salinity (Hu, Schmidhalter, 2005).

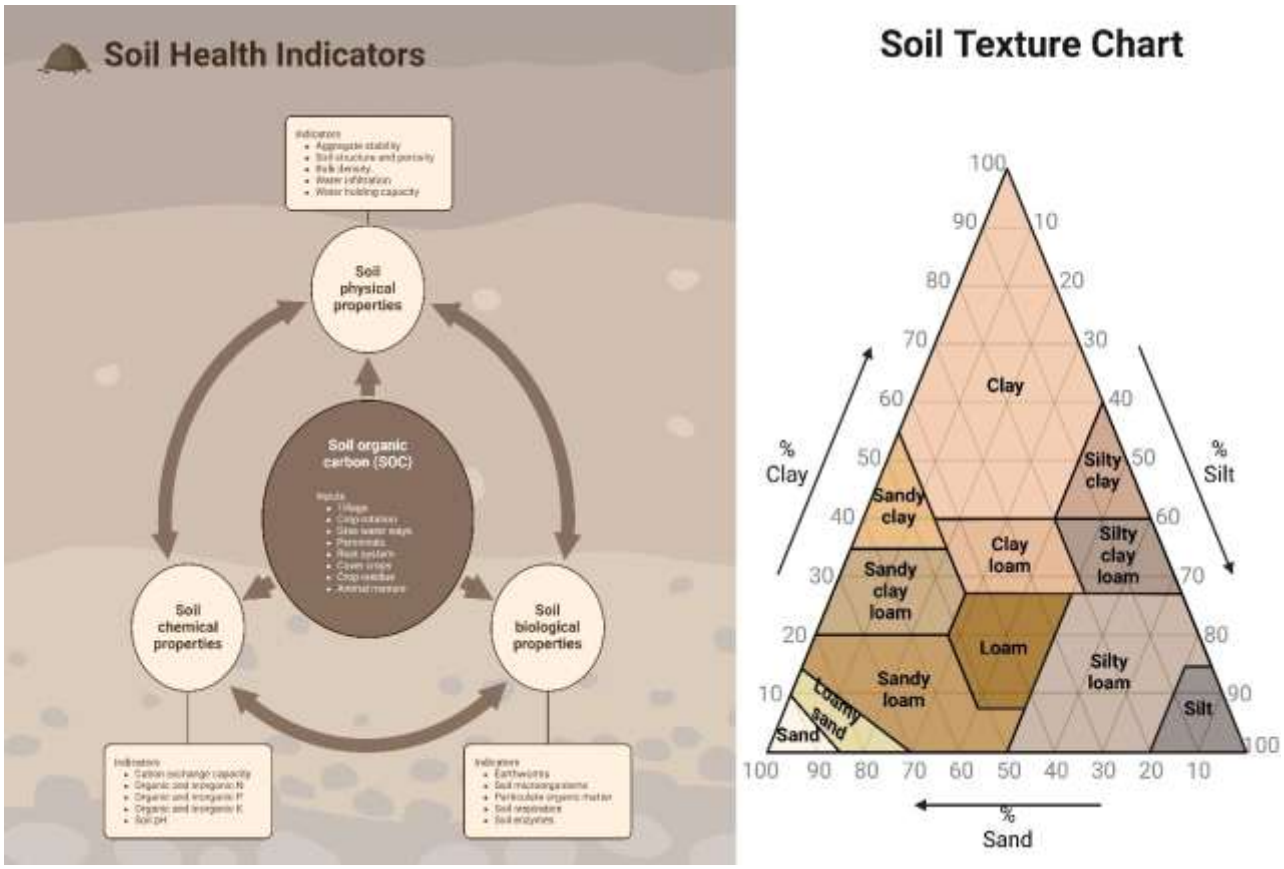

Fig. 1. Different types of soil with their feature

These inadequacies limited protein synthesis and carbon dioxide (CO_2) absorption (Hasana, Miyake, 2017). Various glycophytic crops, including rice, wheat, and maize, fail to achieve optimal yields when grown in saline soil conditions (Zheng et al., 2023). Modern agronomic practices such as *hydrophilic polymer, sulphur acids, green manuring, humic substance, farm yard manures, irrigation systems, salt-tolerant crops, salt scraping, seed bed preparation* and *sub-soiling* are some of the methods used by plant scientists to lower soil salinity levels (Meena et al., 2020; Shahid et al., 2018; Shilev, 2020). Many organic amendments, including *vermicompost (VC), vermiwash (VW), biochar (BC), plant growth promoting rhizobacteria (PGPR),* and biofertilizers (BF), have recently been utilized to reduce the detrimental effects of soil salinity (Ali et al., 2021; Hannan et al., 2020; Hoque et al., 2022; Imran et al., 2022; Kanwal et al., 2018). The main goal of this review paper is to find out how different organic amendments help plants deal with salt stress. In this review we also analysis that efficacy of organic amendments can help plants recover from salinity stress by restoring their morphophysiological and biochemical characteristics.

2. Results and discussion

Salinity Stress Impact on Soil and Plant Physio-Biochemical Properties

Impact on Soil Physio-Biochemical Properties

A high concentration of dissolved salts such sodium (Na^+), calcium (Ca^{2+}), potassium (K^+), magnesium (Mg^{2+}), chloride (Cl^-), sulphate (SO_4^{2-}), carbonate (CO_3^{2-}), and bicarbonate (HCO_3^-) are the defining characteristics of saline soils. Soils with an electrical conductivity (EC) above 4 dS m^{-1} at 25 °C are of this type. The permeability, structural stability, and bulk density of soil are all negatively impacted by an excess of Na^+ (Liu, She, 2017). Soil water retention and infiltration rates are both reduced as a result. Nitrogen (N_2) release in soil for plant growth is inhibited when salt concentrations are high because nitrifying bacteria are unable to carry out their work (Bai et al., 2012). When soil is too saline it inhibits respiration and enzyme activities. Soil enzyme activity, organic carbon (OC), and organic matter (OM) all get negatively impacted with higher EC under salinity stress (Sritongon et al., 2022).

Impact on Plants Physio-Biochemical Properties

The microbial activity in the rhizosphere controls the availability of nutrients which further reduces plant growth and production while under salt stress (Zhang et al., 2019). Salinity leads to osmotic stress, stunted shoot growth, and stomatal closure because Na^+ and Cl^- accumulate in the leaves, the site of photosynthesis (Singh et al., 2022; Singh et al., 2022). By accelerating chl breakdown, it also speeds up the aging of older leaves (Shivangi et al., 2024; Singh et al., 2023). Elevated Na^+ levels inside cells can hinder enzyme activity, leading to diminished water interactions, photosystem II (PS II), and CO_2 absorption in plants (Rajput et al., 2020). It has been found that foxtail millet shoot biomass can be reduced by 24-41 % and grain production by 7-30 % when exposed to salinity stress (Rajput et al., 2024; Rajput et al., 2024a; Singh et al., 2022). High salt levels reduce antioxidant activity, lead to lipid peroxidation, protein and nucleic acid denaturation, and an increase in reactive oxygen species (ROS), which in turn cause damage to cells (Singh et al., 2023).

Organic Amendments Based Salinity Stress Management

Biochar

Biochar is a substance that is produced when biomass is burned into charcoal. Biochar, a substance resembling charcoal produced through the pyrolysis of biomass waste under oxygen-restricted conditions for soil improvement (Lehmann et al., 2006), demonstrates potential in addressing salinization issues (Farhangi-Abriz, Torabian, 2017; Lashari et al., 2015; Lehmann et al., 2006; Sadegh-Zadeh et al., 2018a). It is rich in carbon and contains hydrogen, sulfur, oxygen, nitrogen, and minerals. C constitutes almost 70 % of its composition, with the rest varying based on the feedstock. Recent years have seen increased soil and crop production as a result of its positive environmental and economic effects. In addition to improving soil fertility (Yang et al., 2015), biochar modifies pH (Rasa et al., 2018), increases CEC (Yadav et al., 2019), sequesters carbon and increases phosphate availability (Saifullah et al., 2018). Furthermore, biochar improves the biological environment of the rhizosphere, which in turn increases soil enzyme activity and microbial development (Rasa et al., 2018; Yadav et al., 2019; Yang et al., 2015). It helps plants absorb nutrients easily and keeps them in the soil's micropores (Saifullah et al., 2018). Reduced oxidative stress from NaCl, reduced Na^+ adsorption ratios, and the replacement of Na^+ from exchangeable soil sites all work together to reduce salinity (Allen, 2007; Cheng et al., 2006; Rasa et al., 2018; Saifullah et al., 2018; Yadav et al., 2019). This potential is attributed to various mechanisms, including salt adsorption (Akhtar et al., 2015; Amini et al., 2015; Sadegh-Zadeh et al., 2018b) displacement of Na^+ from soil particle exchange sites (Amini et al., 2015; Sadegh-Zadeh et al., 2018b) lowering of the sodium adsorption ratio (Farhangi-Abriz, Torabian, 2017; Sadegh-Zadeh et al., 2018b), alleviation of NaCl-induced oxidative stress (Akhtar et al., 2015), and reduction of salt levels in plant seedlings (Zhang et al., 2019). Furthermore, biochar significantly enhances soil water retention capacity (Allen, 2007; Cheng et al., 2006). These properties suggest the possibility of soil desalination under altered water supply conditions. Nevertheless, biochar itself exhibits high salinity and sodicity (Lee et al., 2022; Sadegh-Zadeh et al., 2018a), particularly when produced from arid region biomass, which can contain approximately 2 and 25 times the salinity and sodium content, respectively, compared to humid region biochar (Yang et al., 2015). Additionally, the increased water holding capacity promotes soil moisture content, potentially leading to greater water loss through evaporation. The efficacy of using such a saline, sodic, and evaporation-enhancing material for managing salt-related issues under reduced water availability

requires further investigation. The study found that the combined application of biochar and jasmonic acid can improve salt stress tolerance in wheat (Alharbi, Alaklabi, 2022). The application of biochar and jasmonic acid reduced growth traits, nutrients, and leaf gas exchange traits under salt stress. The combination of biochar and jasmonic acid also enhanced antioxidant enzyme activities and glyoxylase system enzymes. The accumulation of osmolytes and secondary metabolites was more evident under joint biochar and jasmonic acid treatments. Another study also shows that the impact of biochar + Arbuscular mycorrhizal fungi (AMF) on maize plants under saline stress in a greenhouse. The results show that the combined application of biochar and AMF significantly improved maize growth under saline stress (Ndiate et al., 2021). The superior mitigating effect of biochar + AMF was attributed to its ability to improve soil nutrient content, plant nutrient uptake, antioxidant enzyme activities, and the contents of various acids (Ndiate et al., 2021). Similarly, another experiment explores the long-term effects of biochar amendment on saline soil in arid and semiarid regions (Yue et al., 2023). Using silage maize, biochar improved soil physical and chemical properties, leading to increased maize growth. However, the effect diminished over three years. This study also suggests that biochar is a promising soil amendment that can enhance maize growth in saline soil for at least three years, providing valuable insights for sustainable agricultural practices in salt-affected regions (Yue et al., 2023).

Three saline irrigations (0, 25, and 50 mm NaCl solutions) and two levels of biochar (0 % and 5 % W/W) treatments were applied to the potato plants from tuber bulking to harvesting (Akhtar et al., 2015). The ability of biochar to adsorb Na^+ was also investigated in an adsorption investigation. Biochar was found to be able to reduce salt stress by absorbing Na^+. Shoot biomass, root length and volume, tuber yield, photosynthetic rate (An), stomatal conductance (gs), and midday leaf water potential were all significantly reduced as salinity level increased. On the other hand, the quantity of abscisic acid (ABA) in both the xylem and leaf sap increased (Akhtar et al., 2015). As compared to the corresponding non-biochar control, biochar addition at each salinity level improved shoot biomass, root length and volume, tuber production, An, gs, midday leaf water potential, and reduced ABA concentration in the leaf and xylem sap. Biochar supplementation ameliorated salt stress in potato plants as evidenced by decreased Na^+, increased K^+ content in xylem, and a decrease in the Na^+/K^+ ratio. Based on the findings, biochar incorporation could be a great way to improve agricultural yields in soils damaged by salt.

Vermicompost, Vermiwash and Humic Acid

The solid byproduct of earthworm digestion of organic materials in an aerobic environment is called vermicompost (Figure 2). Thus, vermicompost is the result of a non-thermophilic biodegradation process including earthworms and microorganisms (Tammam et al., 2023). Humus, macro and microelements, and a diverse and active microbial community are abundant in this colorless, odorless byproduct of vermicomposting. Soil physical qualities, including texture, structure, and tilth, impact a land's agronomic potential; vermicompost promotes soil health, crop yield, and tilth. Root penetration, rooting volume, water availability, nutrient mobility and uptake, and aeration are all significantly affected by the physical qualities of the soil. A soil's cation exchange capacity and other chemical characteristics are significantly impacted by its texture. In order to improve soil aeration, maintain excellent soil aggregation, defend against soil erosion, and boost nutrient availability, it is highly useful to apply vermicompost to sandy soils. This is because it helps increase the soil organic matter composition. Plants benefit from the increased nutrient content found in vermicompost because it includes a variety of nutrients that plants need, including nitrogen, potassium, sulfur, sulfur dioxide, calcium, magnesium, iron, manganese, zinc, copper, and boron. To mitigate the detrimental effects of salt, numerous research have investigated the use of different organic fertilizers on plants (Tammam et al., 2023).

Vermiwash, a liquid biofertilizer derived from decomposed organic matter and earthworm secretions, enhances soil fertility and plant growth due to its nutrient-rich, biologically active composition. It contains auxins, cytokinins, potassium, and water-soluble nutrients like nitrogen, phosphorus, and potassium, along with beneficial microbes that reduce plant diseases and promote nutrient cycling. Environmentally friendly, it serves as a sustainable alternative to synthetic fertilizers, improving soil quality without harming wildlife or human health. Being liquid, it is easily absorbed when sprayed on leaves or applied to soil. It boosts soil microbial activity, increases organic matter and nutrient availability, promotes seed germination, root growth, and photosynthesis, and mitigates abiotic stressors such as salinity, drought, and heavy metal toxicity.

Humic acid (HA), considered a bio-stimulant, is believed to play a crucial role in enhancing

plant growth. Studies by Canellas and Olivares (2014) and Canellas et al. (2015) indicate that HA can stimulate plant development and improve resistance to abiotic stress by modifying primary and secondary metabolic processes associated with stress tolerance. The application of exogenous humic acid has been shown to boost plant growth, increase root and shoot dry weight, and elevate stress tolerance (Rose et al., 2014). Investigations have revealed that humic acid enhances cellular membrane stability, thereby facilitating water absorption, potassium uptake, protein and hormone synthesis, root cell elongation, and the production of non-enzymatic antioxidants linked to the shikimic pathway. It is proposed that humic acid supplementation enables plants to mount an enzymatic defense against salt stress (Çimrin et al., 2010). To mitigate the detrimental effects of salt stress and foster salt tolerance, humic acid may also stimulate root growth, alter mineral uptake, and reduce membrane damage (Canellas, Olivares, 2014; Canellas et al., 2015). Moreover, it is theorized that humic acid application can improve yield components in plants grown under salt stress conditions (Paksoy et al., 2010).

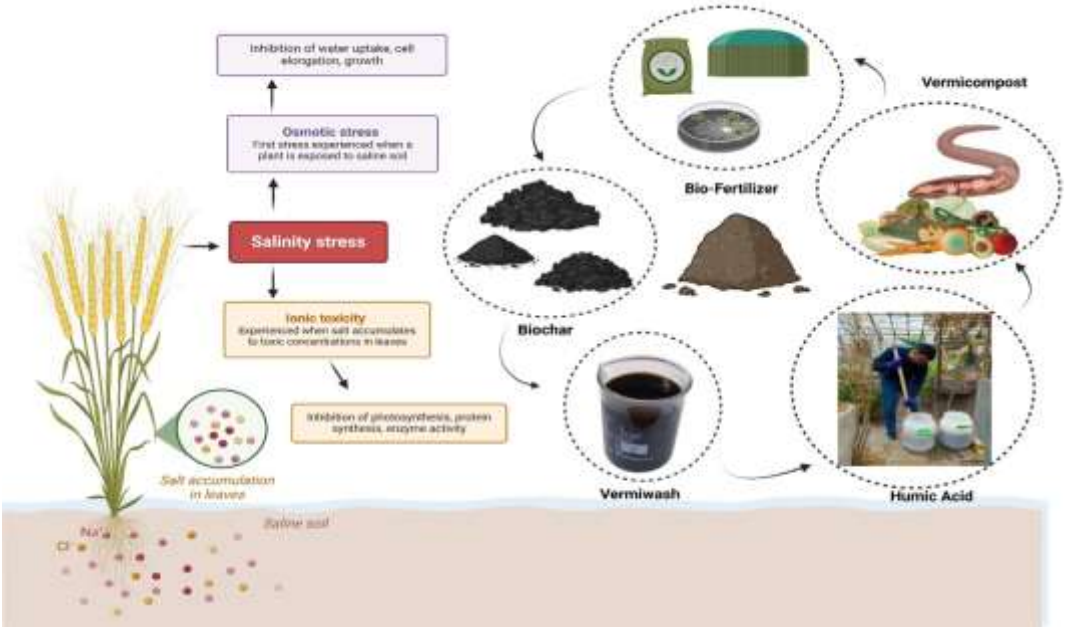

Fig. 2. Impact of salt stress and utilization of various organic amendments to mitigate salt stress effects on plants and improve soil health

Vermicompost and vermiwash mitigated the impact of salinity stress on *Solanum tuberosum* L. growth and tuber attributes in a central point design study with 15 treatments and three replicates (Pérez-Gómez et al., 2017). Physiological measurements, including height, stem diameter, fresh and dry weight, and tuber properties such as fresh weight, pH, electric conductivity, and °Brix, were assessed which improved after application of vermicompost and vermiwash. Optimal results were obtained with 580 g plant^{-1} vermicompost and 15 ml plant^{-1} vermiwash for plant height and stem diameter, while 860 g/plant vermicompost, 15 ml/plant vermiwash, and 15 mM salinity stress led to higher tuber pH and lower electrical conductivity (Pérez-Gómez et al., 2017). In another investigation show the impact of vermicompost on salinity tolerance in tomato plants (*Solanum lycopersicum* L., var. Firenze) through greenhouse pot experiments. Plants were grown on four substrates: a control "T" (100 % organic soil), a vermicompost treatment "Vc" (80 % organic soil + 20 % vermicompost), a compost treatment "C" (80 % organic soil + 20 % compost), and a mixture treatment "M" (80 % organic soil + 10 % vermicompost + 10 % compost). These groups were subjected to three NaCl concentrations (0, 50, and 150 mM) in a completely randomized block design. Plant responses to salinity stress were assessed via morphological (shoot length, stem diameter, leaf number, root length, shoot and root fresh and dry weight), physiological (Chla, Chlb, and carotenoid), and biochemical (malondialdehyde (MDA) and catalase (CAT)) parameters. Significant differences were observed among the four soil treatments. Plants on the Vc substrate exhibited enhanced growth and better salinity resistance. Organic matter (vermicompost, compost, and their mixture) positively influenced the measured parameters by gradually releasing minerals and providing soluble

nutrients, thereby mitigating abiotic stresses. Thus, vermicompost is a promising method for reducing salt stress in tomato plant growth, addressing challenges in cultivating crops in drier, saline environments (Bziouech et al., 2022). Vermicompost leachate (VCL) derived from earthworms is a potent biostimulant, but its hormonal impact on plants under salt stress remains unexplored. A study was conducted on *Solanum lycopersicum* L. plants grown in nutrient solution and exposed to 125 mM NaCl for a week, with or without VCL (18 mL.L^{-1}) (Benazzouk et al., 2020). The researchers examined mineral nutrition, hydration, and hormonal status in roots, young and old leaves, considering the phytohormone concentration in VCL. Plants treated with VCL exhibited improved growth and reduced Na^+ accumulation under salt stress. The treatment mitigated young leaf senescence by reducing ethylene production and increasing proline and anthocyanin levels. VCL contains high concentrations of salicylic acid, benzoic acid, and ACC, but low levels of jasmonates, cytokinins, and proline. In salt-stressed plants, VCL application did not enhance abscisic acid or ACC accumulation. However, it increased jasmonate levels and modified the cytokinin profile, promoting dihydrozeatin-types in older leaves and N6-(Δ2-isopentenyl) adenine-types in younger ones. The study concluded that VCL mitigates the impact of salinity on leaf senescence by influencing endogenous phytohormones rather than through passive absorption of exogenous hormones (Benazzouk et al., 2020).

In another study examines the use of humic fertilizer and vermicompost to mitigate salt-induced stress by influencing soil bacterial communities and aggregates during various growth stages of winter wheat (Liu et al., 2019). The research assessed soil salinity, aggregates, nutrient availability, soil bacterial community composition through next-generation high-throughput sequencing, and wheat yield. Findings revealed that both humic fertilizer and vermicompost effectively reduced salt accumulation in topsoil (by 16.8–41.1% and 13.3–42.7%, respectively) by hindering resalinisation and enhancing the proportion of soil macroaggregates (by 26.7–85.9% and 31.6–105.5%, respectively) throughout wheat growth stages. The predominant genera identified in the soil were *Skermanella, Arthrobacter* and *Sphingomonas*. Both treatments improved soil total N (by 4.7–15.6% and 2.4–25.2 %, respectively), available P (by 15.9 % and 7.3–64.4 %, respectively), and exchangeable K (by 3.9–18.4 % and 0.7–12.1 %, respectively) by boosting the abundance of *Arthrobacter* and *Pedobacter*. This subsequently led to increased shoot biomass (by 41.1 % and 52.8 %, respectively) and grain yield (by 45.1 % and 60.2 %, respectively) in wheat. In conclusion, vermicompost and humic fertilizer alleviate salt-induced stress in coastal saline soil through a comprehensive enhancement of soil physical, chemical, and biological properties. The impact of soil amendments (control, vermicompost, biochar, and vermicompost+biochar) on wheat plant growth and yield in saline sodic soil (Hafez et al., 2021). Results show that vermicompost improves wheat growth and yield, while biochar-treated plants have higher growth performance and yield. Vermicompost-biochar mixture application, followed by biochar as a singular application, leads to significant improvements in water content, chlorophyll content, stomatal conductance, cytotoxicity, leaf K^+ content, and nutrient uptake. The combination of vermicompost and biochar also eliminates the detrimental effects of soil salinity and water stress, enhancing crop production.

Crop development is hindered by irrigation, and salts found in all water sources can build up in soil and plants, preventing their full potential (dos Santos et al., 2019). One option to lessen the impact of salts on plants is to use vermicompost. In addition to enriching soil, this organic compost also provides plants with essential nutrients. The purpose of this study was to compare the effects of irrigation water salinity on noni (*Morinda citrifolia* L.) growth and chlorophyll levels in substrates that included and did not contain vermicompost. Three soil substrates (without humus, with 33.33 and 66.66 % of humus) were tested in a totally randomized design with a 4 × 3 factorial system, representing four levels of electrical conductivity of the irrigation water (0.5, 1.5, 3.0 and 4.5 dS m^{-1}) (dos Santos et al., 2019). Plant height, stem diameter, leaf count, chlorophyll index (a, b, and total) in leaves, and fresh and dry matter of shoots and roots were among the characteristics assessed three months after seedling germination. Regardless of the salinity of the irrigation water, substrates with humus improve the fertility and support the growth of noni plants; however, the beneficial effect diminishes as the electrical conductivity of the water intensifies, and the growth in height, stem diameter, biomass production, chlorophyll a, and total indexes is negatively affected by increasing salinity. The impact of vermicompost (V) on macro and micronutrients in lettuce (*Lactuca sativa* Var. crispa) under salt stress was observed that upregulated the cultivation of lettuce crop (Demir, Kıran, 2020). The experiment utilized various

salt stress levels: control (SS0) at 0 dS m^{-1} NaCl, medium stress (SS4) at 4 dS m^{-1} NaCl, and severe stress (SS8) at 8 dS m^{-1} NaCl. Vermicompost was applied at 0, 2.5 % (V1), and 5 % (V2) (w/w). Plants were cultivated in a greenhouse with controlled conditions (50-55 % relative humidity, 24/20 °C day/night temperature) for 46 days to facilitate nutrient assessment. Medium and severe salt stress increased N and Na concentrations whilst significantly reducing P, K, Mg, Fe, Mn, and Zn levels compared to the control. Vermicompost application decreased sodium concentration but substantially increased other mineral elements, with the most notable improvements observed at 5% V application. The SS x V interaction positively influenced N, P, Mg, Na, Fe, Mn, and Zn, whilst K, Ca, and Cu showed no statistically significant changes. The findings suggest that applying vermicompost in saline-affected areas may mitigate the detrimental effects of salt on plants and restore nutritional balance in lettuce cultivation (Demir, Kıran, 2020).

3.4. Bio-Fertilizer

A more sustainable agricultural practice can be advanced with the use of eco-friendly biofertilizers rather than chemical fertilizers (Olanrewaju et al., 2017). One definition of a biofertilizer is *"a substance which contains living microorganisms which, when applied to seed, plant surfaces, or soil, colonizes the rhizosphere or the interior of the plant and promotes growth by increasing the supply or availability of primary nutrients to the host plant"* (Vessey, 2003). These microbes are commonly known as plant-growth-promoting microbes (PGPM), plant-growth-promoting bacteria (PGPB), or plant-growth-promoting rhizobacteria (PGPR). In 1895, a product called *"Nitragin"* was introduced on the market. It contained rhizobium strains that could fix nitrogen (Soumare et al., 2020). To make soil phosphorus usable by plants, biofertilizers containing bacteria that dissolve phosphorus were first employed in the 1950s (Wang et al., 2020). Multiple studies have now demonstrated BF's capacity to enhance salt tolerance. Wheat seedlings exposed to BF exhibited improved growth and yield, with salt having a reduced impact due to increased chlorophyll levels and decreased proline content (Khalilzadeh et al., 2018; Mahmoud, 2008). A greenhouse experiment was conducted to investigate the effects of saline-irrigation water on okra plant growth and yield. The soil was irrigated with tap water, and biofertilizer Nitroben and ascorbic acid were applied. Results showed that salt stress reduced growth variables, but combined treatments of biofertilizer and ascorbic acid improved growth parameters. The best treatment was T11 (Soil + S2 (2.00 dSm^{-1}) + ascorbic acid (100 $mg.l^{-1}$) + biofertilizer), which increased total chlorophyll and ascorbic acid contents (Mahdy, Fathi, 2012). The study used microbial treatments, including *Cyanothece* sp. and *Enterobacter cloacae*, and nanomaterials like graphene, graphene oxide, and carbon nanotubes, in combination with biofertilizers at high salinity levels. Results showed that salinity stress inhibited growth, but microbial treatments reduced its effects, especially when combined with methyl salicylate. Smart use of nanomaterials could mitigate salinity inhibitory effect (El Semary et al., 2020). Salinity is a significant abiotic factor that affects safflower development and yield. A study found that zinc oxide nanoparticles (ZnO-NPs) and biofertilizer (BF) can improve salt tolerance in safflower plants (Yasmin et al., 2021). A ZnO-NP concentration of 17 mg L^{-1} was sufficient to protect safflower by increasing productivity, water content, and osmolyte levels. Coapplication of ZnO-NPs and Phytoguard protected plants from salinity stress by improving antioxidant enzyme activities and decreasing proline and malondialdehyde levels. The combined treatment improved agronomic parameters under salinity stress (Yasmin et al., 2021). Another study examined the impact of humic acid concentration and biofertilization treatments on olive seedlings grown under different levels of saline water. Results showed that salinity levels (2000 ppm) produced the highest significant parameters for olive seedlings, while salinity levels (4000 ppm) led to a decline in these parameters. Increasing humic acid levels from 0.5 to 1.5 ml L^{-1} significantly increased these parameters. Biofertilization treatments enhanced growth and plant biomass, with mixed treatments having a significant effect on seedling growth. The study recommends using humic acid (1.5 ml L^{-1} %) with biofertilizer treatments like *Mycorrhiza* and *Azotobacter chroococcum* to mitigate the negative impact of salinity on olive seedlings (El-Shazly, Ghieth, 2019). The agricultural sector in Indonesia faces a land shortage, necessitating the use of salinity-stressed land for plant growth. Amaranth, a popular vegetable is cultivated on this land. Biofertilizers, organic fertilizers containing beneficial bacteria, are used to ensure plant growth. This study showed that biofertilizer application increased the stem metaxylem diameter of amaranth plants in salinity-stressed environments. The application did not affect plant height or leaf count (Riesty, Siswanti, 2021).

Exploring the Potential and Limitations of Organic Amendments in Addressing Salinity Stress

Soil properties and plant growth in salt-affected environments are considerably impacted by

organic amendments. However, these techniques come with certain disadvantages, including increased demands on labour, time, space, and resources for their preparation. Moreover, some organic methods produce unpleasant odours and attract insects, whilst others generate harmful moulds and bacteria. Nevertheless, organic amendments have demonstrated effectiveness in mitigating agricultural constraints, such as salt stress. The detection and management of salinization can be enhanced through interdisciplinary approaches, including remote sensing, artificial intelligence, machine learning, and big data analysis. Additional studies are necessary to elucidate the morphological, physio-biochemical, transcriptomic, and proteomic aspects of organic amendment application in saline conditions to enhance crop yields.

3. Conclusion

Abiotic stressors, such as salinity, significantly reduce agricultural yields worldwide. These stressors cause cellular damage, inhibit growth, and affect plant morphology and biochemistry. However, biochar, vermicompost, vermiwash and bio-fertilizers can reduce these negative effects by promoting plant growth, increasing salt tolerance, and maintaining ionic homeostasis. Further research is needed to understand their molecular, biochemical, and physiological functions in salt stress-affected crops.

Ethics declarations

Ethics approval: Not applicable.

Consent to participate: Not applicable.

Consent for publication: The authors are willing to permit the Journal to publish the article.

Funding: Not applicable.

Competing Interests: The authors declare no competing interests.

Availability of data and materials: Not applicable.

4. Acknowledgements

AS expresses deep gratitude to Yerevan State University for its internal grant program (2024). KG conveys sincere appreciation to Yerevan State University for its internal grant program (2023).

References

Akhtar et al., 2015 – *Akhtar, S.S., Andersen, M.N., Liu, F.* (2015). Biochar Mitigates Salinity Stress in Potato. *Journal of Agronomy and Crop Science*. 201(5): 368-378. DOI: https://doi.org/10.1111/JAC.12132

Alharbi, Alalklabi, 2022 – *Alharbi, K., Alaklabi, A*. (2022). Alleviation of salinity induced growth and photosynthetic decline in wheat due to biochar and jasmonic acid application involves up-regulation of ascorbate-glutathione pathway, glyoxylase system and secondary metabolite accumulation. *Rhizosphere*. 24(100603). DOI: https://doi.org/10.1016/J.RHISPH.2022.100603

Ali et al., 2021 – *Ali, M., Kamran, M., Abbasi, G.H., Saleem, M.H., Ahmad, S., Parveen, A., Malik, Z., Afzal, S., Ahmar, S., Dawar, K.M., Ali, S., Alamri, S., Siddiqui, M.H., Akbar, R., Fahad, S.* (2021). Melatonin-Induced Salinity Tolerance by Ameliorating Osmotic and Oxidative Stress in the Seedlings of Two Tomato (Solanum lycopersicum L.) Cultivars. *Journal of Plant Growth Regulation*. 40(5): 2236-2248. DOI: https://doi.org/10.1007/S00344-020-10273-3

Allen, 2007 – *Allen, M.F.* (2007). Mycorrhizal Fungi: Highways for Water and Nutrients in Arid Soils. *Vadose Zone Journal*. 6(2): 291-297. DOI: https://doi.org/10.2136/VZJ2006.0068

Amini et al., 2015 – *Amini, S., Ghadiri, H. Chen, C., Marschner,* P. (2015). Salt-affected soils, reclamation, carbon dynamics, and biochar: a review. *Journal of Soils and Sediments*. 16(3): 939-953. DOI: https://doi.org/10.1007/S11368-015-1293-1

Bai et al., 2012 – *Bai, J., Gao, H., Xiao, R., Wang, J., Huang, C.* (2012). A Review of Soil Nitrogen Mineralization as Affected by Water and Salt in Coastal Wetlands: Issues and Methods. *CLEAN – Soil, Air, Water*. 40(10): 1099-1105. DOI: https://doi.org/10.1002/CLEN.201200055

Balasubramaniam et al., 2023 – *Balasubramaniam, T., Shen, G., Esmaeili, N., Zhang, H.* (2023). Plants' Response Mechanisms to Salinity Stress. *Plants*. 12: 2253. DOI: https://doi.org/10.3390/PLANTS12122253

Benazzouk et al., 2020 – *Benazzouk, S., Dobrev, P.I., Djazouli, Z.E., Motyka, V., Lutts, S.* (2020). Positive impact of vermicompost leachate on salt stress resistance in tomato (Solanum lycopersicum L.) at the seedling stage: a phytohormonal approach. *Plant and Soil*. 446(1–2): 145-162. DOI: https://doi.org/10.1007/S11104-019-04361-X

Bziouech et al., 2022 – *Bziouech, S.A., Dhen, N., Helaoui, S., Ammar, I.B., Al Mohandes Dridi, B.* (2022). Effect of vermicompost soil additive on growth performance, physiological and biochemical responses of tomato plants (Solanum lycopersicum L. var. Firenze) to salt stress. *Emirates Journal of Food and Agriculture*. 34(4): 316-328. DOI: https://doi.org/10.9755/EJFA.2022.V34.I4.2844

Canellas, Olivares, 2014 – *Canellas, L.P., Olivares, F.L.* (2014). Physiological responses to humic substances as plant growth promoter. *Chemical and Biological Technologies in Agriculture*. 1(1): 1-11. DOI: https://doi.org/10.1186/2196-5641-1-3/FIGURES/9

Canellas, Olivares, 2015 – *Canellas, L.P., Olivares, F.L., Aguia, N.O., Jones, D.L., Nebbioso, A., Mazzei, P., Piccolo, A.* (2015). Humic and fulvic acids as biostimulants in horticulture. *Scientia Horticulturae*. 196: 15-27. DOI: https://doi.org/10.1016/J.SCIENTA.2015.09.013

Celleri et al., 2022 – *Celleri, C., Pratolongo, P., Arena, M.* (2022). Spatial and temporal patterns of soil salinization in shallow groundwater environments of the Bahía Blanca estuary: Influence of topography and land use. *Land Degradation & Development*. 33(3): 470-483. DOI: https://doi.org/10.1002/LDR.4162

Cheng et al., 2006 – *Cheng, C.H., Lehmann, J., Thies Janice E., Burton, S.D., Engelhard, M.H.* (2006). Oxidation of black carbon by biotic and abiotic processes. *Organic Geochemistry*. 37(11): 1477-1488. DOI: https://doi.org/10.1016/J.ORGGEOCHEM.2006.06.022

Çimrin et al., 2010 – *Çimrin, K.M., Türkmen, Ö., Turan. M., Tuncer, B.* (2010). Phosphorus and humic acid application alleviate salinity stress of pepper seedling. *African Journal of Biotechnology*. 9(36): 5845-5851.

Demir, Kıran 2020 – *Demir, Z., Kıran, S.* (2020). Effect of Vermicompost on Macro and Micro Nutrients of Lettuce (Lactuca Sativa Var. Crispa) Under Salt Stress Conditions. *Kahramanmaraş Sütçü İmam Üniversitesi Tarım ve Doğa Dergisi*. 23(1): 33-43. DOI:https://doi.org/10.18016/KSUTARIMDOGA.VI.579695

Dos Santos et al., 2019 – *dos Santos, D.G., Diniz, B.L.M.T., Diniz Neto, M.A., Silva, J.H.C.S., de Oliveira Filho, W.N., Ferreira Filho, R.M.* (2019). Growth and chlorophyll in noni seedlings irrigated with saline water in substrate with vermicompost. *Revista Brasileira de Engenharia Agrícola e Ambiental*. 23(8): 586-590. DOI: https://doi.org/10.1590/1807-1929/AGRIAMBI.V23N8P586-590

El Semary et al., 2020 – *El Semary, N.A.H., Alouane, M.H.H., Nasr, O., Aldayel, M.F., Alhaweti, F.H., Ahmed, F.* (2020). Salinity Stress Mitigation Using Encapsulated Biofertilizers for Sustainable Agriculture. *Sustainability*. 12(21): 9218. DOI: https://doi.org/10.3390/SU12219218

El-Shazly, Ghieth, 2019 – *El-Shazly, M.M., Ghieth, W.M.* (2019). Effect of Some Biofertilizers and Humic Acid Application on Olive Seedlings Growth under Irrigation with Saline Water. *Alexandria Science Exchange Journal*. 40: 263-279. DOI: https://doi.org/10.21608/ ASEJAIQJSAE.2019.33657

Farhangi-Abriz, Torabian, 2017 – *Farhangi-Abriz, S., Torabian, S.* (2017). Antioxidant enzyme and osmotic adjustment changes in bean seedlings as affected by biochar under salt stress. *Ecotoxicology and Environmental Safety*. 137: 64-70. DOI: https://doi.org/10.1016/J.ECOENV.2016.11.029

Grattan, Grieve, 1998 – *Grattan, S.R., Grieve, C.M.* (1998). Salinity–mineral nutrient relations in horticultural crops. *Scientia Horticulturae*. 78(1–4): 127-157. DOI: https://doi.org/10.1016/S0304-4238(98)00192-7

Hafez et al., 2022 – *Hafez, E.M., Omara, A.E.D., Alhumaydhi, F.A., El-Esawi, M.A.* (2021). Minimizing hazard impacts of soil salinity and water stress on wheat plants by soil application of vermicompost and biochar. *Physiologia Plantarum*. 172(2): 587-602. DOI: https://doi.org/10.1111/PPL.13261

Hannan et al., 2022 – Hannan, A.H., Hoque, Md.N., Hassan, L., Robin, A.H.K. (2020). Adaptive Mechanisms of Root System of Rice for Withstanding Osmotic Stress. Recent Advances in Rice Research. *IntechOpen*. DOI: https://doi.org/10.5772/INTECHOPEN.93815

Hasana, Miyake, 2017 – *Hasana, R., Miyake, H.* (2017). Salinity Stress Alters Nutrient Uptake and Causes the Damage of Root and Leaf Anatomy in Maize. *KnE Life Sciences*. 3(4): 219. DOI: https://doi.org/10.18502/KLS.V3I4.708

Hoque et al., 2022 – *Hoque, Md.N., Hannan, A., Imran, S., Paul, N.C., Mondal, Md.F., Sadhin, Md.M.R., Bristi, J.M., Dola, F.S., Hanif, Md.A., Ye, W., Bretic, M., Rhaman, M.S.* (2022). Plant Growth-Promoting Rhizobacteria-Mediated Adaptive Responses of Plants Under Salinity Stress. *Journal of Plant Growth Regulation*. 42(3): 1307-1326. DOI: https://doi.org/10.1007/S00344-022-10633-1

Hu, Schmidhalter, 2005 – *Hu, Y., Schmidhalter, U.* (2005). Drought and salinity: A comparison of their effects on mineral nutrition of plants. *Journal of Plant Nutrition and Soil Science*. 168(4): 541-549. DOI: https://doi.org/10.1002/JPLN.200420516

Imran et al., 2022 – *Imran, S., Sarker, P., Hoque, Md.N., Paul, N.C., Mahamud, Md.A., Chakrobortty, J., Tahjib-Ul-Arif, Md., Hamed, A.A., Latef, A., Hasanuzzaman, M., Rhaman, M.S.* (2022). Biochar actions for the mitigation of plant abiotic stress. *Crop and Pasture Science*. 74: 6-20. DOI: https://doi.org/10.1071/CP21486

Kanwal et al., 2018 – *Kanwal, S., Ilyas, N., Shabir, S., Saeed, M., Gul, R., Zahoor, M., Batul, N., Mazhar, R.* (2018). Application of biochar in mitigation of negative effects of salinity stress in wheat (Triticum aestivum L.). *Journal of Plant Nutrition*. 41(4): 526-538. DOI: https://doi.org/10.1080/01904167.2017.1392568

Khalilzadeh et al., 2018 – *Khalilzadeh, R., Sharifi R.S., Jalilian, J.* (2018). Growth, physiological status, and yield of salt-stressed wheat (Triticum aestivum L.) plants affected by biofertilizer and cycocel applications. *Arid Land Research and Management*. 32(1): 71-90. DOI: https://doi.org/10.1080/15324982.2017.1378282

Lashari et al., 2015 – *Lashari, M.S., Ye, Y., Ji, H., Li, L., Kibue, G.W., Lu, H., Zheng, J., Pan, G.* (2015). Biochar–manure compost in conjunction with pyroligneous solution alleviated salt stress and improved leaf bioactivity of maize in a saline soil from central China: a 2-year field experiment. *Journal of the Science of Food and Agriculture*. 95(6): 1321-1327. DOI: https://doi.org/10.1002/JSFA.6825

Lee et al., 2022 – *Lee, X., Yang, F., Xing. Y., Huang, Y., Xu, L., Liu, Z., Holtzman, R., Kan, I., Li, Y., Zhang, L., Zhou, H.* (2022). Use of biochar to manage soil salts and water: Effects and mechanisms. *CATENA*. 211: 06018. DOI: https://doi.org/10.1016/J.CATENA.2022.106018

Lehmann et al., 2006 – *Lehmann, J., Gaunt, J., Rondon, M.* (2006). Bio-char sequestration in terrestrial ecosystems - A review. *Mitigation and Adaptation Strategies for Global Change*. 11(2): 403-427. DOI: https://doi.org/10.1007/S11027-005-9006-5/METRICS

Liu et al., 2019 – *Liu M., Wang, C., Wang, F., Xie. Y.* (2019). Vermicompost and humic fertilizer improve coastal saline soil by regulating soil aggregates and the bacterial community. *Archives of Agronomy and Soil Science*. 65(3): 281-293. DOI: https://doi.org/10.1080/03650340.2018.1498083

Liu, She, 2017 – *Liu, D., She, D.* (2017). Can rock fragment cover maintain soil and water for saline-sodic soil slopes under coastal reclamation? *CATENA*. 151: 213-224. DOI: https://doi.org/10.1016/J.CATENA.2016.12.020

Mahajan, Tuteja, 2005 – *Mahajan, S., Tuteja, N.* (2005). Cold, salinity and drought stresses: An overview. *Archives of Biochemistry and Biophysics*. 444(2): 139-158. DOI: https://doi.org/10.1016/j.abb.2005.10.018

Mahdy, Fathi, 2012 – *Mahdy, A.M., Fathi, N.O.* (2012). Interactive effects between biofertilizer and antioxidant on salinity mitigation and nutrition and yield of Okra plants (Abelmoschus esculentus L.). *Journal of Soil Sciences and Agricultural Engineering*. 3(2): 189-205. DOI: https://doi.org/10.21608/JSSAE.2012.53845

Mahmoud, 2008 – *Mahmoud, A.A.* (2008). Impact of biofertilizers application on improving wheat (Triticum aestivum L.) resistance to salinity. *Research J. of Basic and Applied Sci.* 4(5).

Meena et al., 2020 – *Meena, K.K., Bitla, U.M., Sorty, A.M., Singh, D.P., Gupta, V.K., Wakchaure, G.C. Kumar, S.* (2020). Mitigation of Salinity Stress in Wheat Seedlings Due to the Application of Phytohormone-Rich Culture Filtrate Extract of Methylotrophic Actinobacterium Nocardioides sp. NIMMe6. *Frontiers in Microbiology*. 11. DOI: https://doi.org/10.3389/FMICB.2020.02091

Ndiate et al., 2023 – *Ndiate, N.I., Saeed, Q., Haider, F.U., Liqun, C., Nkoh, J.N., Mustafa, A.* (2021). Co-Application of Biochar and Arbuscular mycorrhizal Fungi Improves Salinity Tolerance, Growth and Lipid Metabolism of Maize (Zea mays L.) in an Alkaline Soil. *Plants*. 10(11): 2490. DOI: https://doi.org/10.3390/PLANTS10112490

Nikolić et al., 2023 – *Nikolić, N., Ghirardelli, A., Schiavon, M., Masin, R.* (2023). Effects of the salinity-temperature interaction on seed germination and early seedling development: a comparative study of crop and weed species. *BMC Plant Biology*. 23(1). DOI: https://doi.org/10.1186/S12870-023-04465-8

Niste et al., 2014 – *Niste, M.G., Vidican, R., Rotar, I., Stoian, V., Pop, R., Miclea.* R. (2014). Plant Nutrition Affected by Soil Salinity and Response of Rhizobium Regarding the Nutrients Accumulation Ioan Rotar Plant Nutrition Affected by Soil Salinity and Response of Rhizobium

Regarding the Nutrients Accumulation. *ProEnvironment*. 7: 71-75. [Electronic resource]. URL: http://journals.usamvcluj.ro/index.php/promediu

Olanrewaju et al., 2017 – *Olanrewaju, O.S., Glick, B.R., Babalola, O.O.* (2017). Mechanisms of action of plant growth promoting bacteria. *World Journal of Microbiology and Biotechnology*. 33(197): 1-16. DOI: https://doi.org/10.1007/S11274-017-2364-9

Pérez-Gómez et al., 2017 – *Pérez-Gómez, J. de J., Abud-Archila, M., Villalobos-Maldonado, J.J., Enciso-Saenz, S., Hernández de León, H., Ruiz-Valdiviezo, V. M., Gutiérrez-Miceli, F.A.* (2017). Vermicompost and Vermiwash Minimized the Influence of Salinity Stress on Growth Parameters in Potato Plants. *Compost Science & Utilization*. 25(4): 282-287. DOI: https://doi.org/10.1080/1065657X.2017.1333932

Qin et al., 2010 – *Qin J., Dong W.Y., He K.N., Yu Y., Tan G.D., Han L., Dong, M., Zhang, Y.Y., Zhang, D., Li, A.Z., Wang Z.L.* (2010). NaCl salinity-induced changes in water status, ion contents and photosynthetic properties of Shepherdia argentea (Pursh) Nutt. seedlings. *Plant, Soil Environ*. 56(7): 325-332. DOI: https://doi.org/10.17221/209/2009-PSE

Rahman et al., 2015 – *Rahman, S., Matsumuro, T., Miyake, H., Takeoka, Y.* (2015). Salinity-Induced Ultrastructural Alterations in Leaf Cells of Rice (Oryza sativa L.). *Plant Production Science*. (4): 422-429. DOI: https://doi.org/10.1626/PPS.3.422

Rajput et al., 2024 – *Rajput, V.D., Singh, A., Ghazaryan, K., Minkina, T.M., Al-Tawaha, A.R.M.* (2024). Sustainable agriculture: Nanotechnology and biotechnology for crop production and protection. *Sustainable Agriculture: Nanotechnology and Biotechnology for Crop Production and Protection*. Pp. 1-492. DOI: https://doi.org/10.1515/9783111234694

Rajput et al., 2024a – *Rajput, V.D., Singh, A., Tomar, B., Minkina, T., Movsesyan, H.S., Elshikh, M.S., Chena, S-M., Singh, R.K., Ghazaryan, K.* (2024). Nanoparticle-Mediated Approaches in Agriculture Addressing Abiotic Stress From Soil to Plant Cells. *Nanotechnology Applications and Innovations for Improved Soil Health*. DOI: https://doi.org/10.4018/979-8-3693-1471-5.CH005

Rasa et al., 2018 – *Rasa, K., Heikkinen, J., Hannula, M., Arstila, K., Kulju, S., Hyväluoma, J.* (2018). How and why does willow biochar increase a clay soil water retention capacity? *Biomass and Bioenergy*. 119: 346-353. DOI: https://doi.org/10.1016/J.BIOMBIOE.2018.10.004

Riesty, Siswanti, 2014 – *Riesty, O.S., Siswanti D.U.* (2021). Effect of biofertilizer on growth and metaxylem diameter of Amaranthus tricolor L. in salinity stress condition. *Biogenesis: Jurnal Ilmiah Biologi*. 9(2): 178-188. DOI: https://doi.org/10.24252/BIO.V9I2.22232

Rose et al., 2014 – *Rose, M.T., Patti, A.F., Little, K., Brown, A., Jackson, R., Cavagnaro, T.R.* (2014). A Meta-Analysis and Review of Plant-Growth Response to Humic Substances: Practical Implications for Agriculture. *Advances in Agronomy*. 124: 37-89. DOI: https://doi.org/10.1016/B978-0-12-800138-7.00002-4

Sadegh et al., 2018 – *Sadegh-Zadeh, F., Parichehreh, M., Jalili, B., Bahmanyar, M.A.* (2018b). Rehabilitation of calcareous saline-sodic soil by means of biochars and acidified biochars. *Land Degradation & Development*. 29(10): 3262-3271. DOI: https://doi.org/10.1002/LDR.3079

Saifullah et al., 2018 – *Saifullah, Dahlawi, S., Naeem, A., Rengel, Z., Naidu, Z.* (2018). Biochar application for the remediation of salt-affected soils: Challenges and opportunities. Science of The Total Environment. 625: 320-335. DOI: https://doi.org/10.1016/J.SCITOTENV.2017.12.257

Shahid et al., 2018a – *Shahid, S.A., Zaman, M.., Heng, L.* (2018). Salinity and Sodicity Adaptation and Mitigation Options. Guideline for Salinity Assessment, Mitigation and Adaptation Using Nuclear and Related Techniques. Pp. 55-89. DOI: https://doi.org/10.1007/978-3-319-96190-3_3

Shilev, 2020 – *Shilev, S.* (2020). Plant-Growth-Promoting Bacteria Mitigating Soil Salinity Stress in Plants. *Applied Sciences*. 10(20): 7326. DOI: https://doi.org/10.3390/APP10207326

Singh et al., 2022 – *Singh, A., Sengar, R.S., Rajput, V.D., Minkina, T., Singh, R.K.* (2022). Zinc Oxide Nanoparticles Improve Salt Tolerance in Rice Seedlings by Improving Physiological and Biochemical Indices. *Agriculture*. 12(7): 1014. DOI: https://doi.org/10.3390/AGRICULTURE12071014

Singh et al., 2022a – *Singh, A., Sengar, R.S., Shahi, U.P., Rajput, V.D., Minkina, T., Ghazaryan, K.A.* (2022). Prominent Effects of Zinc Oxide Nanoparticles on Roots of Rice (Oryza sativa L.) Grown under Salinity Stress. *Stresses*. 3(1): 33-46. DOI: https://doi.org/10.3390/stresses3010004

Singh et al., 2023 – *Singh, A., Rajput, V.D., Sharma, R., Ghazaryan, K., Minkina, T.* (2023). Salinity stress and nanoparticles: Insights into antioxidative enzymatic resistance, signaling, and

defense mechanisms. *Environmental Research*. 235: 116585. DOI: https://doi.org/10.1016/J.ENVRES. 2023.116585

Singh et al., 2024 – *Shivangi, S., Singh, O., Shahi, U.P., Singh, P.K., Singh, A., Rajput, V., Ghazaryan, K.* (2024). Carbon Sequestration through Organic Amendments, Clay Mineralogy and Agronomic Practices: A Review. *Egyptian Journal of Soil Science*. 64(2): 581-598. DOI: https://doi.org/10.21608/EJSS.2024.260719.1707

Singh et al., 2024 – *Singh, A., Tomar, B., Margaryan, G., Rajput, P., Minkina, T., Mandzhieva, S., Elshikh, M.S., Chena, S-M., Singh, R.K., El-Ramady, H.R., Singh, A.K., Singh, O., Ghazaryan K.* (2024). Emerging Technologies for Sustainable Soil Management and Precision Farming. *Nanotechnology Applications and Innovations for Improved Soil Health:* 210-235. DOI: https://doi.org/10.4018/979-8-3693-1471-5.CH010

Soumare et al., 2020 – *Soumare, A., Diedhiou, A.G., Thuita, M., Hafidi, M., Ouhdouch, Y., Gopalakrishnan, S., Kouisni, L.* (2020). Exploiting Biological Nitrogen Fixation: A Route Towards a Sustainable Agriculture. *Plants*. 9(8): 1011. DOI: https://doi.org/10.3390/PLANTS9081011

Sritongon et al., 2022 – *Sritongon, N., Sarin, P., Theerakulpisut, P., Riddech, N.* (2022). The effect of salinity on soil chemical characteristics, enzyme activity and bacterial community composition in rice rhizospheres in Northeastern Thailand. *Scientific Reports*. 12(1): 1-12. DOI: https://doi.org/10.1038/s41598-022-24902-2

Tammam et al., 2023 – *Tammam, A.A., Shehata, M.R.A.S., Pessarakli, M., El-Aggan, W.H.* (2023). Vermicompost and its role in alleviation of salt stress in plants – I. Impact of vermicompost on growth and nutrient uptake of salt-stressed plants. *Journal of Plant Nutrition*. 46(7): 1446-1457. DOI: https://doi.org/10.1080/01904167.2022.2072741

Vessey, 2023 – *Vessey, J.K.* (2003). Plant growth promoting rhizobacteria as biofertilizers. *Plant and Soil*. 255(2): 571-586. DOI: https://doi.org/10.1023/A:1026037216893/METRICS

Wang et al., 2020 – *Wang, X.i, Xie, H., Ku, Y., Yang, X., Chen, Y., Yang, N., Cao, C.* (2020). Chemotaxis of Bacillus cereus YL6 and its colonization of Chinese cabbage seedlings. *Plant and Soil*. 447(1–2): 413-430. DOI: https://doi.org/10.1007/S11104-019-04344-Y

Yadav et al., 2019 – *Yadav, V., Karak, T, Singh, S., Singh, A.K., Khare, P.* (2019). Benefits of biochar over other organic amendments: Responses for plant productivity (Pelargonium graveolens L.) and nitrogen and phosphorus losses. *Industrial Crops and Products*. 131: 96-105. DOI: https://doi.org/10.1016/J.INDCROP.2019.01.045

Yamane et al., 2012 – *Yamane, K., Taniguchi, M., Miyake, H.* (2012). Salinity-induced subcellular accumulation of H 2O 2 in leaves of rice. *Protoplasma*. 249(2): 301-308. DOI: https://doi.org/10.1007/S00709-011-0280-7

Yang et al., 2015 – *Yang, F., LEE, X., Wang, B.* (2015). Characterization of biochars produced from seven biomasses grown in three different climate zones. *Chinese Journal of Geochemistry*. 34(4): 592-600. DOI: https://doi.org/10.1007/S11631-015-0072-4

Yasmin et al., 2021 – *Yasmin, H., Mazher, J., Azmat, A., Nosheen, A., Naz, R., Hassan, M.N., Ahmad, P.* (2021). Combined application of zinc oxide nanoparticles and biofertilizer to induce salt resistance in safflower by regulating ion homeostasis and antioxidant defence responses. *Ecotoxicology and Environmental Safety*. 218. DOI: https://doi.org/10.1016/J.ECOENV. 2021.112262

Yue et al., 2023 – *Yue, Y., Lin, Q., Li, G., Zhao, X., Chen, H.* (2023). Biochar Amends Saline Soil and Enhances Maize Growth: Three-Year Field Experiment Findings. *Agronomy*. 13(4): 1111. DOI: https://doi.org/10.3390/AGRONOMY13041111

Zhang et al., 2019 – *Zhang, J., Bai, Z., Huang, J., Hussain, S., Zhao, F., Zhu, C., Zhu, L., Cao, X., Jin, Q.* (2019). Biochar alleviated the salt stress of induced saline paddy soil and improved the biochemical characteristics of rice seedlings differing in salt tolerance. *Soil and Tillage Research*. 195: 104372. DOI: https://doi.org/10.1016/J.STILL.2019.104372

Zhang et al., 2019 – *Zhang, W-W., Wang, C., Xue, R., Wang, Li-J.* (2019). Effects of salinity on the soil microbial community and soil fertility. *Journal of Integrative Agriculture*. 18(6): 1360-1368. DOI: https://doi.org/10.1016/S2095-3119(18)62077-5

Zheng et al., 2023 – *Zheng, C., Liu, C., Liu, L., Tan, Y., Sheng, X., Yu, D., Sun, Z., Sun, X., Chen, J., Yuan, D., Duan, M.* (2023). Effect of salinity stress on rice yield and grain quality: A meta-analysis. *European Journal of Agronomy*. 144: 126765. DOI: https://doi.org/10.1016/J.EJA. 2023.126765

Published in the USA
Biogeosystem Technique
Issued since 2014.
E-ISSN: 2413-7316
2025. 12(1): 48-60

DOI: 10.13187/bgt.2025.1.48
https://bgt.cherkasgu.press

Assessment of Soil Erosion and Mitigation Strategies in Nghe An Province, Vietnam under Tropical Monsoon Conditions

Ha Thi Nguyen Thuy [a, *], Tamara S. Astarkhanova [b], Alla A. Okolelova [c], Van Tran Quang [d]

[a] School of Agriculture and Resources, Vinh University, Nghe An, Vietnam
[b] Agrarian Technological Institute, Patrice Lumumba Peoples' Friendship University of Russia, Moscow, Russian Federation
[c] Volgograd State Technical University, Russian Federation
[d] Tan Trao University, Tuyen Quang, Vietnam

Paper Review Summary:
Received: 2025, February 28
Received in revised form: 2025, April 15
Acceptance: 2025, April 26

Abstract

This study on soil erosion in Thanh Chuong, Nghe An Province (Vietnam) utilized GIS, remote sensing, and the RUSLE model to assess and quantify erosion dynamics. It was found that soil erosion is primarily influenced by the intensity and duration of monsoon rainfall, while the erosion resistance of landscapes is determined by factors such as slope, vegetation cover, and precipitation. High erosion rates were observed in areas where land use was mismatched with local agro-climatic conditions, leading to significant soil loss. The agroecological assessment revealed that 18 % of the study area experiences high to very high erosion, with an average annual soil loss of 25 T/ha. Erosion data were categorized based on three agricultural systems: tea and citrus cultivation along contour lines, annual crops on sloping lands, and perennial crops such as acacia and cassava. Using remote sensing and GIS, erosion was classified into five levels, ranging from very low to very high, while LS-Factor assessments from Landsat 8 images were divided into eight classes. To combat erosion, the study proposes several mitigation measures, including evaluating vegetation cover for anti-erosion efficiency, constructing trenches and embankments, creating terraced slopes, and optimizing agricultural and forestry practices through the SALT models for heavily eroded lands.

Keywords: soil erosion, RUSLE model, SALT model.

1. Introduction

Soil erosion is a critical exogenous geological process characterized by the detachment, transport, and deposition of soil particles due to hydrodynamic forces from surface water (water erosion) or aeolian activity (wind erosion or deflation). Its intensity is governed by soil properties, granulometric composition, vegetation cover, regional geomorphology, and land management practices (Aksoy, Kavvas, 2005). Globally, approximately 70 % of nations experience soil erosion and desertification, affecting 30 % of the continental landmass (Tian et al., 2008). In Vietnam,

* Corresponding author
E-mail addresses: hantt_dly@vinhuni.edu.vn (H. Thi Nguyen Thuy)

approximately 40 % of the national territory is subject to erosion, threatening agricultural productivity and socio-economic stability, particularly in East Asian nations such as Nepal, Malaysia, and Vietnam. Wischmeier and Smith identified topography, climate, soil characteristics, and anthropogenic influences as primary drivers of erosion (Le et al., 2022; Wischmeier, Smith, 1978).

Soil erosion leads to landscape degradation, water quality deterioration, and adverse socio-economic consequences (Golkarian et al., 2023). Unsustainable agricultural practices, deforestation, and climate change intensify its impacts (Adornado et al., 2009). In Vietnam's mountainous regions, agricultural activities on steep slopes (>25°) accelerate erosion, resulting in rapid soil depletion and a reduction in arable land (Committee T.C.D.P.s, 2021). Additionally, deforestation for artificial plantations, particularly acacia, exacerbates soil erosion. Research indicates that young acacia plantations are highly vulnerable due to insufficient vegetation cover, whereas mature plantations improve soil stability through extensive root networks. To promote sustainable development, the identification of erosion-prone areas is essential for implementing targeted mitigation measures (Yesuph, Dagnew, 2019). Nghe An Province, Vietnam, experiences a tropical monsoon climate, with annual precipitation ranging from 1,800 to 2,200 mm, and diverse topographical features (elevations from 10 m to 1,500 m). The interplay between land use, agricultural activities, and precipitation variability heightens erosion risks (Committee T.C.D.P.s, 2021). Soil erosion diminishes humus horizon thickness, agricultural output, and economic resilience, thereby exacerbating poverty and environmental degradation (Dung et al., 2020). Increased precipitation intensity further accelerates topsoil depletion and quality decline, while future land degradation is expected to escalate due to climate change and suboptimal land management practices. Implementing sustainable agricultural and forestry models is imperative to enhance socio-economic resilience and mitigate erosion. This study, conducted in Thanh Chuong District, Nghe An Province, Vietnam, evaluates the current soil erosion dynamics in a tropical monsoon environment.

2. Materials and methods

2.1. Meteorological and Geographical Conditions of the Study Area

The study area, Thanh Chuong District in Nghe An Province, spans approximately 1,228 km² and is located 45 km west of Vinh City (18°34'42"–18°53'33" N, 104°56'07"–105°36'06" E). It borders Anh Son and Do Luong districts (north), Huong Son district, Ha Tinh Province (south), Do Luong and Nam Dan districts (east), and Bolikhamxai Province, Laos (west).

The region experiences a tropical monsoon climate with distinct seasons: a hot, humid, and rainy summer (May–October) and a cooler, drier winter (November–April). Annual rainfall ranges from 1,800 to 2,200 mm, concentrated (85 %) between August and October. Relative humidity varies from 84 % to 86 %, with seasonal differences of 17–20 %. Annual evaporation is 700–940 mm. The average temperature is 23.5°C–24.5°C, peaking at 35°C–36°C in June–July and dropping to 13°C–14°C in December–February. Sunshine duration ranges from 1,500 to 1,700 hours per year. The district is influenced by the northeast monsoon (winter) and the southwest foehn wind (summer), which exacerbates drought and heat stress, impacting agriculture.

Geologically, the district comprises sedimentary, metamorphic, volcanic, and alluvial formations, with ferruginous soils dominating hilly regions and alluvial soils along river floodplains. The terrain transitions from low hills in the northeast to high mountains (900–1,026 m) in the southwest, including the Vu Tru range. The Ca River (375 km total length, 32 km within Thanh Chuong) and six other rivers provide abundant surface water. However, steep slopes, narrow river channels, and concentrated seasonal rainfall contribute to frequent floods, flash floods, and soil erosion.

2.2. Characteristics of Study Objects

To assess erosion intensity at study sites, spatio-temporal land use distribution maps were generated using Landsat (https://glovis.usgs.gov) and Sentinel (https://scihub.copernicus.eu) satellite imagery. High-resolution (30 m) image datasets spanning 2000–2021 were utilized (Appendix. Table S1).

Prior to classification, remote sensing images were preprocessed using ENVI software (version 4.7). To enhance accuracy and ensure comprehensive coverage of the study area, atmospheric correction was applied, aligning the vegetation spectral curve with real spectral reflectance. Additionally, image processing involved radiometric, atmospheric, geometric, and topographic corrections to improve data quality and analytical precision.

2.3. Land Use Spatio-Temporal Distribution Maps

Satellite Imagery. To achieve the objectives of this study, land use spatio-temporal distribution maps were generated using Landsat (https://glovis.usgs.gov) and Sentinel (https://scihub.copernicus.eu) satellite imagery. The datasets, with a spatial resolution of 30 m, were acquired for the period 2000–2021. Prior to classification, the images were processed using ENVI software (version 4.7). Atmospheric correction was applied to ensure the vegetation spectrum curve closely matched real vegetation spectra. Additional pre-processing steps included radiometric, atmospheric, geometric, and topographic corrections to enhance image accuracy.

GIS Data Utilization. The digital elevation model (DEM) dataset was selected using the grid referencing method to ensure spatial consistency across all resampled images. To enhance image quality, satellite data underwent atmospheric correction, and resolution was resampled from 30 m to 10 m. GIS-managed digital datasets were obtained from the Department of Natural Resources and Environment, including administrative maps, current land use maps, and soil maps.

Additional data sources included. Reports from the Department of Natural Resources and Environment of Nghe An Province, the Department of Agriculture and Rural Development of Nghe An Province, and the People's Committee of Thanh Chuong District. Statistical Yearbooks of Nghe An Province and Thanh Chuong District**.**

2.4. Field Survey Method

Field surveys were conducted to validate data on vegetation cover, cultivation practices, and soil erosion factors. Soil erosion severity was assessed across six land cover types: (1) natural forest restoration, (2) forest vegetation, (3) perennial vegetation, (4) annual vegetation, (5) shrub vegetation, and (6) bare land.

Cropping practices were categorized into: (1) contour cultivation of tea and citrus on hilly terrain, (2) intercropping annual crops on slopes, and (3) monoculture of acacia and cassava.

Erosion severity was classified into five levels: very low (0–5 T ha^{-1} yr^{-1}), low (5–10T ha^{-1} yr^{-1}), moderate (10–20 T ha^{-1} yr^{-1}), high (20–50 T ha^{-1} yr^{-1}), and very high (>50 T ha^{-1} yr^{-1}). Survey points were systematically distributed across Thanh Chuong District, Nghe An Province, Vietnam, ensuring representativeness

2.5. Remote Sensing Method

Pre-processing of satellite images involved stitching, straightening, filtering, and enhancement. Land cover classification was performed using the maximum likelihood classification algorithm, with accuracy assessed through ground truth validation. Field verification included marking virgin and plantation forests, perennial and annual crops, other vegetation, and water bodies using GPS-referenced field data.

Classification accuracy for Landsat images was 93 % and 88 %, while Sentinel images achieved 84 %. Land cover change (LCC) maps for 2010, 2015, and 2021, developed using the RUSLE model, were validated against ground truth data. The model demonstrated high reliability, with overall accuracy exceeding 90 %, confirming its effectiveness in simulating soil loss in the study area.

2.6. Soil Erosion Estimation Using an Optimized RUSLE Model

This study refines the Revised Universal Soil Loss Equation (RUSLE) to enhance soil erosion assessment accuracy. The RUSLE model, an advancement of the Universal Soil Loss Equation (USLE) (Wischmeier, Smith, 1978) predicts average annual soil loss through the integration of five key factors: rainfall aggressiveness (R), soil erodibility (K), slope length and steepness (LS), land cover (C), and erosion control practices (P). The optimized RUSLE model facilitates data acquisition by converting Digital Elevation Model (DEM) data into satellite imagery, improving precision compared to traditional erosion models. Our optimized RUSLE model determines the average annual soil loss using the following formula (1): $\mathbf{A=R\times K\times LS\times C\times P}$

The R-factor, representing precipitation-induced soil erosion, is computed using the equation: $\mathbf{R=79+0{,}363\times X_a}$

where X_a is the average annual precipitation (mm), derived from data collected at six observation stations (2010–2021). The Kriging interpolation method, integrated with ArcGIS, converts precipitation data into raster layers.

The K-factor quantifies soil loss potential and is determined using soil texture, organic matter content, and permeability, computed as:

$$\mathbf{K = 27.66 \times 10^{1.14} \times 10^{-8} \times (12 - a) + 0.0043 \times (b - 2) + 0.0033 \times (c - 3)}$$

where a is organic matter (%), b is soil texture, and c is soil permeability.

The LS-factor, indicating topographic influence, is calculated by:

$$\mathbf{LS} = \left[\frac{\mathbf{Q_a M}}{\mathbf{22.13}}\right]^{\mathbf{y}} \times \left(\mathbf{0.065 + 0.045 \times S_g + 0.0065 \times S_g^2}\right)$$

where Qa is flow accumulation, M is grid size, Sg is slope (%), and y is an exponent (0.2–0.5).

The C-factor accounts for vegetation cover, obtained from LUMP-based lookup tables. The P-factor, which represents conservation practices, is computed as:

$$\mathbf{P = 0.2 + 0.03 \times S}$$

where S is slope (%), using the Wener approach. This optimized RUSLE model enables precise soil loss estimation by integrating high-resolution meteorological, topographical, and land use data. Its applicability enhances erosion assessment and supports sustainable land management strategies.

3. Results and discussion

3.1. Results of Soil Erosion Monitoring Using Satellite Imagery

The study utilized three satellite image sources: Landsat 5 TM, Landsat 8 OLI, and Sentinel 2A, providing comprehensive information on the study area. The diagram below (Figure 1) outlines the research stages and data processing step.

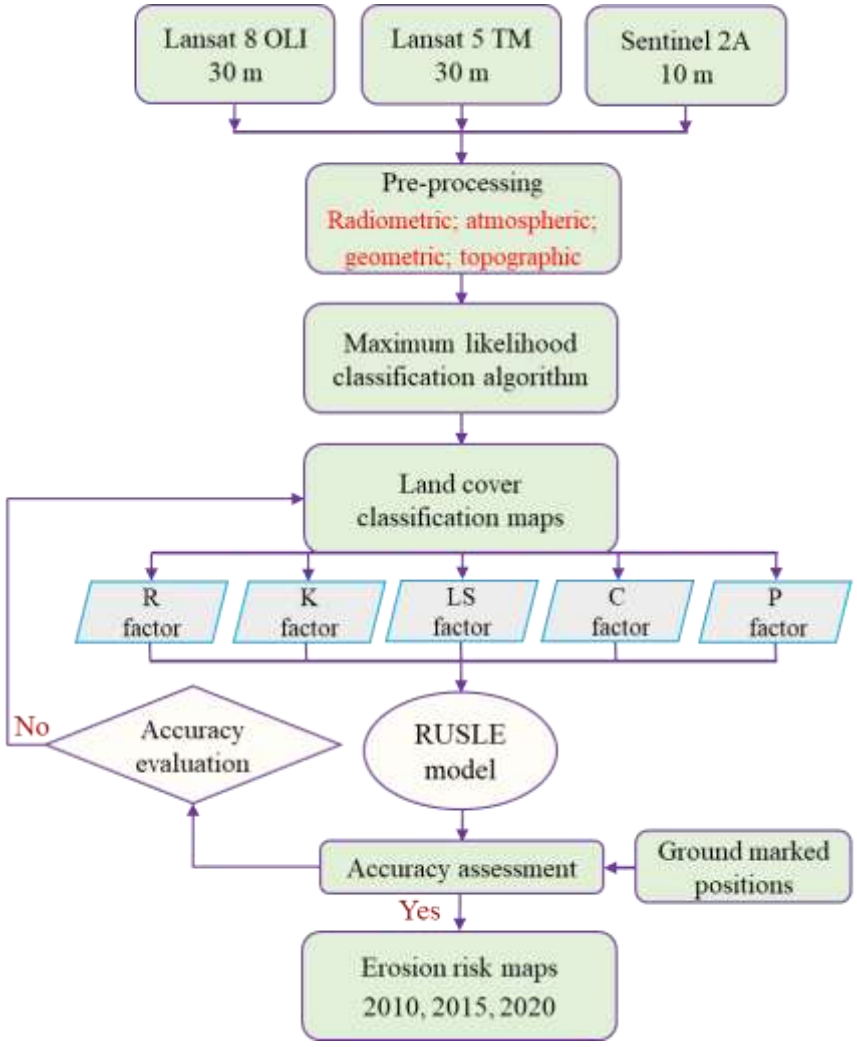

Fig. 1. Image processing workflow for erosion risk map generation

3.2. Influence of Rainfall on Soil Erosion (R-Factor)

Tropical cyclones and orographic effects significantly influence rainfall patterns in the Central Region. The Thanh Chuong study area experiences two distinct seasons: a dry season (December–April) and a rainy season (May–November). The dry season accounts for approximately 12 % of the annual rainfall, with January and February being the driest months

(33.64 mm and 24.33 mm, respectively, for 2010–2021) (Table 1).

The rainy season, contributing about 88 % of the annual precipitation, peaks from August to October, with average rainfall values of 269.46 mm (August), 468 mm (September), and 402.25 mm (October). Rainfall is primarily driven by tropical storms, often coinciding with the hurricane and flood seasons.

Table 1. Frequency of Heavy Rainfall Events and Maximum Daily Rainfall in the Study Area (2010–2021)

Year	Jan.	Feb.	Mar.	Apr.	May.	Jun.	July.	Aug.	Sep.	Oct.	Nov.	Dec.	Total Rainfall	Time
2010	0	0	0	0	0	1	0	7	0	5	0	0	211.3	25/8
2011	0	0	0	0	1	2	3	0	4	1	0	0	130.4	10/9
2012	0	0	0	0	3	0	0	2	2	0	2	0	365.9	6/9
2013	0	0	0	0	0	1	1	1	4	1	0	0	321.8	23/6
2014	0	0	0	0	0	1	0	1	1	0	0	0	152.5	13/6
2015	0	0	1	0	1	2	0	1	2	0	0	0	132.0	17/9
2016	0	0	0	0	0	0	0	0	0	1	1	0	254.1	15/10
2017	0	0	1	0	3	1	4	2	1	3	0	0	161.9	10/10
2018	0	0	0	0	0	0	4	0	2	0	1	2	188.5	19/7
2019	0	0	0	0	1	0	1	3	1	1	0	0	89.3	3/9
2020	0	0	0	0	0	0	0	2	3	4	0	0	508.6	30/10
2021	0	0	0	2	0	1	2	0	4	3	0	0	128.8	24/9
Total	**0**	**0**	**2**	**2**	**9**	**9**	**15**	**19**	**24**	**19**	**4**	**2**		

Notes: Data source is from the hydrometeorological station in the study area.

Unlike Northern Vietnam, where the rainy season begins in May under the influence of the southwest monsoon, Thanh Chuong experiences a delayed onset due to the foehn effect of southwest winds from May to August. With an annual precipitation range of 1,800–2,200 mm, the region is highly susceptible to soil erosion, particularly in mountainous areas. Although the frequency of extreme rainfall events (51–100 mm/day) is relatively low, the total precipitation is significant. Table 1 provides a summary of heavy rainfall occurrences (>50 mm/day) and maximum daily precipitation recorded between 2010 and 2021.

The highest concentration of rainfall events (Table 2) occurs from May to November, with peak daily precipitation in August, September, and October. Rainfall dynamics in the study area deviate from typical storm-induced precipitation patterns observed in other regions of Vietnam. The variability in heavy daily rainfall is significant, ranging from 89.3 mm (September 3, 2019) to 508.6 mm (October 30, 2020), the latter causing widespread flooding and high soil erosion risk.

Table 2. Annual Precipitation in the Study Area (2010–2021) (mm)

Year	Jan.	Feb.	Mar.	Apr.	May.	Jun.	July.	Aug.	Sep.	Oct.	Nov.	Dec.	Total Rainfall
2010	57.20	12.00	13.10	86.00	80.20	100.50	140.00	743.40	82.60	683.60	28.30	14.70	2,041.60
2011	41.60	11.70	77.90	21.90	126.40	291.90	384.30	172.00	538.50	272.10	76.50	46.40	2,061.20
2012	21.40	27.10	44.70	18.10	398.60	66.20	60.80	293.00	613.60	78.80	185.10	43.60	1,851.00
2013	23.30	16.50	22.00	39.30	104.00	349.20	254.50	224.90	646.50	471.70	66.30	32.40	2,250.60
2014	25.30	31.50	28.90	39.10	88.70	285.80	156.90	356.00	519.40	206.40	66.00	21.90	1,825.90
2015	30.80	27.80	154.90	78.10	78.40	163.60	160.00	266.20	560.90	190.90	125.70	49.40	1,886.70
2016	86.50	17.60	25.30	92.00	61.40	11.20	125.20	178.50	624.70	371.50	206.40	41.70	1,842.00
2017	49.70	10.70	96.30	20.20	345.80	106.50	456.70	298.20	338.40	437.40	37.10	40.20	2,237.20
2018	8.20	52.00	34.90	56.60	79.10	45.30	701.00	157.60	231.40	15.10	170.80	253.90	1,805.90
2019	20.60	19.90	29.50	51.20	81.40	1.00	134.60	186.10	587.70	577.80	139.10	42.10	1,871.00

Year	Jan.	Feb.	Mar.	Apr.	May.	Jun.	July.	Aug.	Sep.	Oct.	Nov.	Dec.	Total Rainfall
2020	31.10	23.60	82.40	83.40	102.00	17.30	65.30	288.60	259.30	1,108.90	67.80	18.30	2,148.00
2021	8.00	41.60	56.10	315.60	28.70	188.30	301.20	69.00	613.00	412.80	64.50	24.70	2,123.50

Notes: Data source is from the hydrometeorological station in the study area (2010-2021)

Besides the primary rainy season (August–October), a secondary peak occurs in May–June due to the Tropical Convergence Zone. The annual rainfall-runoff erosion coefficient (R-factor) quantifies rainfall intensity's impact on erosion and requires detailed precipitation data for accurate assessment (Wischmeier, Smith, 1978). The R-factor in the study area varies between 0.69 and 0.87 MJ mm ha^{-1} h^{-1}, with higher values recorded in southern communes (Thanh Lam, Thanh Xuan, Thanh Mai, Thanh Tung, Thanh Yen, Thanh Ha, Thanh Giang) and lower values in northern communes (Cat Van, Thanh Nho, Thanh Duc, Thanh Hoa). The R-factor is classified into six ranges: 0.69–0.72, 0.72–0.75, 0.75–0.78, 0.78–0.81, 0.81–0.84, and 0.84–0.87 MJ mm ha^{-1} h^{-1}.

Average annual precipitation data from the local hydrometeorological station were utilized to calculate the rainfall erosivity (R-factor) (Figure 2). These data serve as a basis for assessing the impact of precipitation on soil erosion dynamics in the study area.

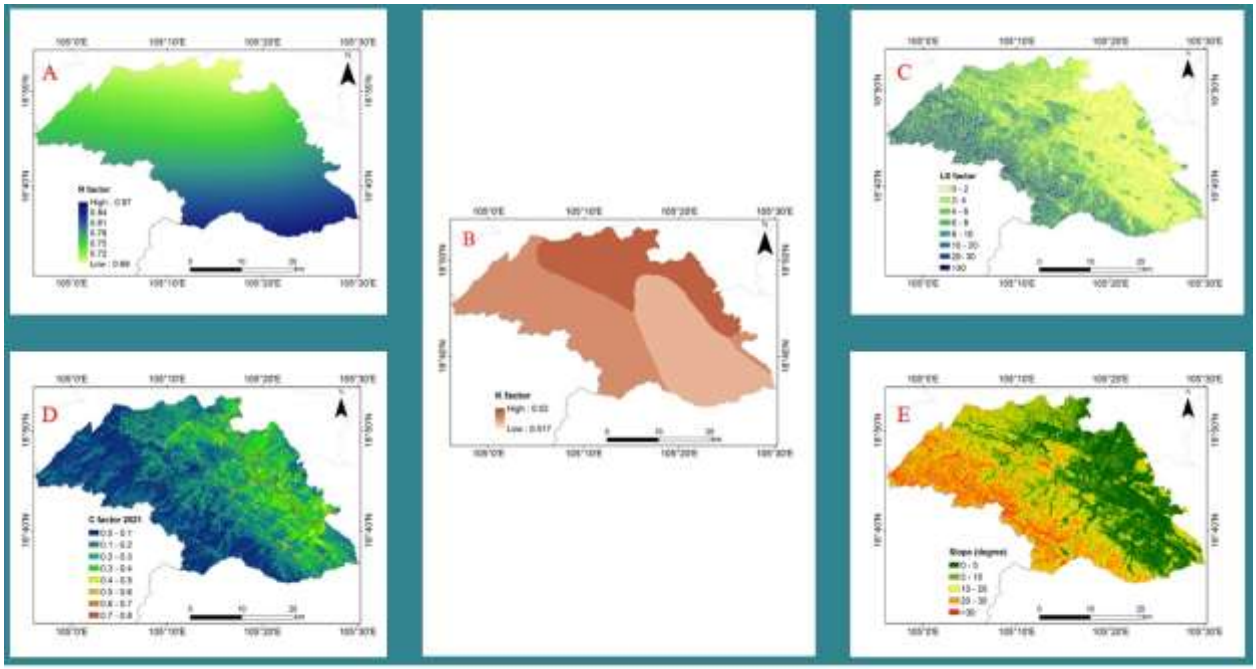

Fig. 2. Spatial Distribution of Erosion Factors in the Study Area

(A) R-Factor: Rainfall erosivity factor indicating the impact of precipitation on soil erosion; (B) K-Factor: Soil erodibility factor representing the susceptibility of soil particles to detachment and transport; (C) LS-Factor: Combined effect of slope length and steepness on erosion potential; (D) C-Factor: Land cover and management factor reflecting the influence of vegetation on soil protection; (E) P-Factor: Erosion control practices factor assessing the effectiveness of conservation measures.

3.3. Effect of Soil Type on Erosion in the Study Area (K)

The soil types in Thanh Chuong District, as identified in the Land Use Planning Report to 2030, significantly influence erosion processes.

Alluvial Soil (P). Formed by the annual deposition from the Lam and Giang River systems, alluvial soils cover approximately 17,780 hectares along both riverbanks. Their texture ranges from sandy loam to medium loam, with a pH_{KCl} value of 6.7–7.2, indicating neutral to slightly acidic conditions. These soils contain 0.25% total nitrogen, adequate phosphorus, and available potassium.

Alluvial soils on river terraces, prevalent in Thanh Van, Xuan Tuong, Thanh Duong, and Thanh Luong communes, exhibit a pH_{KCl} range of 5.8–6.8 and a texture varying from loamy to clayey. They consist of 25–50 % sand, 30–50 % humus, and 10–30 % clay, with relatively low nutrient content (total nitrogen 0.08–0.13 %, total phosphorus 0.06–0.07 %, total potassium

0.15–0.25 %). These soils typically support single-season rice cultivation, while areas with irrigation infrastructure enable double-cropping.

At higher elevations, alluvial soils are modified by agricultural activities, altering their properties. In communes such as Xuan Tuong, Thanh Van, and Vo Liet, soils exhibit greater acidity (pH_{KCl} < 5.0) and a texture ranging from medium to light loam. These soils contain minimal humus and lower concentrations of nitrogen and phosphorus (total nitrogen ~0.1%, total phosphorus 0.04–0.05 %). The presence of conglomerates in some areas further affects their erosion susceptibility.

Ferralitic Soil in the Transition Zone (Fl). Ferralitic soil (Fl) covers approximately 7,700 ha in the transition zone between hills and plains or mountains and valleys. It is characterized by strong degradation, particularly at depths of 12–25 cm, with a texture ranging from sandy loam to medium loam. The soil is highly acidic (pH_{KCl} <5.0) and has low nutrient content (N: 0.05–0.08 %, P: 0.006–0.010 %, K: 0.10–0.26 %).

In terraced fields at the base of hills, prolonged rice cultivation has altered the upper soil layer. Weathering and rainwater transport contribute to soil deposition in valley transition zones. This soil type is prevalent in Thanh Xuan, Thanh Khe, Thanh Thuy, Thanh Lam, Xuan Tuong, and Ngoc Son, with localized variations in texture and organic matter decomposition.

Yellow-Red Ferralitic Soil (Fs). This soil type originates from the weathering of shale parent rocks, exhibiting a yellow-red or red-yellow coloration. It spans approximately 29,900 hectares, predominantly distributed across various communes in the region. Thegranulometric composition varies, ranging from sandy loam to heavy silt and clay. The soil is acidic, with values pH_{KCl} ranging from 4.2 to 4.3. Organic matter content is low, varying from 1.65 % to 3.51 %, and total nitrogen ranges from 1.06% to 0.19%. Total phosphorus concentrations in the surface layer are low to moderate, while total potassium content in the upper horizon ranges from 0.93 % to 1.19 %, with a higher concentration in the deeper layers. Easily available potassium fluctuates between 7.3 and 11.2 mg/100 g of soil. The soil also contains small amounts of calcium and magnesium, and elevated concentrations of Fe_3^+ and Al_3^+.

Red-Yellow Ferralitic Soil (Fq). Formed from the weathering of sandstone, quartzite, and conglomerate, this soil type covers about 2,000 hectares, primarily in the Han Lam commune and some adjacent areas. It has a sandy loam texture with a high proportion of large sand fractions. Both its chemical and physical properties are characterized by low values.

Eroded-to-Stone Ferralitic Soil (E). This soil is derived from the weathering of various parent rocks, including shale, chalk, and quartzite, and covers an area of approximately 12,000 hectares. Historically, these areas featured thick, heavily weathered soils and dense forests with large trees. However, due to unsustainable land use practices such as indiscriminate exploitation and poor agricultural methods, significant erosion has occurred, resulting in a considerable reduction in topsoil thickness.

Yellow Mountain Ferralite Soil (H). Yellow Mountain Ferralite soil is prevalent in the mountainous regions of the study area, covering approximately 47,250 hectares, primarily between 200 to 800 meters above sea level in the western mountainous zones. The granulometric composition of this soil varies from light to medium loam. It is nitrogen-rich, with concentrations ranging from 0.1 % to 0.2 %, but is poor in phosphorus, with values ranging from 0.03 % to 0.04 %. Potassium content fluctuates between 0.2 % and 1.5 %, and the soil exhibits high acidity, with values pH_{KCl} less than 5.0. This soil type is typically covered by natural forests, though past exploitation has led to the presence of shrubbery or even bare hills in some areas. It is primarily utilized for forestry purposes.

At altitudes between 800 to 2,000 meters, the soil remains acidic, characterized by a slow rate of organic matter decomposition and a high humus content. These areas are also predominantly covered by natural forests and are mainly designated for forestry.

Soil Erosion Potential (K-Factor). The K-Factor is a critical measure of soil erosion potential, influenced by soil texture, structure, organic matter content, and water permeability (Abdo, Salloum, 2017). In the study area, the K-Factor varies as follows:

Low K-Factor (0.017 to 0.018 Mg h MJ^{-1} mm^{-1}): This range is common in the southern communes, including Thanh Lam, Thanh Xuan, Thanh Giang, Thanh Tung, Thanh Long, Vo Liet, Thanh Khe, Dong Van, and Thanh Chuong.

Medium to High K-Factor (0.018 to 0.019 Mg h MJ^{-1} mm^{-1}): Found in communes such as Thanh Thuy, Ngoc Lam, Thanh Son, Hanh Lam, and Thanh Duc.

High K-Factor (0.019 to 0.02 Mg h MJ^{-1} mm^{-1}): The highest values are observed in the

northern communes, including Cat Van, Phong Thinh, Thanh Hoa, Thanh Nho, Thanh Phong, Thanh Hung, and Thanh Van. Higher K-Factor values correspond to a higher potential for soil erosion. These findings underline the importance of soil management in relation to erosion risks, particularly in areas with higher K-Factor values.

3.4. Effect of Terrain on Soil Erosion in Thanh Chuong District (LS Factor)

The terrain of Thanh Chuong District is categorized into three primary types: Plains (26 % of the total area) are primarily located along the Lam River, with small, scattered distributions. Approximately 12 % of this land experiences annual flooding. Alluvial plains support agricultural activities, including rice, corn, potatoes, and short-term industrial crops.

Hills (30 % of the area) are characterized by undulating or bowl-shaped topography, with elevations typically below 100 m. These soils, primarily formed on shale, are suitable for perennial industrial crops, fruit trees, and livestock grazing. However, unsustainable land use has resulted in soil degradation, reducing fertility and exposing rocky surfaces.

Mountains (44 % of the area) are primarily located along the Vietnam-Laos border and feature steep slopes with significant elevation variations. High mountains (>800 m) constitute 17 % of the total area, while low mountains (200–800 m) make up the remainder. The complex topography exacerbates soil erosion risk.

The LS factor, representing the impact of slope length and steepness on erosion, was analyzed using slope accumulation data. The lowest LS values were recorded in the eastern Lam River Valley (e.g., Thanh Giang, Thanh Yen, Thanh Tung), whereas the highest LS values were associated with steep, folded terrain in the southwest (e.g., Thanh Ha, Thanh Thuy, Ngoc Lam). LS values in the study area are classified into eight categories, ranging from 0 to >30, indicating increasing erosion susceptibility. Areas with steep slopes and high LS values require targeted soil conservation measures to mitigate erosion risks.

3.5. Effect of Vegetation Cover on Soil Erosion in Thanh Chuong District (C)

A comparative analysis of land cover data for 2010, 2015, and 2021 revealed significant changes in vegetation distribution across the study area (Table 3; Figure 3). Six land cover classes were identified: primary forests, forest plantations, annual plantations, perennial plantations, other land types, and water bodies.

Table 3. The land cover change during the period from 2010–2021

Cover types	Total cover area (ha)			Changed trends in periods (%)		
	2010	2015	2021	2010-2015	2015-2021	2010–2021
Primary forest	37200.2	35117.4	32797.0	-1.86	-2.07	-3.92
Plantation forest	23223.8	20233.3	20027.3	-2.67	-0.18	-2.85
Perennial plant	5659.9	4006.2	8667.6	-1.47	+4.16	+2.68
Annual plants	12002.5	17881.2	17702.9	+5.24	-0.16	+5.08
Other land	32832.0	33554.5	30951.5	+0.64	-2.32	-1.67
Water	1247.5	1377.9	2012.1	+0.12	+0.57	+0.68

In 2010, primary forests occupied the largest area (37,200.2 ha), followed by other land types (32,832.0 ha) and forest plantations (23,223.8 ha). Annual and perennial plantations covered 12,002.5 ha and 5,659.9 ha, respectively, while water bodies accounted for 1,247.5 ha. By 2015, the area of primary forests had decreased by 2,082.8 ha, shelterbelts by 2,990.5 ha, and perennial plantations by 1,653.7 ha. Concurrently, agricultural expansion led to an increase in annual plantations (+5,878.2 ha), other land types (+722.5 ha), and water bodies (+130.4 ha). This shift was primarily driven by the conversion of forested areas into agricultural land, notably for acacia and cassava cultivation (Dinh, Shima, 2022).

Between 2015 and 2021, deforestation accelerated, with forested areas shrinking by an additional 7,599.7 ha. Other vegetation types declined by 1,880.5 ha, while annual and perennial plantations expanded by 8,708.1 ha. A slight increase in water bodies (+764.6 ha) was also observed, likely resulting from the loss of forested land.

The continued decline in primary forests and shelterbelts from 2010 to 2021 underscores the intensification of land conversion for agriculture. This transformation has heightened soil erosion

risks and disrupted ecological stability, emphasizing the urgent need for sustainable land management practices to mitigate degradation.

The C-Factor, representing vegetation cover and land management, is a critical parameter influencing soil erosion (El Jazouli et al., 2017). It varies according to land use and management practices (LUMP) and is referenced in established datasets (Ganasri, Ramesh, 2016). The initial C-Factor values used in this study are presented in Appendix. Table S2.

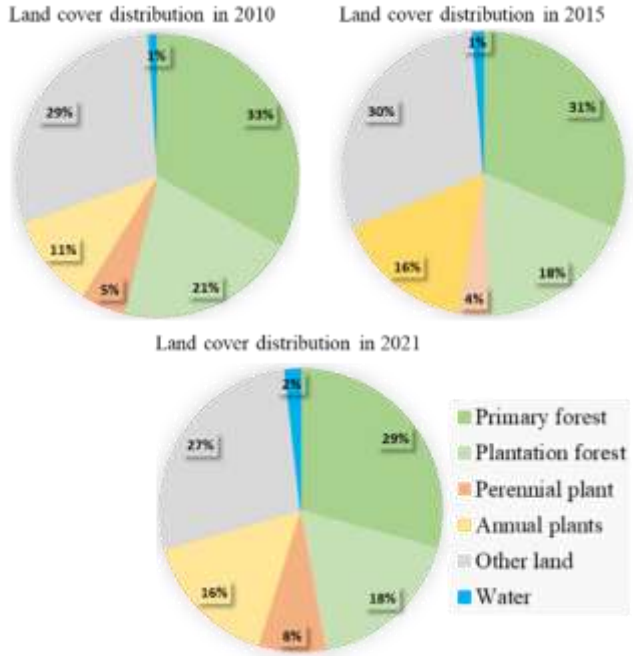

Fig. 3. Land cover distribution in the study area 2010, 2015, and 2021

To categorize the impact of vegetation on erosion, we classified the C-Factor into five ranges: 0 for water bodies, 0–0.1 for primary forests and shelterbelts, 0.1–0.3 for perennial plantations, 0.3–0.5 for annual plantations, and 0.5–0.8 for other land types (Figure 2D). Our findings indicate that a significant portion of the study area is covered by natural forests and shelterbelts, where the C-Factor is low, suggesting reduced susceptibility to soil erosion. Conversely, areas dominated by annual crops and bare soil exhibit higher C-Factor values, indicating increased erosion potential. These results highlight the protective role of forested areas in mitigating soil degradation.

3.6. Impact of Conservation Measures on Soil Erosion (P-Factor)

The P-Factor quantifies soil loss due to anthropogenic influences and is determined based on erosion control measures implemented on slopes. It represents a soil loss coefficient, which is assigned according to specific land management practices (Figure 2E).

Areas with effective soil conservation techniques typically exhibit lower P-Factor values, as these practices reduce runoff velocity and promote sediment deposition on slopes. Soil erosion potential, driven by runoff from precipitation, is influenced by both land management and basin characteristics.

Our analysis indicates that the P-Factor is primarily controlled by slope gradient, which is categorized into five classes: 0–5, 5–10, 10–20, 20–30, and >30. The study area exhibits a clear spatial differentiation in slope distribution, with the highest values observed in the western and southern regions, while a gradual decrease is noted toward the east and southeast (Figure 2E). These findings emphasize the need for targeted conservation strategies in areas with steeper slopes to mitigate soil erosion risks.

3.7. Soil Erosion Map of the Study Area

The soil erosion risk map (Figure 4A) illustrates the spatial distribution of soil loss across the study area, with values ranging from 0 to 50 t ha^{-1} yr^{-1} for the period 2010–2021. The estimated average soil loss of 25 t ha^{-1} yr^{-1}, based on RUSLE model indicators, aligns with field observations.

The analysis reveals that high soil erosion is primarily concentrated in areas with steep slopes and high precipitation intensity, particularly in the southwestern and northeastern regions. In contrast, low

erosion levels are predominant across most of the study area, corresponding to regions with stable vegetation cover and gentler slopes. Approximately 18 % of the total area falls within the high to very high erosion risk categories, with moderate soil erosion occurring along a northwest-to-southwest corridor where steep slopes coincide with unsustainable operational activities (UOA).

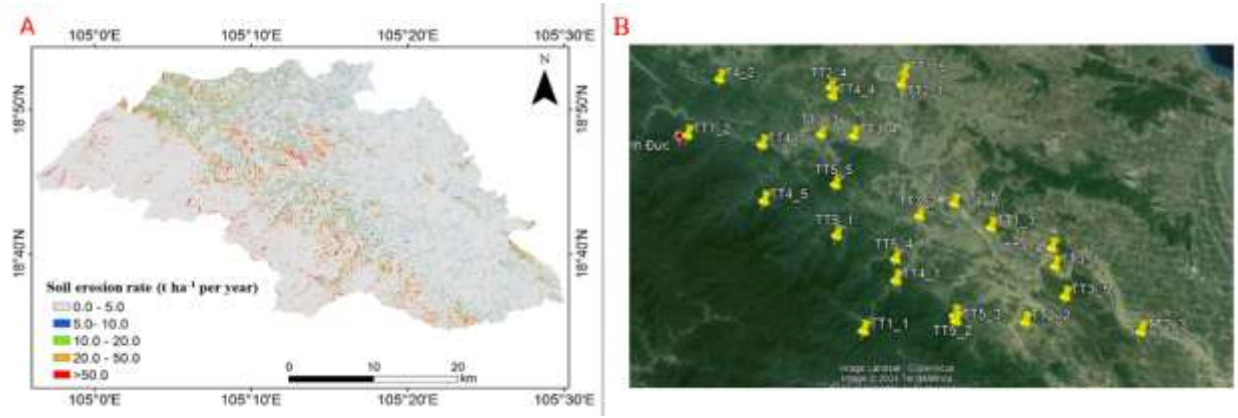

Fig. 4. (A) Soil erosion map of the study area and (B) erosion verification points

The east, southeast, and northwest regions exhibit moderate soil erosion, attributed to lower rainfall intensity and the prevalence of less steep terrain. However, land cover changes particularly the conversion of primary and plantation forests into agricultural and barren lands have contributed to increased soil loss. This is consistent with findings by Brodie & Catherine (2020), which highlight the protective role of forest and plantation vegetation in mitigating soil erosion.

Verification points (Figure 4B) were selected across the study area, focusing on representative locations within Thanh Chuong District, Nghe An Province, Vietnam. Temporal image analyses suggest that fluctuations in land cover significantly influence the C-Factor, thereby accelerating soil loss. These findings underscore the importance of sustainable land management practices to mitigate erosion risks.

3.8. Development of Erosion Control Measures in the Study Area

Impact of Human-Induced Erosion on Forest Soil Degradation. Anthropogenic soil erosion is a major contributor to forest soil degradation worldwide, directly influencing forest stand development and reducing forest productivity. Sustainable forest management requires an accurate assessment of soil loss resulting from various forestry activities. A key factor in this process is rainfall intensity, which affects the volume of rainwater reaching the soil. This is closely linked to phytosanitary conditions, as the stability and health of forest stands depend on canopy consistency and vegetation density.

Determination of Vegetation Cover Threshold and Anti-Erosion Efficiency. In central Vietnam, where 80 % of the land area is characterized by sloping terrain, soil erosion is exacerbated by both natural factors and human activities, leading to severe ecological imbalances. To quantify the erosion control efficiency of forest stands, it is crucial to evaluate parameters such as tree density, seedling biomass, and surface runoff rates. These factors influence precipitation retention capacity, thereby reducing erosion intensity. Determining the optimal number of trees per hectare, alongside the presence of shrubs, seedlings, and forest litter, is essential for minimizing soil loss. Consequently, a comprehensive strategy is required to enhance land-use management practices, particularly in erosion-prone zones at the regional level.

Development of Agricultural and Forestry Models for Heavily Eroded Lands. At the local level, effective erosion control measures remain underdeveloped due to limited methodological frameworks and insufficient technological support. One of the most promising approaches is Sloping Agriculture Land Technology (SALT), an integrated soil conservation and agroforestry system designed for erosion-prone landscapes. SALT incorporates contour farming techniques, where strips of perennial and nitrogen-fixing trees (spaced 3 to 5 meters apart) are planted between rows of food and cash crops. This system enhances soil retention, reduces runoff velocity, and improves land productivity while ensuring sustainable agricultural and forestry land use in severely eroded regions.

Implementation of the SALT 3 Model in Livestock Farming. Anthropogenic soil

erosion often results from poor land management, particularly in livestock farming, where improper waste disposal and overgrazing accelerate land degradation. The SALT 3 model offers an integrated approach that combines small-scale afforestation with food production, ensuring environmental sustainability while enhancing agricultural productivity.

This model promotes an optimal land-use structure of 40 % agricultural land and 60 % forestry, effectively balancing soil conservation and economic benefits. The expansion of forest cover within agricultural systems increases the availability of food, fuelwood, and other forest-based products, directly benefiting farmers' incomes. The SALT 3 model is particularly suitable for land areas of 5-10 hectares and can be adapted to various terrain types.

Experimental application of this model indicates that diversification of perennial crops is crucial for sustainable land use. Ideally, at least 20 % of total planted trees should be perennial species, contrasting with the current trend in the study area, where acacia monoculture dominates.

Application of the SALT 1 Model in Tea Plantations. The SALT 1 model integrates annual and perennial crops in a structured manner, ensuring soil compatibility and consistent harvesting cycles. Currently, tea plantations on hills are cultivated along contour lines, but lack protective strips of nitrogen-fixing trees, which are essential for erosion control, shading, soil enrichment, and sustainable timber production.

Under this model, nitrogen-fixing trees are planted in dense double rows between tea crops. Once these trees reach 1 meter in height, their branches are pruned, and leaves are used as organic mulch, enhancing soil fertility and moisture retention. In Thanh My and Thanh Huong communes, the cropping pattern follows a 75 % agricultural – 25 % forest crop distribution, with agricultural lands divided into 50 % annual and 25 % perennial crops.

The SALT 1 model has proven economically beneficial, increasing farmers' income by 1.5 times compared to traditional cassava cultivation. Additionally, it reduces soil erosion by 50 % compared to conventional farming methods on sloping terrain. In areas where tea plantations lack forest buffers, it is essential to plant additional contour-aligned trees, prioritizing nitrogen-fixing species. These practices prevent soil erosion, enhance shade coverage, improve soil fertility, and support timber production. In Thanh Mai, Thanh An, and Thanh Thuy communes, the SALT 1 model proposes a 75 % tea plantation – 25 % forest tree structure, offering a more sustainable alternative to the existing tea cultivation systems in these hilly regions.

The SALT 4 model integrates citrus cultivation (e.g., orange and grapefruit) with food crops, focusing on perennial trees to enhance soil stability and reduce erosion. This model, effective in Thanh Nho, Thanh Duc, Thanh Lien, Thanh Thinh, and Thanh My communes, promotes soil fertility through nitrogen-fixing plants and offers economic benefits via the production of marketable fruit.

To mitigate soil erosion, trenching and embankment construction divide slopes into smaller sections, reducing runoff speed and improving water infiltration. The spacing between barriers varies with slope steepness: 3–4 meters for steep slopes and 5–6 meters for moderate ones. In areas with rocky terrain, stone barriers provide an alternative solution. In gentle slopes, the construction of terraces is an effective strategy for long-term erosion control. This involves determining terrace dimensions based on soil type, constructing embankments to slow runoff, and redistributing fertile topsoil to enhance productivity.

The SALT 4 model emphasizes the cultivation of perennial crops, such as oranges, which offer benefits including nitrogen fixation, erosion control, and soil improvement while also providing a marketable food product. In contrast, the SALT 1 model applied to tea plantations involves a combination of annual crops interspersed with perennial species to optimize soil conditions and ensure consistent harvests. The cropping structure proposed for this model includes 75 % agricultural crops and 25 % forest crops, with 50 % of agricultural crops being annuals and 25 % perennials. Overall, the SALT models provide a holistic approach to erosion control and sustainable land management, enhancing agricultural productivity while preserving soil integrity.

4. Conclusion

This study provides a comprehensive assessment of soil erosion in Thanh Chuong District, Nghe An Province, Vietnam, under tropical monsoon conditions. Utilizing GIS, remote sensing, and an optimized RUSLE model, it identifies high erosion risk areas and quantifies soil loss, averaging 25 t/ha/year, with 18 % of the region facing high to very high erosion. Key factors influencing erosion include rainfall intensity, slope, soil type, and land use practices. The findings

highlight the urgent need for targeted conservation measures, such as SALT-based agroforestry models, vegetation restoration, and terracing, to promote sustainable land management and mitigate soil degradation in erosion-prone areas.

5. Conflict of interest

The authors have no conflicts of interest to declare that are relevant to the content of this article.

References

Abdo, Salloum, 2017 – *Abdo, H., Salloum, J.* (2017). Mapping the soil loss in Marqya basin: Syria using RUSLE model in GIS and RS techniques. *Environmental Earth Sciences*. 76: 1-10.

Adornado et al., 2009 – *Adornado, H.A., Yoshida, M., Apolinares, H.A.* (2009). Erosion vulnerability assessment in REINA, Quezon Province, Philippines with raster-based tool built within GIS environment. *Agricultural Information Research*. 18(1): 24-31.

Aksoy, Kavvas, 2005 – *Aksoy, H., Kavvas, M.L.* (2005). A review of hillslope and watershed scale erosion and sediment transport models. *Catena*. 64(2-3): 247-271.

Committee T.C.D.P.s, 2021 – Committee T.C.D.P.s. Report on Land Use Planning to 2030 of Thanh Chuong District, 2021.

Dinh, Shima, 2022 – *Dinh, K.H.T., Shima, K.* (2022). Effects of forest reclamation methods on soil physicochemical properties in North-Central Vietnam. *Research on Crops*. 23(1): 110-118.

Dung et al., 2020 – *Dung, N.D. et al.* (2020). Study on the characteristics of sedimentation soil of small and medium reservoirs in Ha Tinh. *Journal of Water resources & Environmental engineering*. 60: 99-106.

El Jazouli et al., 2017 – *El Jazouli, A. Barakat, A., Ghafiri, A, El Moutaki, S, Ettaqy, A. Khellouk, R.* (2017). Soil erosion modeled with USLE, GIS, and remote sensing: a case study of Ikkour watershed in Middle Atlas (Morocco). *Geoscience Letters*. 4(1): 25.

Ganasri, Ramesh, 2016 – *Ganasri, B., Ramesh, H.* (2016). Assessment of soil erosion by RUSLE model using remote sensing and GIS-A case study of Nethravathi Basin. *Geoscience Frontiers*. 7(6): 953-961.

Golkarian et al., 2023 – *Golkarian, A., Khosravi, K., Panahi, M., Clague, J.J.* (2023). Spatial variability of soil water erosion: Comparing empirical and intelligent techniques. *Geoscience Frontiers*. 14(1): 101456.

Le Dinh et al., 2022 – *Le Dinh, H., Shibata, M., Kohmoto, Y., Ho, L.N., Funakawa, S.* (2022). Analysis of the processes that generate surface runoff and soil erosion using a short-term water budget on a mountainous sloping cropland in central Vietnam. *Catena*. 211: 106032.

Tian et al., 2008 – *Tian, W. et al.* (2008). The status of soil and water loss and analysis of countermeasures in China. *Research of soil and water conservation*. 15(4): 204-209.

Wischmeier, Smith, 1978 – *Wischmeier, W.H., Smith, D.D.* (1978). Predicting rainfall erosion losses: a guide to conservation planning. *Department of Agriculture, Science and Education Administration*. P. 537.

Yesuph, Dagnew, 2019 – *Yesuph, A.Y., Dagnew, A.B.* (2019). Soil erosion mapping and severity analysis based on RUSLE model and local perception in the Beshillo Catchment of the Blue Nile Basin, Ethiopia. *Environmental Systems Research*. 8(1): 1-21.

Appendix

Table S1. Satellite imagery data utilized in this study

Data	Projection	Date of receipt	Resolution (m)	Source
Landsat 5 TM	UTM-Zone-48N	2000	30	https://glovis.usgs.gov/
Landsat 5 TM	UTM-Zone-48N	2001	30	https://glovis.usgs.gov/
Landsat 5 TM	UTM-Zone-48N	2002	30	https://glovis.usgs.gov/
Landsat 5	UTM-Zone-48N	2003	30	https://glovis.usgs.gov/

Data	Projection	Date of receipt	Resolution (m)	Source
TM				
Landsat 5 TM	UTM-Zone-48N	2004	30	https://glovis.usgs.gov/
Landsat 5 TM	UTM-Zone-48N	2005	30	https://glovis.usgs.gov/
Landsat 5 TM	UTM-Zone-48N	2006	30	https://glovis.usgs.gov/
Landsat 5 TM	UTM-Zone-48N	2007	30	https://glovis.usgs.gov/
Landsat 5 TM	UTM-Zone-48N	2008	30	https://glovis.usgs.gov/
Landsat 5 TM	UTM-Zone-48N	2009	30	https://glovis.usgs.gov/
Landsat 5 TM	UTM-Zone-48N	2010	30	https://glovis.usgs.gov/
Landsat 5 TM	UTM-Zone-48N	2011	30	https://glovis.usgs.gov/
Landsat 5 TM	UTM-Zone-48N	2012	30	https://glovis.usgs.gov/
Landsat 8 OLI	UTM-Zone-48N	2013	30	https://glovis.usgs.gov/
Landsat 8 OLI	UTM-Zone-48N	2014	30	https://glovis.usgs.gov/
Landsat 8 OLI	UTM-Zone-48N	2015	30	https://glovis.usgs.gov/
Sentinel 2A	UTM-Zone-48N	2016	10	https://scihub.copernicus.eu/
Sentinel 2A	UTM-Zone-48N	2017	10	https://scihub.copernicus.eu/
Sentinel 2A	UTM-Zone-48N	2018	10	https://scihub.copernicus.eu/
Sentinel 2A	UTM-Zone-48N	2019	10	https://scihub.copernicus.eu/
Sentinel 2A	UTM-Zone-48N	2020	10	https://scihub.copernicus.eu/
Sentinel 2A	UTM-Zone-48N	2021	10	https://scihub.copernicus.eu/

Table S2. C-Factor for Various Land Use and Management Practices in the Study Area

Class	C factor range	Mean value
Primary forest	0.001-0.002	0.0015
Plantation forest	0.01-0.02	0.015
Perennial plant	0.1-0.3	0.2
Annual plants	0.3-1.0	0.65
Other land	0.5-1.0	0.75
Waterbody	0	0